CHARACTERIZING SINGLE-CELL BEHAVIOR OF FLAGELLATED PATHOGENIC BACTERIA IN MUCUS AND VISCO-ELASTIC ENVIRONMENTS

By

Nhu Thi Quynh Nguyen

A DISSERTATION

Submitted to
Michigan State University
in partial fulfillment of the requirements
for the degree of

Microbiology and Molecular Genetics–Doctor of Philosophy

2020

ABSTRACT

CHARACTERIZING SINGLE-CELL BEHAVIOR OF FLAGELLATED PATHOGENIC BACTERIA IN MUCUS AND VISCO-ELASTIC ENVIRONMENTS

By

Nhu Thi Quynh Nguyen

Flagellar motility is required for some enteric pathogens to colonize the intestine. Understanding how these pathogens overcome the mucus layer protecting the epithelial tissue is necessary for disease prevention. In this thesis project I examined bacterial motility in mucus to understand factors that facilitate mucus penetration and contrasted this with the motility in different visco-elastic materials.

In this thesis, I used single cell tracking to characterize the flagellar motility of *Vibrio cholerae* and *Salmonella enterica* in different visco-elastic environments. First, I tested if *V. cholerae* and *S. enterica* were still motile in unprocessed pig intestinal mucus. Second, I studied factors that supported their motility in mucus. The first factor I investigated was the effect of pH on *V. cholerae* motility. I also studied the role of curvature in *V. cholerae* motility within mucus and some other visco-elastic environments, including liquid and agar. Last, I began investigation of the role of flagellar number in *S. enterica* motility. In these studies, I focused on analyzing the effective diffusion of bacteria and factors promoting the diffusion in each environment. My findings demonstrate that *V. cholerae* and *S. enterica* are able to swim in mucus, and that the torque, and the curvature of *V. cholerae*, and the flagellar number of *S. enterica*, play a significant role in bacteria motility in mucus and liquid. Moreover, my findings help elucidate the significance of motility in pathogenesis.

ACKNOWLEDGEMENTS

I would like to thank my PI, Dr. Yann Dufour for challenging me to become a better scientist. Six year working in his lab helped me grow up a lot.

I would like to thank Dr. Maxine Caws, who helps boost my confidence. She always supported and encouraged me in my academic life. Thanks to her, I continued to satisfy my curiosity by taking a PhD in the USA.

I would like to thank my lab mates, Josh, John Lee, Alex, and John Chodkowski who encouraged and supported me during the last six years. They would go eat ice cream with me when my research was not on the right path.

I would like to thank my American friends who taught me about your culture and introduced me to the beauty of the U.S.A.

I would like to thank my Vietnamese friends, who consulted and helped me to get through all the culture shocks and homesickness.

I would like to thank my international friends, who shared the feelings and encouraged me a lot.

Lastly, I would like to thank my parents, my brother, my aunt, and cousins for being my family, for letting me know that I always have somewhere to come back.

TABLE OF CONTENTS

LIST OF FIGURES

KEY TO ABBREVIATIONS

V. cholerae	*Vibrio cholerae*
S. enterica	*Salmonella enterica*
C. jejuni	*Campylobacter jejuni*
WT	Wild type
LB	Luria-Bertani
MHB	Mueller Hinton broth
VB	Vogel-Bonner
MC	Methyl cellulose
LMA	Low-melting agarose
MCLMA	Methyl cellulose and low-melting agarose
MSD	Mean-squared displacement

Chapter 1: INTRODUCTION

Bacterial biomass is estimated to be 500 times greater than the biomass of humans (Whitman et al., 1998). The accumulation of bacterial biomass can be attributed to their ability to inhabit various environments, including fresh water, ocean, hot springs, the soil, and animal guts (Flemming and Wuertz, 2019). Some bacteria are ubiquitous, while others have evolved to inhabit specific niches. Each environment imposes a different constraint to bacteria. To survive and thrive in various environments, bacteria have developed different strategies to cope with environmental stressors. One of the solutions is becoming motile. Motility helps bacteria to move towards food sources and escape harsh conditions.

BACTERIAL MOTILITY

Bacterial motility directly and indirectly affects many aspects of human life (Männik et al., 2009). These effects can be both beneficial and detrimental (Moens and Vanderleyden, 1996). For example, in agriculture, bacterial motility allows for colonization of plant roots that form beneficial microbiota (Turnbull et al., 2001). Once established, these bacteria help improve plant growth through nutrient exchange and plant health through competitive exclusion of plant pathogens (Hassani et al., 2018). On the other hand, bacterial motility is reported as a virulence factor upon *Salmonella enterica, Vibrio cholerae* and *Campylobacter jejuni* human infection (Guentzel and Berry, 1975; Jones et al., 1994; Morooka et al., 1985; Richardson, 1991; Schmitt et al., 2001). Nevertheless, there is limited information about how motility helps establish the pathogenesis of these bacteria. For example, how motility helps these enteric pathogens to penetrate through the mucus layer protecting the epithelial tissue before initiating an infection. Thus, knowledge about bacterial motility behavior is necessary to exploit the benefits and limit the negative effects.

Bacteria have low Reynolds number. The Reynolds number is the ratio of inertial to viscous forces on an object (Purcell, 1977). In a majority of environments experienced on Earth (e.g. air and water), larger objects tend to live life at high Reynolds number, where inertial forces predominate. On

the contrary, microscopic objects, have a low Reynolds number. For example, bacteria have a Reynolds number typically in the range of 1×10^{-6} (Rapp, 2017). The Reynolds number quantifies how much the flow is affected by inertia. Due to its size and low inertia forces, bacterial movement is limited by the viscosity of the surrounding environments. Low Reynolds number affects food searching behavior. To search for places with more food, bacteria must be motile enough to perform beyond the Brownian diffusion of both itself and the food molecules. Motility helps bacteria adapt to life at low Reynolds number. Most bacteria develop to swim by corkscrew motion to propel its body (Purcell, 1977).

Flagellar motility is the most prevalent type of motility. The use of flagellar rotation helps bacteria generate corkscrew motion to diffuse and overcome the low Reynolds number (Purcell, 1997). This motion also helps bacteria to respond to some chemical stimuli. Apart from some bacteria with periplasmic flagella, most bacteria have exterior flagella. The flagella may localize to the poles or be distributed around the cell body (peritrichous). The flagellum is divided into three parts: the flagellar filament, the hook, and the motor (Fig. 1.1). The flagellar filament length is two to ten times longer than the body length, from 5-20 μm long and 20 nm in width. The flagellum is rotated by a motor at the base. The motor when rotating produces a torque, making the filament rotate. The rotation of the flagellum propels the cell to go forward. The filament is connected to the motor through a hook. The hook is so flexible that it allows the change of rotation direction of the flagellum enacted by the motor. When this event happens, it changes the swimming direction of bacteria (tumble or reverse event). The flagellar rotation helps bacteria move in various moist environments, including liquid or hydrogel or pockets of water in the soil.

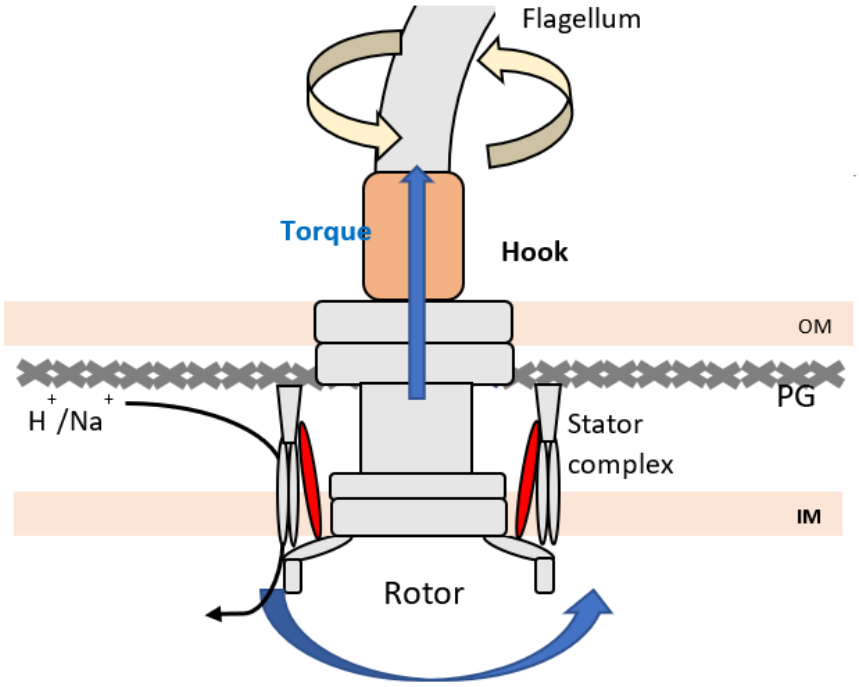

Figure 1.1: Bacterial flagellar motor

Swimming is the most known type of flagellar motility, which is often expressed in aqueous environments. Bacteria can swim at speeds ranging from 1 to 1000 µm/s (Mitchell and Kogure, 2006). When swimming, some bacteria have a "random walk", characterized by intermittent periods of swimming straight and changing direction. Swimming motility is aided by chemotaxis, which biases movement towards food or away from predators. Chemotaxis happens in response to chemical gradients resulting in a "biased random walk".

Swimming motility is costly. The flagellum is a complex machine with thousands of units. In fact, the cost to the cell of flagellar synthesis is 2% of the biosynthetic energy expenditure as found in *Escherichia coli* and *Salmonella enterica* (Moens and Vanderleyden, 1996). Additionally, the rotation of flagella is supported by proton or sodium pumps which requires energy to produce and function. The cost of motility can be clearly seen by its effects on the growth rate (Ni et al., 2020). Moreover, it is

observed that bacteria regulate the use of motility carefully by inhibiting motile behavior when they are close to the surface or substrate (Garrett et al., 2008; Jones et al., 2015). Since swimming is costly, bacteria must develop different strategies to be more efficient in motility.

Although genetic studies suggested the role of flagellar proteins, the contributions of swimming motility to bacterial pathogenesis has been under characterized and lacks quantification due to difficulties in recording swimming behavior. In the human host, mucus is a bio-physical barrier against the microbiota. How swimming motility helps enteric pathogens to compromise this mucus layer needs to be deciphered. Recently, Furter et al. reported that *Salmonella enterica* can swim through the fluid streams in mucus to epithelial cells and initiate an infection in a mouse model (Furter et al., 2019). This paper shows that both mucus structure and flagellar motility are required for S. enterica successful infection. Nevertheless, the role of swimming motility in pathogenesis still needs to be elucidated in more depth to determine which factors or strategies have been used.

ENVIRONMENTAL CONSTRAINTS

Bacterial motility behavior is strongly affected by environmental constraints. First, physic factors such as the viscosity and the elasticity can inhibit bacterial motility. The viscosity can either impede or increase the motility in terms of the proportion of motile cells and swimming speed (Ferrero and Lee, 1988; Schneider and Doetsch, 1974; Takabe et al., 2013). A highly elastic material can trap bacteria in its pores. It was reported that *E. coli* that tumble more frequently can escape the porous environments better (Licata et al., 2016). In addition, it is worth noting that bacterial swimming behavior from the gut and sea water is different. Bacteria from the gut change direction by tumbling whereas bacteria from sea water tends to reverse to counter the stream (Mitchell and Kogure, 2006; Stocker and Seymour, 2012). In addition, factors such as pH, osmolarity, and temperature also regulate motility (Maeda et al., 1976; Soutourina et al., 2002; Takabe et al., 2013). The concentration of nutrients also affects motility as

it regulates the motile versus sessile behavior (Adler and Templeton, 1967; Ni et al., 2020; Wei and Bauer, 1998). To study pathogenesis, it is required to understand how the environments inhibit or promote bacterial swimming motility.

BACTERIAL STRATEGIES

To deal with environmental constraints, bacteria must develop different strategies to be efficient in diffusion. One of them is by regulating the flagellar number. Flagellar production is costly. Therefore, bacteria have developed strategies to minimize costs of motility while satisfying the need to find food. Most ocean bacteria have only one flagellum at the pole, whereas soil bacteria tend to be peritrichous. Some bacteria even change the number of flagella depending on the environments they live in (McCarter, 2005). For example*, V. parahaemolyticus* have one flagellum at the pole when swimming in liquid and express lateral flagella when growing on a solid surface (McCarter, 2001). It was reported that flagellar number affects the transportation efficiency of *Bacillus subtilis* (Najafi et al., 2018). In terms of pathogenesis, more flagella increase the swimming speed of *Helicobacter pylori* in porcine stomach mucin (Martínez et al., 2016). However, bacteria with one flagellum such as *V. cholerae* can still infect the gut. Therefore, it is unknown if more flagellar number benefits bacterial pathogenesis.

Another difference observed between bacteria is the torque. The torque is generated when the motor rotates, which is then translated into swimming speed. Bacteria with sodium motor such as *V. cholerae* tend to generate stronger torque than bacteria with proton motor (Takekawa et al., 2020). Moreover, Beeby et. al,. reported that bacteria with wider stator radii have higher torque (Fig. 1.1) (Beeby et al., 2016). There is little knowledge about why bacterial motors produce different levels of torque. Firstly, it is not known if higher torque is developed based on the environments in which they live. It is suggested that the flagellar motors from other bacteria, such as *Helicobacter pylori* and *Campylobacter jejuni*, are known to generate higher torque and have faster swimming speeds

in high-viscosity environments (Lertsethtakarn et al., 2011). Secondly, it is not known if higher torque promotes bacterial infection. The influence of flagellum torque in helping bacteria overcome environmental constraints remains to be elucidated.

Bacterial cell morphology is greatly affected by its environment. For example, *E. coli* cell size changes under different nutrient conditions (Yao et al., 2012). Having a curved shape could be costly (Schuech et al., 2019). However, it is common that marine bacteria have curved rod shape (La Ferla et al., 2014). The cell shape seems to change depending on type of motility. For example, *E. coli* swarm cells are longer than swim cells (Damton et al., 2010). Previous studies suggest that bacterial morphology contributes to the motility. Bacteria with spiral shape were shown to be more motile in viscous environments compared to their rod shape mutants. In fact, the spiral shape increases the speed of *Helicobacter pylori* in liquid by 15% (Martínez et al., 2016). In addition, the curved shape was predicted to be optimal for bacteria in terms of speed and chemotaxis (Schuech et al., 2019). However, evidence about the effect of cell shape on motility is still scarce.

THESIS OVERVIEW

Motility is an important aspect of pathogenesis, especially in enteric pathogens. Yet, little is known how the motility helps bacteria to overcome the environmental constraint of mucus. A study on the swimming behavior of enteric bacteria in intestinal mucus would be a significant contribution to the understanding of bacterial pathogenesis. The results would help understand how pathogenic bacteria compromise the physical mucus barrier and inform strategies to reduce the risk of gastrointestinal infections in humans and animals. If we understand which factors have the largest effect on motility, we may be able to design a targeted approach to manipulate mucus properties and prevent infection with minimal effect on the normal microbiota.

In this dissertation, I investigated the motility of *V. cholerae* and *S. enterica* in mucus. My goal was to determine if these bacteria could swim in unprocessed intestinal mucus. It is unknown if the torque, the cell shape, and the flagellar number improve the motility of these pathogens. I aimed to decipher the role of these factors that might support the flagellar motility. Traditionally, bacterial motility has been investigated by observing colony morphologies on soft agar plates. However, this method reveals little information about bacterial behavior since the only result is the diameter of the colony. A combination of factors including bacterial growth, nutrient consumption, swimming behavior, mutation rate, and agar visco-elasticity have been shown to affect swimming colony results (Baym et al., 2016; Croze et al., 2011; Wolfe and Berg, 1989). However, the contributions of different factors are difficult to delineate, limiting the information which can be extracted. *In vivo* studies investigating the role of motility in pathogenesis were focused on endpoint results and provided limited insights into cell behavior.

For my thesis, I have use single cell tracking to investigate how bacteria cope with different environmental constraints. With this method, I can track thousands of cells and obtain more information such as the proportion of motile cells, swimming speed and frequency of changing direction. In addition, I had more control over environmental factors. By carefully analyzing the swimming trajectories, I learned more about the motility of *S. enterica*, and *V. cholerae* in different environments. Particularly, in chapter 2, I hypothesized that these enteric pathogens could penetrate through unprocessed intestinal mucus. Using single-cell tracking, I characterized the diffusion and swimming behaviors of these pathogens in mucus in comparison to other highly visco-elastic environments. In chapter 3, I hypothesized that the penetration of *V. cholerae* through mucus using flagellar motility is affected by pH. I will present how physical pH range in mucus affects *V. cholerae* swimming speed. In chapter 4, I hypothesized that the penetration of *V. cholerae* through mucus using flagellar motility is affected by its cell shape. To prove this hypothesis, I investigated the role and cost of curvature in *Vibrio cholerae*

motility in liquid and mucus. Lastly, in chapter 5, I hypothesized that the penetration of *S. enterica* through mucus using flagellar motility is affected by flagellar number. I used an inducible flagellar producing strain to investigate the role of flagellar number in *S. enterica* motility in liquid and mucus**.** In summary, this study provides a more mechanistic understanding on how bacteria overcome environmental constraints.

REFERENCES

REFERENCES

Adler, J., and Templeton, B. (1967). The effect of environmental conditions on the motility of Escherichia coli. J. Gen. Microbiol. *46*, 175–184.

Baym, M., Lieberman, T.D., Kelsic, E.D., Chait, R., Gross, R., Yelin, I., and Kishony, R. (2016). Spatiotemporal microbial evolution on antibiotic landscapes. Science (80-.). *353*, 1147–1151.

Beeby, M., Ribardo, D.A., Brennan, C.A., Ruby, E.G., Jensen, G.J., Hendrixson, D.R., and Hultgren, S.J. (2016). Diverse high-torque bacterial flagellar motors assemble wider stator rings using a conserved protein scaffold. Proc. Natl. Acad. Sci. U. S. A. *113*, 1–10.

Croze, O.A., Ferguson, G.P., Cates, M.E., and Poon, W.C.K. (2011). Migration of Chemotactic Bacteria in Soft Agar: Role of Gel Concentration. Biophys. J. *101*, 525–534.

Damton, N.C., Turner, L., Rojevsky, S., and Berg, H.C. (2010). Dynamics of bacterial swarming. Biophys. J. *98*, 2082–2090.

La Ferla, R., Maimone, G., Caruso, G., Azzaro, F., Azzaro, M., Decembrini, F., Cosenza, A., Leonardi, M., and Paranhos, R. (2014). Are prokaryotic cell shape and size suitable to ecosystem characterization? Hydrobiologia *726*, 65–80.

Ferrero, R.L., and Lee, A. (1988). Motility of Campylobacter jejuni in a viscous environment: comparison with conventional rod-shaped bacteria. J. Gen. Microbiol. *134*, 53–59.

Flemming, H.C., and Wuertz, S. (2019). Bacteria and archaea on Earth and their abundance in biofilms. Nat. Rev. Microbiol. *17*, 247–260.

Furter, M., Sellin, M.E., Hansson, G.C., and Hardt, W.D. (2019). Mucus Architecture and Near-Surface Swimming Affect Distinct Salmonella Typhimurium Infection Patterns along the Murine Intestinal Tract. Cell Rep. *27*, 2665-2678.e3.

Garrett, T.R., Bhakoo, M., and Zhang, Z. (2008). Bacterial adhesion and biofilms on surfaces. Prog. Nat. Sci. *18*, 1049–1056.

Guentzel, M.N., and Berry, L.J. (1975). Motility as a virulence factor for Vibrio cholerae. Infect. Immun. *11*, 890–897.

Hassani, M.A., Durán, P., and Hacquard, S. (2018). Microbial interactions within the plant holobiont. Microbiome *6*, 58.

Jones, B.D., Ghori, N., and Falkow, S. (1994). Salmonella typhlrnurium initiates murine infection by penetrating and destroying the specialized epithelial M cells of the peyer's patches. J. Exp. Med. *180*, 15–23.

Jones, C.J., Utada, A., Davis, K.R., Thongsomboon, W., Zamorano Sanchez, D., Banakar, V., Cegelski, L., Wong, G.C.L., and Yildiz, F.H. (2015). C-di-GMP Regulates Motile to Sessile Transition by Modulating

MshA Pili Biogenesis and Near-Surface Motility Behavior in Vibrio cholerae. PLOS Pathog. *11*, e1005068.

Lertsethtakarn, P., Ottemann, K.M., and Hendrixson, D.R. (2011). Motility and Chemotaxis in Campylobacter and Helicobacter. Annu. Rev. Microbiol. *65*, 389–410.

Licata, N.A.A., Mohari, B., Fuqua, C., and Setayeshgar, S. (2016). Diffusion of Bacterial Cells in Porous Media. Biophys. J. *110*, 247–257.

Maeda, K., Imae, Y., Shioi, J.I., and Oosawa, F. (1976). Effect of temperature on motility and chemotaxis of Escherichia coli. J. Bacteriol. *127*, 1039–1046.

Männik, J., Driessen, R., Galajda, P., Keymer, J.E., and Dekker, C. (2009). Bacterial growth and motility in sub-micron constrictions. Proc. Natl. Acad. Sci. U. S. A. *106*, 14861–14866.

Martínez, L.E., Hardcastle, J.M., Wang, J., Pincus, Z., Tsang, J., Hoover, T.R., Bansil, R., and Salama, N.R. (2016). Helicobacter pylori strains vary cell shape and flagellum number to maintain robust motility in viscous environments. Mol. Microbiol. *99*, 88–110.

McCarter, L.L. (2001). Polar flagellar motility of the Vibrionaceae. Microbiol. Mol. Biol. Rev. *65*, 445–462, table of contents.

McCarter, L.L. (2005). Multiple modes of motility: A second flagellar system in Escherichia coli. J. Bacteriol. *187*, 1207–1209.

Mitchell, J.G., and Kogure, K. (2006). Bacterial motility: Links to the environment and a driving force for microbial physics. FEMS Microbiol. Ecol. *55*, 3–16.

Moens, S., and Vanderleyden, J. (1996). Functions of bacterial flagella. Crit. Rev. Microbiol. *22*, 67–100.

Morooka, T., Umeda, A., and Amako, K. (1985). Motility as an intestinal colonization factor for Campylobacter jejuni. J. Gen. Microbiol. *131*, 1973–1980.

Najafi, J., Shaebani, M.R., John, T., Altegoer, F., Bange, G., and Wagner, C. (2018). Flagellar number governs bacterial spreading and transport efficiency. Sci. Adv. *4*, eaar6425.

Ni, B., Colin, R., Link, H., Endres, R.G., and Sourjik, V. (2020). Growth-rate dependent resource investment in bacterial motile behavior quantitatively follows potential benefit of chemotaxis. Proc. Natl. Acad. Sci. U. S. A. *117*, 595–601.

Purcell, E.M. (1977). Life at low Reynolds number. Am. J. Phys. *45*, 3–11.

Purcell, E.M. (1997). The efficiency of propulsion by a rotating flagellum. Proc. Natl. Acad. Sci. U. S. A. 94, 11307-11311

Rapp, B.E. (2017). Fluids: Prandtl Numbers. Microfluid. Model. Mech. Math. 243–263.

Richardson, K. (1991). Roles of motility and flagellar structure in pathogenicity of Vibrio cholerae: analysis of motility mutants in three animal models. Infect. Immun. *59*, 2727–2736.

Schmitt, C.K., Ikeda, J.S., Darnell, S.C., Watson, P.R., Bispham, J., Wallis, T.S., Weinstein, D.L., Metcalf,

E.S., and O'Brien, A.D. (2001). Absence of all components of the flagellar export and synthesis machinery differentially alters virulence of Salmonella enterica serovar typhimurium in models of typhoid fever, survival in macrophages, tissue culture invasiveness, and calf enterocolitis. Infect. Immun. *69*, 5619–5625.

Schneider, W.R., and Doetsch, R.N. (1974). Effect of viscosity on bacterial motility. J. Bacteriol.117, 696-701.

Schuech, R., Hoehfurtner, T., Smith, D.J., and Humphries, S. (2019). Motile curved bacteria are Pareto-optimal. Proc. Natl. Acad. Sci. U. S. A. *116*, 14440–14447.

Soutourina, O.A., Krin, E., Laurent-Winter, C., Hommais, F., Danchin, A., and Bertin, P.N. (2002). Regulation of bacterial motility in response to low pH in Escherichia coli: The role of H-NS protein. Microbiology.148, 1543-1551.

Stocker, R., and Seymour, J.R. (2012). Ecology and Physics of Bacterial Chemotaxis in the Ocean. Microbiol. Mol. Biol. Rev. *76*, 792–812.

Takabe, K., Nakamura, S., Ashihara, M., and Kudo, S. (2013). Effect of osmolarity and viscosity on the motility of pathogenic and saprophytic Leptospira. Microbiol. Immunol.57, 236-239.

Takekawa, N., Imada, K., and Homma, M. (2020). Structure and Energy-Conversion Mechanism of the Bacterial Na+-Driven Flagellar Motor. Trends Microbiol. *28*, 719–731.

Turnbull, G.A., Morgan, J.A.W., Whipps, J.M., and Saunders, J.R. (2001). The role of bacterial motility in the survival and spread of Pseudomonas fluorescens in soil and in the attachment and colonisation of wheat roots. FEMS Microbiol. Ecol. *36*, 21–31.

Wei, X., and Bauer, W.D. (1998). Starvation-induced changes in motility, chemotaxis, and flagellation of Rhizobium meliloti. Appl. Environ. Microbiol.64, 1708-1714.

Whitman, W.B., Coleman, D.C., and Wiebe, W.J. (1998). Prokaryotes: The unseen majority. Proc. Natl. Acad. Sci. U. S. A. *95*, 6578–6583.

Wolfe, A.J., and Berg, H.C. (1989). Migration of bacteria in semisolid agar. Proc. Natl. Acad. Sci. *86*, 6973–6977.

Yao, Z., Davis, R.M., Kishony, R., Kahne, D., and Ruiz, N. (2012). Regulation of cell size in response to nutrient availability by fatty acid biosynthesis in Escherichia coli. Proc. Natl. Acad. Sci. U. S. A.109, E2561-8.

Chapter 2: MUCUS RESTRICTS *SALMONELLA ENTERICA* AND *VIBRIO CHOLERAE* MOTILITY

INTRODUCTION

Our digestive tract is protected by a mucus layer. Mucus is a semipermeable mesh allowing nutrients or small components to diffuse through while slowing the movement of larger particles such as bacteria and viruses. Mucus is 90 - 98% water and 2-10% mucin, DNA, lipid, peptides, and salts (Allen et al., 2008). Mucin, the major protein of mucus, is a glycoprotein with a peptide core and carbohydrate-side chains. Mucin polymerizes by creating di-sulfide bonds between cysteine residues at a concentration between 14 mg/ml and 30 mg/ml (Bromberg and Barr, 2000). In addition, the interactions between hydrophobic domains and entanglement between mucin strands gives mucus a gel-like property (Leal et al., 2017). Pore sizes in mucus range from 200 to 500 nm. The intestinal mucus has two layers, a dense 15-30 µm thick inner layer and a looser 100-400 µm thick outer layer (Atuma et al., 2001; Gustafsson et al., 2012). The thickness of mucus is therefore about 50 to 200 times the length of a typical bacterium. Thus, mucus is a physical barrier for bacteria.

Mucus is an environmental constraint for bacterial motility. Mucus has high visco-elasticity. The visco-elasticity of mucus varies between individuals and along the length of the gastro-intestinal tract (Bajka et al., 2015; Matsui et al., 2006; Schuster et al., 2013). The visco-elasticity of mucus changes depending on the temperature and pH, and concentrations of mucin, DNA, and lipids (Lai et al., 2009). Information on how the visco-elasticity of mucus limits bacterial diffusion is scarce. Most of current studies on motility are based on tracking bacteria in commercial mucin solution, which is not a gel. Therefore, the role of unprocessed intestinal mucus in limiting the motility of bacteria should be further characterized.

The mucus acts as a barrier between the epithelial cells and the microbiota. This trait is preserved throughout all vertebrates (Leung et al., 2018). However, some enteric pathogens, such as *S. enterica* and *V. cholerae,* can navigate through this mucus to reach the epithelial cells. In fact, it was

shown that *S. enterica* is trapped by the inner mucus layer. Researchers demonstrated in a mouse model that *S. enterica* penetrates to epithelial cells by swimming through the fluid streams in the mucus layer. This finding agrees with genetics results which suggests the role of swimming motility in *Salmonella* infection. Flagellar motility was also shown as an important virulence factor in *V. cholerae* infection (Guentzel and Berry, 1975; Jones et al., 1994; Richardson, 1991; Schmitt et al., 2001). However, how the swimming behavior helps it to compromise mucus requires more studies.

My research aims to answer the question if *S. enterica* and *V. cholerae* are able to swim through mucus. In this research, I used single cell tracking to evaluate the efficiency of mucus in preventing *S. enterica* and *V. cholerae* diffusion and characterized the motility of these bacteria in mucus by analyzing the swimming parameters, such as diffusion coefficients, and proportion of free-swimming cells. In addition, I also investigated the visco-elasticity of mucus in comparison to other visco-elastic materials.

METHODS

Bacterial strains

The strains used in this study were *S. enterica* LT2, and *V. cholerae* El Tor C6706str2. *S. enterica* and *V. cholerae* were fluorescently labelled with green fluorescent protein expressed from a constitutive cytochrome c promoter on a p15a plasmid derivative, pCMW5 (gift from Dr. Christopher Waters).

Growth conditions

Bacteria were grown in conditions promoting their swimming motility. In brief, *S. enterica* was grown in Vogel-Bonner medium supplemented with 2% (w/v) yeast extract (VB2Y) (Koirala et al., 2014) until it reached OD_{600nm} ~1.0. *V. cholerae* was grown in M9 minimal salts (52 mM Na_2HPO_4, 18 mM K_2HPO_4, 18.69 mM NH_4Cl, 2 mM $MgSO_4$) supplemented with 10 µM $FeSO_4$, 20 µM $C_6H_9Na_3O_9$ and 36.4 mM Sodium pyruvate (M9P) until it reached early stationary phase (1.9×10^9 c.f.u./mL). *S. enterica* and

V. cholerae were started at the same OD, 0.01. All cultures were grown at 37°C, and liquid cultures were shaken at 200RPM. Kanamycin was added to 50 μg/ml when needed.

Visco-elastic material preparation

1% methylcellulose (MC) (4000cP, M352-500, Fisher Scientific) was prepared at least 16 hours and stored at 4°C before tracking so that it was dissolved completely. Agarose (LMA) was made by heating 0.3% (w/v) low-melting agarose (BP165-25, Fisher Scientific) to 70° C. MC and LMA were made in VB and M9 minimal salts buffer, accordingly. To make MCLMA, 2% MC and 0.6% LMA are first prepared separately. Later, half the volume of each material is incubated at 37°C before being mixed. Porcine gastric mucin was made at 30 mg/ml concentration in buffer. The solution was left at 4°C for 48 hours to ensure a complete hydration. All materials were brought to 37° C before being used for tracking.

Raw and clarified pig intestinal mucus preparation

Pig intestines were obtained from pigs slaughtered at the Michigan State University meat laboratory with approval from the United States Department of Agriculture. Crude mucus was freshly collected by scraping the small intestines. Mucus was frozen in liquid nitrogen, then stored at -80° C. The mucus was clarified by repeatedly washing with 6M guanidine hydrochloride to solubilize fat and proteins while preserving di-sulfide bonds between mucin monomers (protocol by Dr. Eric Martens). Centrifugation at high speed was applied to separate the mucin gel from soluble particles. Finally, clarified mucus was washed and stored in phosphate buffer saline (PBS). The final product was clear and gel-like.

Raw mucus and clarified mucus were hydrated in 1ml of VB or M9 minimal salts dependent on the bacterium tested. Mucus was incubated at 37° C for ~1 hour. Before tracking, excess liquid was removed by centrifugation at 21,000 g for 40 s.

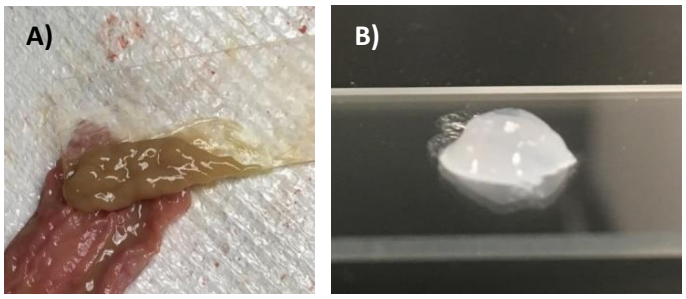

Figure 2.1: A) Raw and B) clarified pig intestinal mucus

Single-cell tracking

Bacterial cells were tracked in liquid following a previously described protocol (Dufour et al., 2016). *S. enterica* grown in VB2Y was washed and tracked in VB supplemented with 0.5% glucose (VBG). *V. cholerae* were tracked in M9P at pH 8.0. For optimal tracking, bacterial cells were diluted to 1.9 x 10^7 cells/mL in VBG or M9P. Cells were incubated at 37° C for 15 minutes before tracking to allow for adaptation of the chemotaxis response. Polyvinylpyrrolidone (PVP, BP431-100, Fisher Scientific) was added at 0.05% w/v to the samples to prevent attachment on the glass slide. 6 µl of each sample dropped on a glass slide and trapped under a 22 x 22 mm, #1.5 coverslip sealed with wax and paraffin to create a thin water film (10±2 µm) for video microscopy. For tracking in mucus, MC, MCLMA, and LMA, a 130 µm spacer was added between the slide and the coverslip and fluorescently labelled cells were used. LMA slides were kept at room temperature for 30 minutes to allow solidification. The samples were kept at 37°C during tracking. Images of swimming cells were recorded using a sCMOS camera (Andor Zyla 4.2, Oxford Instruments) at 20 frames per second using a 40X objective (Plan Fluor 40x, Nikon Instruments, Inc.) mounted on an inverted microscope (Eclipse Ti-E, Nikon Instruments, Inc.). Cell were illuminated using phase contrast in liquid or epifluorescence in mucus and agarose. Images were analyzed to detect and localize cells using custom scripts (Dufour et al., 2016) and cell trajectories were reconstructed using the µ-track package (Jaqaman et al., 2008). The analysis and plots of the cell

trajectory statistics were done in MATLAB (The Mathworks, Inc.) as previously described (Dufour et al., 2016).

Passive micro-rheology of materials used for tracking

The viscoelasticity of mucus and agarose were measured by tracking the passive diffusion of 1 μm beads (F8814, ThermoFisher Scientific). To prevent electrostatic or hydrophobic interactions between the beads and the gels, beads were coated with polyethylene glycol (PEG MW 2,000Da). Coating was done by crosslinking carboxyl groups on the surface of the beads with diamine-PEG following the previously described protocol (Lai et al., 2007). Beads 0.5% w/v and Triton (X-100, Sigma-Aldrich) 0.01% w/v were added to samples and mixed gently. Epifluorescence signals from the beads were recorded using a sCMOS camera (Andor Zyla 4.2, Oxford Instruments) at 100 frames per second using a 40X objective (Plan Fluor 40x, Nikon Instruments, Inc.). Images were analyzed to detect and localize beads using custom scripts and trajectories were reconstructed using the μ-track package (Jaqaman et al., 2008). Diffusion coefficients were calculated to characterize the physical properties of each materials.

RESULTS

Mucus is a hydrogel.

To understand the role of mucus in inhibiting the motion of bacteria, I tracked 1 μm beads in mucus and compared its rheology to other materials. The motion of the beads reflects the properties of each material at microscale. By tracking the diffusion of beads in each environment, I can understand what obstacles are present to bacteria when navigating through each material. I used 1.0% w/v methyl cellulose (MC) to create a highly viscous environment and 0.3% w/v low-melting agarose (LMA) to create a gel-like environment. I mixed MC and LMA to form a high viscous-high elastic material (MCLMA). In addition, I also compared raw pig intestinal mucus to clarified mucus and commercial mucin (PGM).

After analyzing videos to obtain the bead trajectories, I calculated the diffusion coefficients from the x and y coordinates of the beads over time. The diffusion coefficients show how fast a particle spreads in each environment. As expected, all viscous and elastic materials inhibit the diffusion of the beads significantly. Buffer, MC and PGM are homogenous materials with most of the beads diffuse at the same coefficients. LMA, MCLMA, raw, and clarified mucus shown as heterogenous environments in which the beads show highly varied diffusion coefficients. Beads have similar diffusion coefficients in both raw and clarified mucus. Overall, our results suggest that PGM is similar to a viscous material like MC. On the other hand, mucus is similar to a gel-like material like LMA.

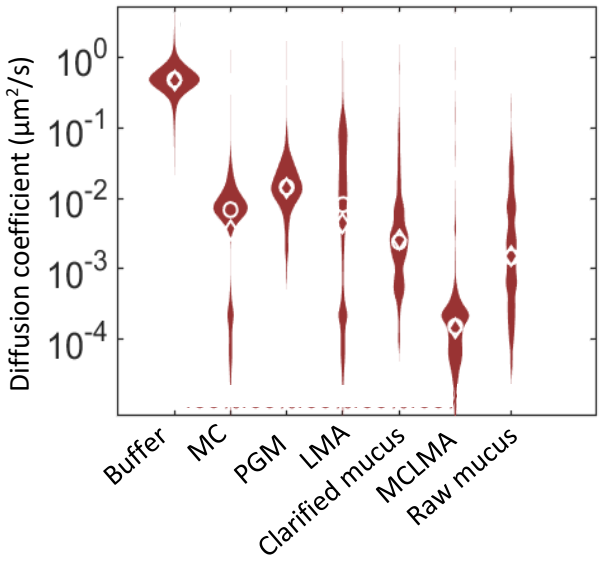

Figure 2.2: The physical properties of materials used in this study. The plot shows the distribution of diffusion coefficients of 1 μm beads in different environments. Data is calculated from the bead trajectories collected from at least three independent replicates (~ 60 beads for each replicate with 35 to 239 minutes of cumulative time). Diamonds: means. Circles: median.

Single cell tracking analysis

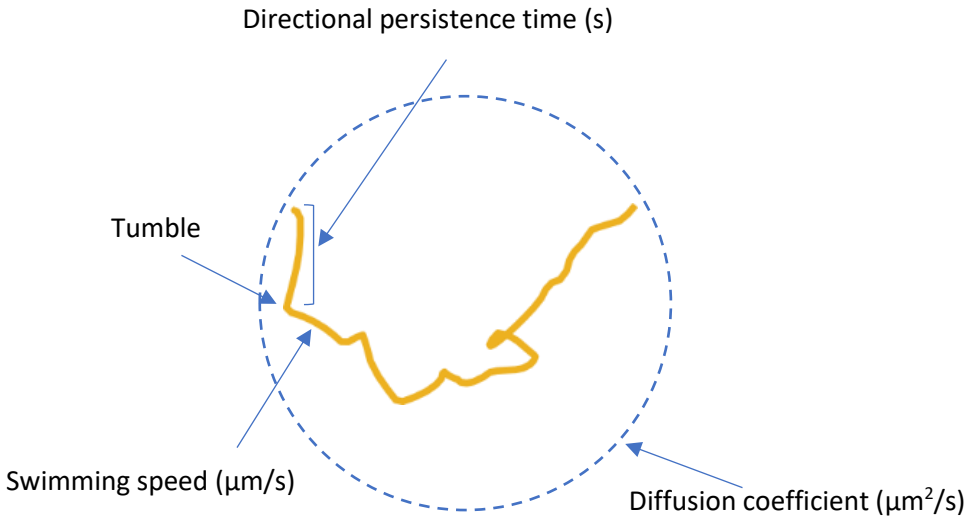

Figure 2.3: Bacterial trajectories and parameters for analysis.

I took videos of bacteria swimming at 40X for 60 seconds. Typically, bacteria swim with stages of running forward and changing direction. Several parameters were calculated from the trajectories to characterize these two stages of swimming behavior.

Swimming speed (μm/s) is the average speed between frames. Swimming speed is affected by many factors, such as bacterial flagellar motor torque, the nutrient condition, and the viscosity of the environment.

Directional persistence time (s) is the autocorrelation in time of the direction of the velocity vectors (regardless of speed). It represents the average time trajectories maintain a specific direction. Directional persistence time is affected by many factors, such as the changing direction frequency of the bacterium and the viscosity and elasticity of the environments.

Diffusion coefficient ($\mu m^2/s$) shows how fast a cell spreads in an environment in one second. Diffusion coefficient is a function of swimming speed and directional persistence time.

Mean-squared displacement (μm) (MSD) shows the expansion of a trajectory as a function of time. If a cell stays in the same position or is trapped in a pore, its MSD remains the same over time. MSD is dependent on swimming speed and directional persistence time.

Speed variance is the variance of the instantaneous speed from a trajectory. The instantaneous speed is calculated between each frame. Speed variance is affected by changing direction frequency and the visco-elasticity of the environment.

Tumble bias is the proportion of time a cell spent tumbling. Tumble bias has an opposite relationship with directional persistence time. Tumble bias changes with bacterium swimming behavior and nutrient condition. In addition, tumble bias is very sensitive to the environment. It cannot be differentiated from changing direction because of obstacles in gels.

Raw mucus is more effective than commercial porcine mucin at inhibiting *S. enterica* and *V. cholerae* movement

To test the effectiveness of mucus in inhibiting bacterial motility, I compared *S. enterica* and *V. cholerae* in mucus with different visco-elastic materials. I calculated swimming parameters from thousands of cells in each environment to characterize the swimming behavior of bacteria. In this research, I want to see how the visco-elastic environments inhibit the motility in comparison to liquid, where bacteria can swim freely.

S. enterica is a rod shape, peritrichous bacterium. Each of its flagellum is powered by a proton-driven motor. In VB supplemented with 0.5% glucose (liquid), *S. enterica* swims at an average speed of ~32.5 μm/s (Fig. 2.5B). *S. enterica* shows near-surface motility with circular trajectories when swimming at near the glass surface (Fig. 2.4A). In high visco-elastic materials, *S. enterica* show short trajectories and small diffusion coefficients in LMA and mucus (Fig. 2.5CEF) but not in MC and PGM (Fig. 2.5BD). Overall, *S. enterica* has decreased diffusion and swimming speed in all conditions comparing to liquid. *S.*

enterica is especially trapped and shows high speed variance in LMA and mucus (Fig. 2.5D). These results agree with the bead tracking where it shows that gels are heterogenous. Interestingly, the raw mucus can inhibit motile cells four times more effective than PGM (mean diffusion coefficients 2.8 vs 11.3 $\mu m^2/s$) (p-value < 10^{-4}). On the other hand, *S. enterica* does not diffuse in clarified mucus as well as in raw mucus even though the bead tracking results suggested that they have similar heterogeneity (Fig. 2.2). This result suggests that the soluble components in mucus might promote the motility of *S. enterica*.

I also tested the motility of *V. cholerae* in raw mucus. *V. cholerae* has a single polar flagellum powered by a sodium-driven motor. Except for when swimming in liquid, *V. cholerae* trajectories in high visco-elastic are similar to *S. enterica* trajectories, suggesting that their motility is strongly affected by the environment. *V. cholerae* has a high swimming speed in buffer of up to 150 µm/s. The speeds decrease to ~85.0% in MC (112.0 vs 16.4 µm/s) and ~95.0% in LMA (112.0 vs 5.2 µm/s) (Fig. 2.7B). Most *V. cholerae* cells were not motile in LMA and clarified mucus (Fig. 2.7A). The low number of motile cells in these materials may explain for the high-speed variation (Fig. 2.7D). The addition of viscous factor (MC) seems to improve the motility of *V. cholerae* in LMA with more motile cells in MCLMA (p-value < 10^{-4}) (Fig. 2.7A). Additionally, I found that the diffusion of *V. cholerae* in clarified mucus is less than the diffusion in raw mucus.

The heterogeneity of the environments seems proportional to speed variation. In particular, the speed variation is highest in LMA, the most heterogenous material among the gels tested (Fig. 2.2).

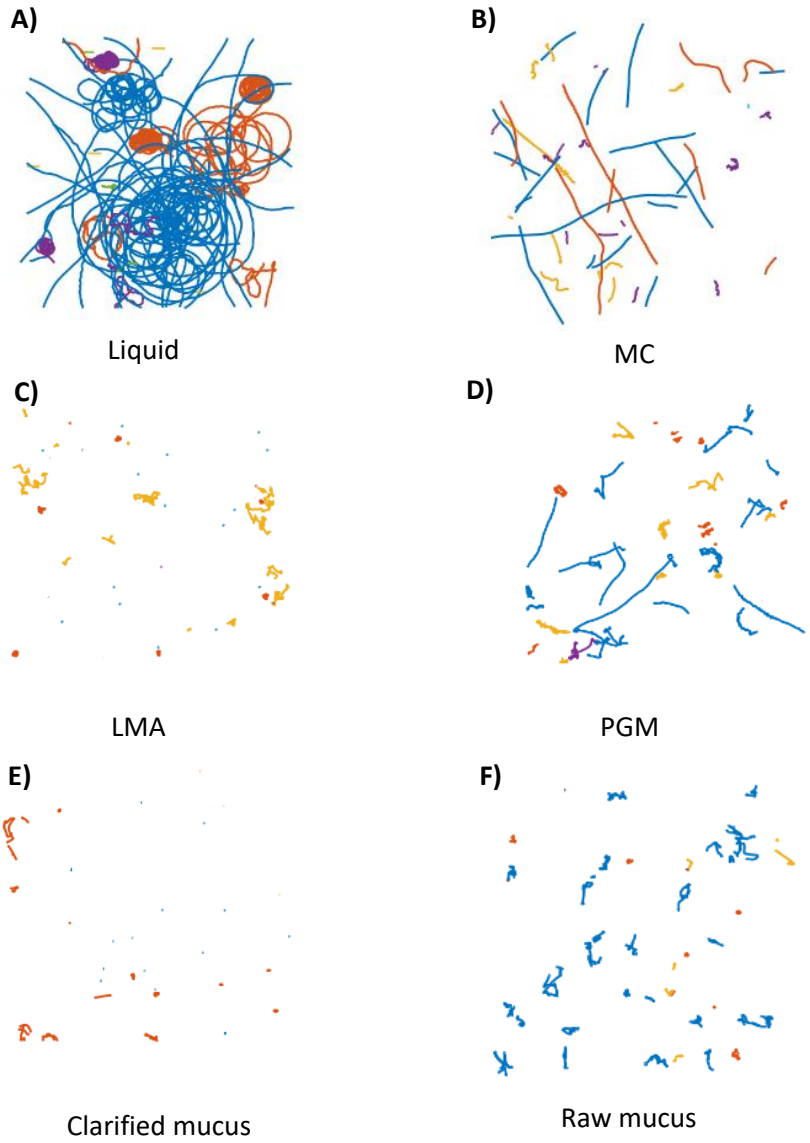

Figure 2.4: *S. enterica* trajectories in different visco-elastic conditions, A) Liquid, B) 1.0% w/v methyl cellulose, C) 0.3% w/v LMA, D) porcine gastric mucin, E) clarified mucus, and F) raw mucus. *S. enterica* trajectories are shown in different colors.

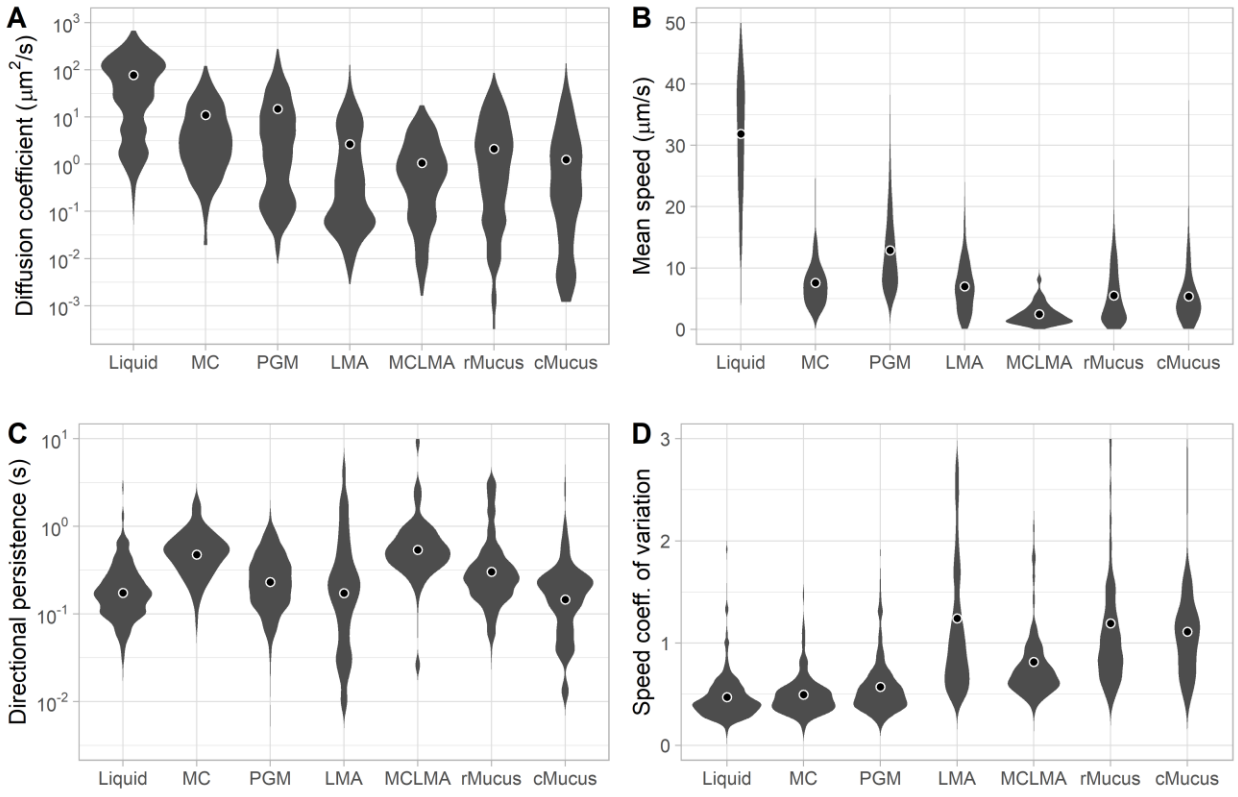

Figure 2.5: *S. enterica* motility in different visco-elastic environments. Distributions of A) diffusion coefficient, B) swimming speed, C) directional persistence time and D) speed variance extracted from *S. enterica* trajectories when swimming in different visco-elastic conditions. The circle represents the mean. Data is calculated from between 200 to 6,000 trajectories collected from at least three independent replicates for each condition.

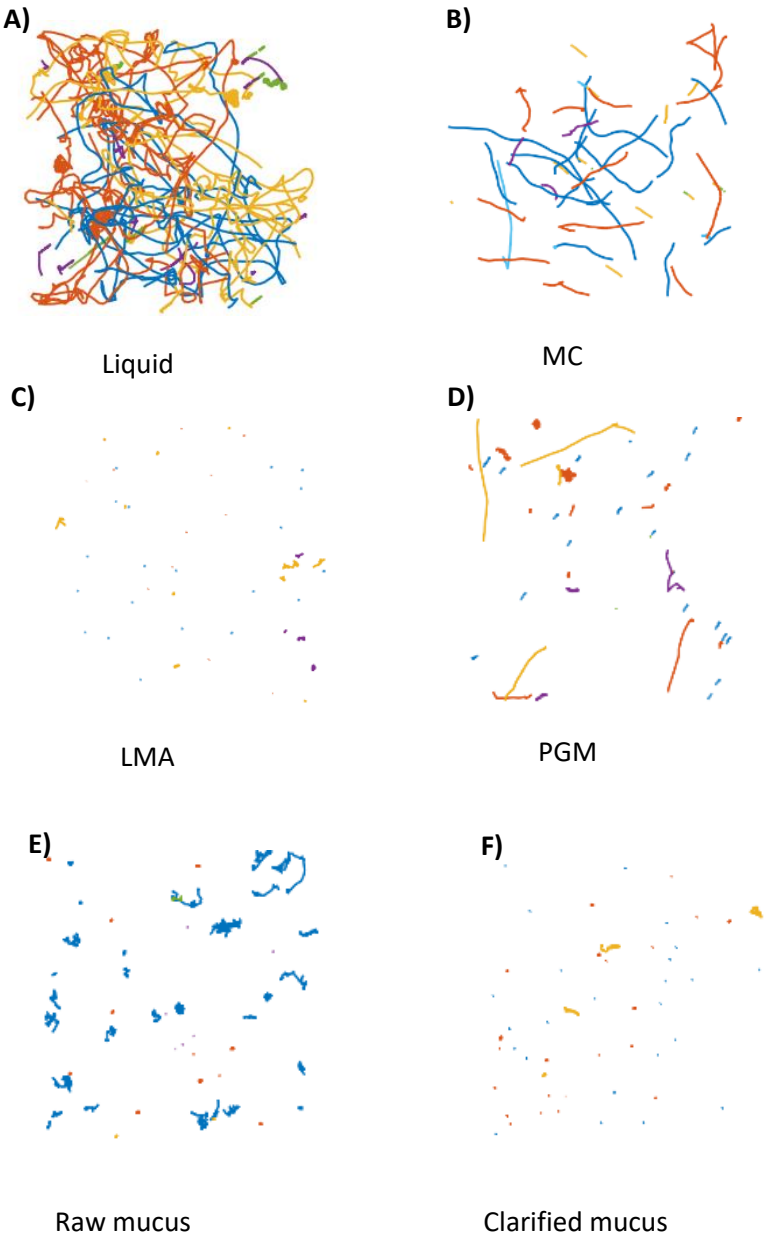

Figure 2.6: *V. cholerae* trajectories in different visco-elastic conditions, A) Liquid, B) 1.0% w/v methyl cellulose, C) 0.3% w/v LMA, D) porcine gastric mucin, E) raw mucus, and F) clarified mucus. *V. cholerae* trajectories are shown in different colors.

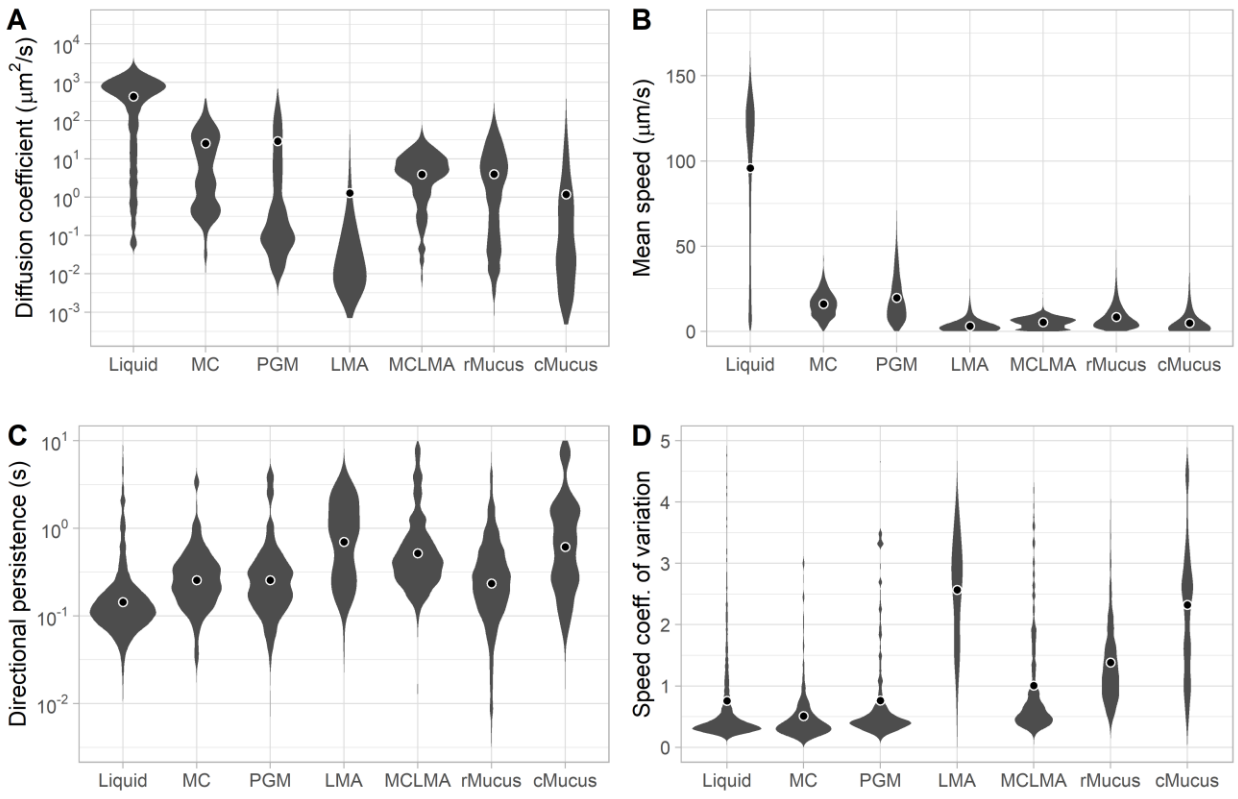

Figure 2.7: *V. cholerae* motility in different visco-elastic environments. Distributions of A) diffusion coefficient, B) swimming speed, C) directional persistence time and D) speed variance extracted from V. cholerae trajectories when swimming in different visco-elastic conditions. The circle represents the mean. Data is calculated from between 200 to 25,000 trajectories collected from at least three independent replicates for each condition.

DISCUSSION

In this chapter, I evaluated the role of raw mucus in restricting the motility of bacteria. I used mucus collected from pig intestine since it is more closely resembles to human mucus among mucus sampled from animal models (Varum et al., 2012). Single-particle tracking revealed that mucus can trap the diffusion of 1 µm beads which have similar size to bacterial cells. Moreover, mucus is more closely resembles LMA, a hydrogel, than MC, a highly viscous material. Since raw mucus is a nutrient-rich

environment, I clarified it to remove the effects from the soluble components on bacterial motility behavior. The clarified mucus has similar properties to raw mucus. The use of clarified mucus may be promising since it can help determine the role of each mucus component in motility.

I reported here that mucus immobilizes ~80.0% free-swimming bacteria. Although some bacterial cells still can move in raw mucus, I expect that bacteria face more challenges when navigating though mucus in the gut. One of the challenges is the growing rate of mucus (240 µm/hour) that can push bacteria away from epithelial layer (Gustafsson et al., 2012). In addition, immune factors such as antibody and antimicrobial peptides can inhibit the growth and penetration of bacteria. Nevertheless, I also found that *S. enterica* and *V. cholerae* can navigate in raw mucus better than in clarified mucus. Clarified mucus can inhibit up to ~98.0% of free-swimming *S. enterica*. This finding suggests that soluble components in mucus might support the motility of bacteria. First, raw mucus can be a rich nutrient source and promotes the flagellar rotation of *S. enterica* and *V. cholerae*. In fact, glycan from mucin was found as a carbon source for the microbiota and pathogens (Schroeder, 2019; Stecher et al., 2008). Second, the soluble component of mucus may become a spacer between mucin strands and enlarge the mucin pore. These soluble components while limiting the vibration of the beads, allow bacteria with strong motor torque to move between pores.

PGM is not as effective as mucus in inhibiting the motility of bacteria. PGM has been widely used as a replacement for mucus to investigate motility (Martínez et al., 2016)**.** In this study, I found that PGM is more similar to MC than pig mucus. Therefore, *S. enterica* and *V. cholerae* can easily spread in PGM with long trajectories and high diffusion. On the other hand, gel materials like agarose, and mucus are heterogenous. They can limit the movement of bacteria in pockets of liquid, showing by short track and low diffusion. Therefore, the application of PGM in research about bacterial motility behavior should be limited.

I also investigated strategies to diffuse in mucus. Comparing between the two bacteria, *V. cholerae* seems to navigate through mucus better than *S. enterica* with higher diffusion coefficients. Although *V. cholerae* has only one flagellum, it has a stronger torque which is advantageous in mucus (Beeby et al., 2016). Moreover, *V. cholerae* has a higher speed variance, suggesting that it changes direction more often than *S. enterica*. It was reported earlier that tumbling is beneficial to bacteria to escape the porous environments (Licata et al., 2016). Future studies should investigate the role of strong torque in bacterial movement through mucus.

In summary, mucus is efficient in limiting the diffusion of *S. enterica* and *V. cholerae*. Nevertheless, some bacteria can navigate through mucus with high speed. Understanding how these population navigate the mucus is necessary to prevent their spreading in the gut. I will discuss about the role of several factors, including motor torque, cell shape, and flagellar number in promoting *V. cholerae* and *S. enterica* motility in mucus in the following chapters.

REFERENCES

REFERENCES

Allen, A., Hutton, D.A., Pearson, J.P., and Sellers, L.A. (2008). Mucus Glycoprotein Structure, Gel Formation and Gastrointestinal Mucus Function. In Mucus and Mucosa, pp. 137–156.

Atuma, C., Strugala, V., Allen, A., and Holm, L. (2001). The adherent gastrointestinal mucus gel layer: thickness and physical state in vivo. Am. J. Physiol. Liver Physiol. *280*, G922–G929.

Bajka, B.H., Rigby, N.M., Cross, K.L., Macierzanka, A., and Mackie, A.R. (2015). The influence of small intestinal mucus structure on particle transport ex vivo. Colloids Surfaces B Biointerfaces *135*, 73–80.

Beeby, M., Ribardo, D.A., Brennan, C.A., Ruby, E.G., Jensen, G.J., Hendrixson, D.R., and Hultgren, S.J. (2016). Diverse high-torque bacterial flagellar motors assemble wider stator rings using a conserved protein scaffold. Proc. Natl. Acad. Sci. U. S. A. *113*, 1–10.

Bromberg, L.E., and Barr, D.P. (2000). Self-Association of Mucin. Biomacromolecules *1*, 325–334.

Dufour, Y.S., Gillet, S., Frankel, N.W., Weibel, D.B., and Emonet, T. (2016). Direct Correlation between Motile Behavior and Protein Abundance in Single Cells. PLoS Comput. Biol. *12*, e1005149.

Guentzel, M.N., and Berry, L.J. (1975). Motility as a virulence factor for Vibrio cholerae. Infect. Immun. *11*, 890–897.

Gustafsson, J.K., Ermund, A., Johansson, M.E.V. V., Schütte, A., Hansson, G.C., and Sjövall, H. (2012). An ex vivo method for studying mucus formation, properties, and thickness in human colonic biopsies and mouse small and large intestinal explants. Am. J. Physiol. Liver Physiol. *302*, G430–G438.

Jaqaman, K., Loerke, D., Mettlen, M., Kuwata, H., Grinstein, S., Schmid, S.L., and Danuser, G. (2008). Robust single-particle tracking in live-cell time-lapse sequences. Nat. Methods. *5*, 695-702.

Jones, B.D., Ghori, N., and Falkow, S. (1994). Salmonella typhlrnurium initiates murine infection by penetrating and destroying the specialized epithelial M cells of the peyer's patches. J. Exp. Med. *180*, 15–23.

Koirala, S., Mears, P., Sim, M., Golding, I., Chemla, Y.R., Aldridge, P.D., and Rao, C. V. (2014). A nutrient-tunable bistable switch controls motility in Salmonella enterica serovar Typhimurium. MBio *5*, 01611–01614.

Lai, S.K., O'Hanlon, D.E., Harrold, S., Man, S.T., Wang, Y.-Y., Cone, R., and Hanes, J. (2007). Rapid transport of large polymeric nanoparticles in fresh undiluted human mucus. Proc. Natl. Acad. Sci. *104*, 1482-1487.

Lai, S.K., Wang, Y.-Y.Y., Wirtz, D., and Hanes, J. (2009). Micro- and macrorheology of mucus. Adv. Drug Deliv. Rev. *61*, 86–100.

Leal, J., Smyth, H.D.C., and Ghosh, D. (2017). Physicochemical properties of mucus and their impact on transmucosal drug delivery. Int. J. Pharm. *532*, 555–572.

Leung, J.M., Graham, A.L., and Knowles, S.C.L. (2018). Parasite-microbiota interactions with the vertebrate gut: Synthesis through an ecological lens. Front. Microbiol. *9*, 9:843.

Licata, N.A.A., Mohari, B., Fuqua, C., and Setayeshgar, S. (2016). Diffusion of Bacterial Cells in Porous Media. Biophys. J. *110*, 247–257.

Martínez, L.E., Hardcastle, J.M., Wang, J., Pincus, Z., Tsang, J., Hoover, T.R., Bansil, R., and Salama, N.R. (2016). Helicobacter pylori strains vary cell shape and flagellum number to maintain robust motility in viscous environments. Mol. Microbiol. *99*, 88–110.

Matsui, H., Wagner, V.E., Hill, D.B., Schwab, U.E., Rogers, T.D., Button, B., Taylor, R.M., Superfine, R., Rubinstein, M., Iglewski, B.H., et al. (2006). A physical linkage between cystic fibrosis airway surface dehydration and Pseudomonas aeruginosa biofilms. Proc. Natl. Acad. Sci. U. S. A. *103*, 18131–18136.

Richardson, K. (1991). Roles of motility and flagellar structure in pathogenicity of Vibrio cholerae: analysis of motility mutants in three animal models. Infect. Immun. *59*, 2727–2736.

Schmitt, C.K., Ikeda, J.S., Darnell, S.C., Watson, P.R., Bispham, J., Wallis, T.S., Weinstein, D.L., Metcalf, E.S., and O'Brien, A.D. (2001). Absence of all components of the flagellar export and synthesis machinery differentially alters virulence of Salmonella enterica serovar typhimurium in models of typhoid fever, survival in macrophages, tissue culture invasiveness, and calf enterocolitis. Infect. Immun. *69*, 5619–5625.

Schroeder, B.O. (2019). Fight them or feed them: How the intestinal mucus layer manages the gut microbiota. Gastroenterol. Rep. *7*, 3-12.

Schuster, B.S., Suk, J.S., Woodworth, G.F., and Hanes, J. (2013). Nanoparticle diffusion in respiratory mucus from humans without lung disease. Biomaterials *34*, 3439–3446.

Stecher, B., Barthel, M., Schlumberger, M.C., Haberli, L., Rabsch, W., Kremer, M., and Hardt, W.D. (2008). Motility allows S. Typhimurium to benefit from the mucosal defence. Cell. Microbiol. *10*, 1166–1180.

Varum, F.J.O., Veiga, F., Sousa, J.S., and Basit, A.W. (2012). Mucus thickness in the gastrointestinal tract of laboratory animals. J. Pharm. Pharmacol. *64*, 218–227.

Chapter 3: ALKALINE PH INCREASES SWIMMING SPEED AND FACILITATES MUCUS PENETRATION FOR *VIBRIO CHOLERAE*

Work presented in the chapter has been submitted to Journal of Bacteriology as Nguyen T. Q. Nhu, John S. Lee, Helen J. Wang, and Yann S. Dufour. Alkaline pH increases swimming speed and facilitates mucus penetration for *Vibrio cholerae.*

INTRODUCTION

Vibrio cholerae is the cause of an ongoing cholera pandemic with up to 4 million cases per year from regions of the world that do not have access to potable water (Ali et al., 2015). Without proper rehydration and antibiotic treatments, severe diarrhea triggered by the cholera toxin can be fatal (Sack et al., 2004). Preventative measures and vaccines against *V. cholerae* have had partial success (Bi et al., 2017; Taylor et al., 2015), but cholera outbreaks are still a significant burden for populations living in developing regions or after natural disaster, such as Bangladesh and Haiti (Ali et al., 2015).

V. cholerae is represented by more than 200 serogroups that are endemic to sea and brackish waters and often found associated with copepods (Chatterjee and Chaudhuri, 2003; Huq et al., 1983). However, only the O1 and 0139 serogroups have been associated with cholera, the diarrheal disease in humans (Calia et al., 1994). Within the O1 serogroup, the Classical biotype dominated the first 6 recorded cholera pandemics. The ongoing 7th pandemic is dominated by the El Tor biotype, which has rapidly displaced the Classical biotype in the environment (Baine et al., 1974; Hu et al., 2016). Although similar, the two biotypes have differences in their genetic makeups, signaling dynamics, and behaviors (Beyhan et al., 2006; Hammer and Bassler, 2009; Son et al., 2011). The relative importance of these unique traits has not been fully elucidated yet.

V. cholerae colonize the mucus of the small intestine without invading epithelial cells. When reaching the intestinal crypts, *V. cholerae* secreted the cholera toxin, which targets epithelial cells to activate the chlorine channels proteins and consequently trigger a massive efflux of chlorine ions and water into the intestinal lumen. Many aspects of *V. cholerae* physiology and the regulation virulence

factor expression have been investigated to recapitulate the dynamics of infection after ingestion (Lee et al., 1999, 2001a; Schild et al., 2007), such as pili production (Krebs and Taylor, 2011), type 6 secretion system (Miyata et al., 2010), quorum sensing (Zhu et al., 2002), biofilm formation (Zhu and Mekalanos, 2003), and flagellar motility (Richardson, 1991). While these different behaviors have been shown to contribute to *V. cholerae* success during infection, the specific sequence of events and site-specific activities in the intestine are still under investigation.

Flagellar motility is essential for *V. cholerae* infection. Studies of transcription profiles and screens of mutant libraries during the infection of animal models and humans identified genes involved in chemotaxis and motility functions (Lombardo et al., 2007). Non-motile *V. cholerae* mutants have reduced virulence and intestinal colonization (Guentzel and Berry, 1975; Lee et al., 2002; Silva and Benitez, 2016). In addition, previous work supports that protective immunity is mostly provided by mucosal antibodies that inhibit *V. cholerae* motility through bivalent binding of the O-antigen (Shen et al., 2017). Motility may not be required for survival and growth in the intestine since non-motile mutants do not appear to suffer a large competitive disadvantage when inoculated with motile *V. cholerae* (Millet et al., 2014). However, flagellar motility is likely necessary to penetrate the mucus layer protecting the intestinal tissue and reach epithelial cells to deliver the cholera toxin.

Mucus is a complex hydrogel made of mucins (2-10% w/v), lipids, and DNA (Allen et al., 2008) and is difficult for motile bacteria to penetrate. Mucins are large and highly glycosylated proteins cross-linked by disulfide bonds reinforced by hydrophobic interactions to form a tight mesh. The intestinal mucus layer is continuously renewed by secretion of highly O-glycosylated MUC2 mucin by goblet cells (240 ± 60 µm per hour) (Gustafsson et al., 2012). Consequently, mucus forms a selective diffusion barrier undergoing continuous regeneration, which rate can increase in response to threat such as the cholera toxin (Leitch, 1988). Histological analyses revealed that the inner part of the mucus layer is mostly free of bacteria (Johansson et al., 2008). In the small intestine, the mucus layer is thinner in the

proximal part (~200 μm) than the distal part (~500 μm) (Atuma et al., 2001). These observations raise the questions of how *V. cholerae* can penetrate mucus and why it preferably infects the distal small intestine where the mucosa is thicker.

Few studies have directly observed the motile behavior of individual bacteria in mucus to characterize the strategy used to compromise the protective layer. *Helicobacter pylori*, which colonizes the thick mucus layer of the stomach, facilitates flagellar motility through mucus by enzymatically increasing the local pH to liquify the mucus gel structure (Bansil et al., 2005, 2013). It is also believed that the helical cell shape of both *H. pylori* and *Campylobacter jejuni*, which colonizes the thick mucus layer of the cecum, facilitates mucus penetration by allowing the body to push against the mucin matrix like a corkscrew (Lauga, 2016; Lertsethtakarn et al., 2011). Recent work demonstrated that the peritrichous rod-shaped bacteria, *Escherichia coli* and *Bacillus subtilis*, are able to penetrate cervical mucus by taking advantage of water channels created by shear forces during secretion (Figueroa-Morales et al., 2019). The behavior of *V. cholerae* in mucus has not been described.

In this study, we characterized the behavior of individual cells from two *V. cholerae* strains in unprocessed porcine intestinal mucus and tested if *V. cholerae* alters the rheological properties of mucus over time. We demonstrated that *V. cholerae* is able to swim through porcine intestinal mucus even without measurable changes in mucus rheology and measured that porcine intestinal mucus is not sensitive to change in pH between 6 and 8. However, alkaline conditions dramatically increase swimming speed and mucus penetration for *V. cholerae*. These results shed light on how *V. cholerae* is able to overcome the defensive mucus layer and the role of intestinal pH during the initial stage of infection.

METHODS

Bacterial strains

V. cholerae strains used in this study were El Tor C6706str2 (Thelin and Taylor, 1996) and Classical O395 (Anthouard and DiRita, 2013) biotypes. Our wild type El Tor strain has a functional *lux*O gene. Strains were fluorescently labelled with the expression of the green fluorescent protein expressed from a constitutive cytochrome c *V. cholerae* promoter on a p15a plasmid derivative (gift from Dr. Christopher Waters). The inactivation of *mshA* in the El Tor C6706 background was generated by recombining genomic DNA of mutant EC4926 from the defined transposon mutant library (Cameron et al., 2008) using natural transformation (Dalia, 2018). The El Tor *flrA* mutant was generated from previous work (Srivastava et al., 2013).

Growth conditions

M9 minimal salts (52 mM Na_2HPO_4, 18 mM K_2HPO_4, 18.69 mM NH_4Cl, 2 mM $MgSO_4$) were supplemented with 10 µM $FeSO_4$, 20 µM $C_6H_9Na_3O_9$ and 36.4 mM Sodium pyruvate. The pH of the growth medium was adjusted with HCl to the desired value. *V. cholerae* was grown shaking (200 r.p.m.) in liquid cultures at 37°C. Kanamycin was added to 50 µg/ml when needed. For all experiments, *V. cholerae* cultures were sampled at early stationary phase (1.9 x 10^9 c.f.u./mL). Soft agar plates were prepared with the same medium with the addition of 0.1% w/v Tryptone and 0.3% w/v Bacto agar (BD). Plates were inoculated with 5 µl of saturated liquid cultures (5.8 x 10^6 cells) on the agar surface and incubated at 37°C for 12 hours before measuring colony size.

Mucus preparation

Small intestines were obtained from a freshly slaughtered adult pig at the Meat Lab at Michigan State University (USDA permit #137 from establishment #10053). The animal was slaughtered as part of the normal work of the abattoir according to the rules set by the Michigan State University Institutional Animal Care and Use Committee (IACUC). The small intestines were acquired from the abattoir with

prior consent. The mucosa was gently scraped from the medial part of small intestine and frozen in liquid nitrogen before storage at -80°C. For each experiment, mucus samples were warmed to 37°C temperature and equilibrated for 1 hour in 10 volumes excess of M9 salts buffered to the desired pH. Bovine submaxillary gland mucin (M3895, Sigma-Aldrich) solution was prepared at 3% w/v in LB medium adjusted to pH 8.0 with sodium hydroxide. Non soluble particles were separated from the preparation by centrifugation at 21,130 r.c.f for 10 minutes. Porcine stomach (M2378, Sigma-Aldrich) mucin solution was prepared at 3% w/v in M9 salts at pH 8.0. The survival rate of *V. cholerae* in BSG was calculated by enumerating colonies on LB agar plate supplemented with 50 µg/ml kanamycin. Fluorescent beads were added to the samples at 0.15% w/v and gently mixed.

Single cell tracking

V. cholerae cells were tracked in liquid medium following the protocol previously described (Dufour et al., 2016). Briefly, *V. cholerae* cells in the early stationary growth phase were diluted to 1.9 x 10^7 cells/mL in fresh medium adjusted to pH 6, 7, or 8. Cells were incubated shaking at 37°C for 15 minutes before tracking to allow for adaptation of the chemotaxis response. Polyvinylpyrrolidone (PVP) was added at 0.05% w/v to the samples to prevent attachment on the glass slide. 6 µl of each sample dropped on a glass slide and trapped under a 22 x 22 mm, #1.5 coverslip sealed with wax and paraffin to create a thin water film (10±2 µm) for video microscopy. For tracking in mucus or low-melting temperature agarose, a 130 µm spacer was added between the slide and the coverslip and fluorescently labelled cells were used. The samples were kept at 37°C during tracking. Images of swimming cells were recorded using a sCMOS camera (Andor Zyla 4.2, Oxford Instruments) at 20 frames per second using a 40X objective (Plan Fluor 40x, Nikon Instruments, Inc.) mounted on an inverted microscope (Eclipse Ti-E, Nikon Instruments, Inc.). Cell were illuminated using phase contrast in liquid or epifluorescence in mucus and agarose. Images were analyzed to detect and localize cells using custom scripts (Dufour et al., 2016) and cell trajectories were reconstructed using the µ-track package (Jaqaman et al., 2008). The

analysis and plots of the cell trajectory statistics were done in MATLAB (The Mathworks, Inc.) as previously described (Dufour et al., 2016).

Passive microrheology of mucus and agarose gel

The viscoelasticity of mucus and agarose were measured by tracking the passive diffusion of 1 µm fluorescent polystyrene beads (F8814, ThermoFisher Scientific). To prevent electrostatic or hydrophobic interactions between the beads and the gels, beads were coated with polyethylene glycol (PEG MW 2,000Da). Coating was done by crosslinking carboxyl groups on the surface of the beads with diamine-PEG following the previously described protocol (Lai et al., 2007). Beads 0.5% w/v and Triton (X-100, Sigma-Aldrich) 0.01% w/v were added to samples and mixed gently. Epifluorescence signal from the beads were recorded using a sCMOS camera (Andor Zyla 4.2, Oxford Instruments) at 100 frames per second using a 100X objective (Plan Fluor 100x, Nikon Instruments, Inc.) and a 1.5X multiplier mounted on an inverted microscope (Eclipse Ti-E, Nikon Instruments, Inc.). Images were analyzed to detect and localize beads using custom scripts and trajectories were reconstructed using the µ-track package (Jaqaman et al., 2008). The beads trajectories were manually inspected to remove artifact and erroneous linking. Systematic drift of the trajectories was corrected prior to calculating the bead average mean-squared displacement (MSD) and velocity autocorrelation (VAC) as a function of time. The VAC was fitted to a degree six polynomial multiplied by an exponential decay function. The VAC function was integrated according the Green-Kubo relation (Green, 1954; Kubo, 1957) to obtain a function that can also be fitted to the MSD with the same parameters. The VAC and MSD were fitted simultaneously using nonlinear least-square regression to separate the dynamic properties of the beads from the tracking noise. The fitted parameters were then used to calculate the storage and loss moduli of the sample according to the generalized Stokes–Einstein equation (Mason, 2000). The analysis and plots of the bead diffusive behavior were done in MATLAB (The Mathworks, Inc.).

Growth rate analysis

The growth rates of bacterial cultures were calculated by recording the change in optical density at 590 nm of 200 µL cultures in 96-well plates (Corning, CLS3595) using a Sunrise plate reader (Tecan Trading AG, Switzerland). Cultures were inoculated with 1.6 x 10^6 c.f.u./mL cells in the exponential growth phase and incubated at 37°C with intermittently shaking every 10 mins for 24 hours. Precautions were taken to limit evaporation.

c-di-GMP quantification

The concentration of c-di-GMP was measured as previously described (Massie et al., 2012). Briefly, 2x10^8 cells sampled during the exponential growth phase were collected on a PTFE membrane filter (0.2 µm) from each condition. Membranes were submerged and mixed in extraction buffer (40% v/v acetonitrile, 40% v/v methanol, 0.1 N formic acid) for 30 minutes. The extraction solution was spiked with a known amount of N^{15}-labeled c-di-GMP to normalize sample loss across samples during extraction. Non-soluble cell debris were separated by centrifugation (21,130 r.c.f. for 2 minutes). The soluble fractions were dried in vacuum overnight and resuspended in 100µl distilled water prior to identification and quantification using mass spectrometry (Quattro Premier XE mass spectrometer, Waters Corp.). c-di-GMP and N^{15}-labeled c-di-GMP were detected simultaneously at *m/z* 699.16 and at *m/z* 689.16, respectively.

Statistical analyses

Statistical significance of the different effects was calculated using Bayesian sampling of linear mixed-effect models taking into account experimental treatments and random effects from replication. The effect of pH on motility in mucus and in liquid was modeled as Response ~ Strain*pH + (1|Replicate) using a log normal link function. The addition of HQNO was modeled as an additional interaction with concentration modeled as a monotonic relationship. The effect of pH on motility in soft agar and growth rate was modeled as Response ~ Strain*pH + (1|Replicate) using a normal link function. Models were

compiled and sampled using the RSTAN (Stan Development Team, 2019) and BRMS packages (Bürkner, 2017, 2018) in R (R Core Team, 2019). The plots were generated using the ggplot2 (Wickham, 2009) and tidybayes (Kay, 2019) packages.

RESULTS

V. cholerae can penetrates intestinal mucus using flagellar motility

We tracked fluorescently labeled *V. cholerae* Classical O395 in unprocessed mucus that was scraped from the medial part of the small intestine of an adult pig (Fig. 3. 1AB). Porcine mucus has been shown to be the most comparable to human mucus regarding structure and thickness when compared to several animal models and also act as a physical barrier between intestinal tissues and bacteria in the lumen (Engevik et al., 2019; Varum et al., 2012). As expected, the movement of *V. cholerae*, as quantified by the trajectory effective diffusion coefficient (Fig. 3.1C), is severely impaired in mucus when compared to swimming in a liquid environment (Fig. 3.1D). To determine the proportion of cells using flagellar motility to swim through mucus, we also measured the effective diffusion coefficient of non-flagellated cells (*flrA* mutant) and determined that a diffusion coefficient above $10^{-0.5}$ $\mu m^2/s$ was evidence of flagellar motility (Fig. 3.1D). Most wild-type cells (~75%) were trapped and unable to swim through the mucus mesh. The rest of the population (~25%) was able to swim through the mucus while being caught in the mucus mesh only intermittently. Because cells were not moving freely and did not have a constant diffusion coefficient, the reported diffusion coefficient represents an average over the entire length of each trajectory.

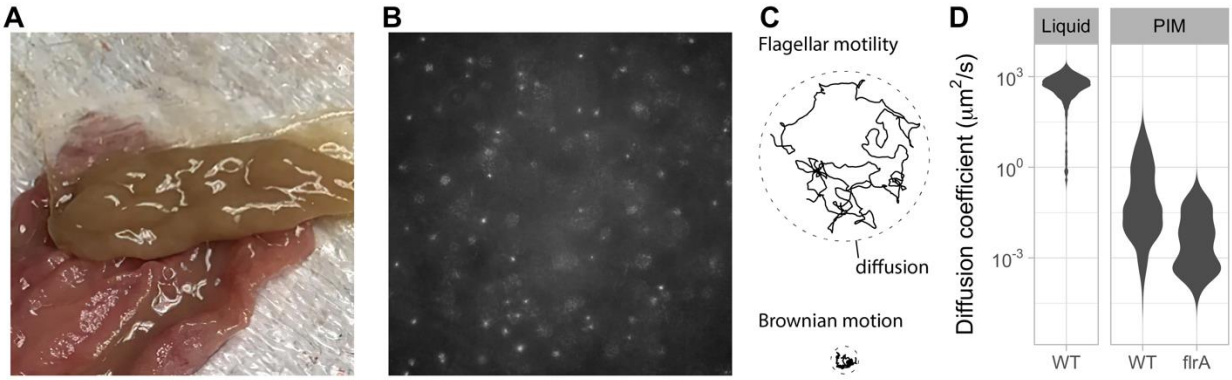

Figure 3.1: *V. cholerae* Classical O395 flagellar motility through unprocessed porcine intestinal mucus (PIM). (A) Mucus scraped from the medial part of the small intestine of an adult pig. (B) Epi-fluorescence image of fluorescent *V. cholerae* Classical O395 in PIM. (C) Motile cells can be distinguished from non-` motile by comparing the trajectories effective diffusion coefficients. (D) Distributions of diffusion coefficients from individual trajectories in liquid and PIM. Motile wild-type *V. cholerae O395* (WT) was compared to a non-motile mutant (*flrA*) in PIM. Each distribution represents 3 to 12 replicates combining between 500 and 6,000 individual trajectories (between 250 and 1,700 minutes of cumulative time).

Alkaline pH improves the motility of *V. cholerae* in intestinal mucus

V. cholerae appears to colonize preferentially the lower part of the small intestine (ileum) where the mucus layer is thicker (Atuma et al., 2001). The ileum is also the most alkaline region of the small intestine (pH 7-8), whereas the jejunum (upper part) is slightly acidic (pH 6-7) (Fallingborg et al., 1989). Therefore, we tested if pH influenced the motile behavior of *V. cholerae* in intestinal mucus. We equilibrated unprocessed porcine intestinal mucus with phosphate saline buffer at pH 6, 7, and 8. We then tracked the swimming behavior of both *V. cholerae* Classical O395 and El Tor C6706 in mucus at each pH. The proportions of swimming cells and the swimming speeds increased as pH increased for both strains (p-values < 10^{-4}) (Fig. 3.2AB). At pH 8, 51% of Classical 0395 and 76% of El Tor C6706 were

able to swim through the mucus. Directional persistence (the time scale at which cells change direction) did not show a response indicating that the reversal frequency of the flagellar motor was not affect by the change in pH (Fig. 3.2C). Overall, alkaline pH improves the motility of *V. cholerae* in mucus, but pH could be affecting either the rheological properties of mucus or the physiology of *V. cholerae.*

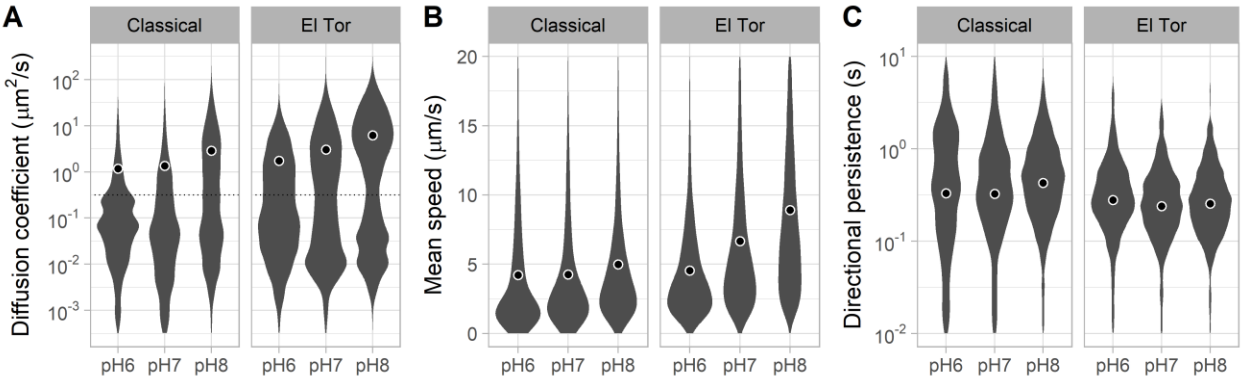

Figure 3.2: Effects of pH on the motility of *V. cholerae* through porcine intestinal mucus. (A) Distributions of diffusion coefficient from individual trajectories in mucus buffered at different pH. Cells with a diffusion coefficient < $10^{-0.5}$ μm^2/s were categorized as non-motile or trapped and were excluded from the following analyses. (B) Distributions of swimming speed from the motile cell populations. (C) Distributions of directional persistence time scales from the motile cell populations. Each distribution represents 8 to 12 replicates combining between 6,000 and 19,000 individual trajectories (between 1,000 and 2,600 minutes of cumulative time). Circles: means for the motile populations.

Change in pH between 6 and 8 had little effects on the mucus rheological properties

To test if pH affects the structure of mucus, we tracked the motion of 1 μm fluorescent polystyrene beads coated with polyethylene glycol that were mixed in the same mucus samples used to track *V. cholerae*. The thermally driven diffusive behavior of beads is affected by the viscoelastic properties of mucus. The 1 μm beads had a sub-diffusive behavior (slope of the mean-squared

displacement < 1) indicating that the motion of the beads was constrained by the mucin matrix (Fig. 3.3A) (Allen et al., 2008). The mucin matrix pore sizes were previously estimated to be ~240 nm using electron microscopy (Bajka et al., 2015; Gustafsson et al., 2012). Consequently, the diffusive motion of 1 µm beads and similarly sized bacteria such as *V. cholerae* are severely diminished in mucus.

The loss (viscous) and storage (elastic) moduli of the mucus can be calculated from mean-squared displacement of the beads with respect to time using the generalized Stokes-Einstein relation (Squires and Mason, 2010). This analysis indicated that the viscosity and elasticity of the porcine intestinal mucus did not change substantially when pH was equilibrated at 6, 7, or 8 (Fig. 3.3BC). We also determined that a prolonged incubation (1 hour) of mucus with *V. cholerae* El Tor C6706 had no measurable effect on the mucus rheology at pH 8. The average diffusion coefficient of non-motile *V. cholerae* (*flrA*) decreased slightly after 1 hour in mucus when compared to 15 minutes. Therefore, we concluded that the improved motility of *V. cholerae* in mucus at pH 8 is likely not attributed to changes in the mucus structure.

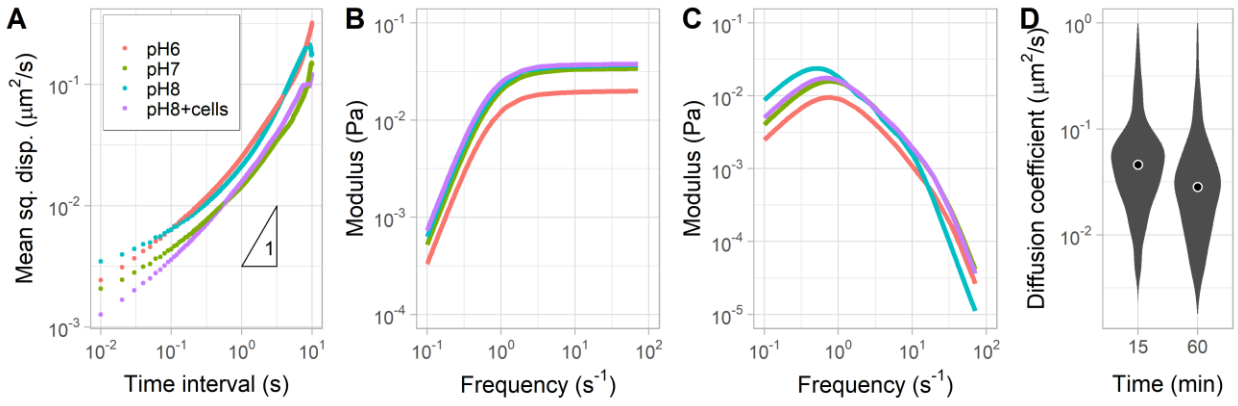

Figure 3.3: Passive microrheology of porcine intestinal mucus. (A) Mean-squared displacement (Mean sq. disp.) of PEG-coated 1 µm polystyrene beads with respect to time at different pH and after incubation with *V. cholerae* (colors). The data points (circles) are the average of trajectories from 4 to 6 replicates (10 to 25 individual trajectories). The hypotenuse of the triangle represents for the slope of 1.

Figure 3.3 (cont'd)

A polynomial fit to the data was used to calculate the storage and loss moduli using the generalized Strokes-Einstein relation. (B) Storage moduli (elasticity) of porcine intestinal mucus at different pH (color). (C) Loss moduli (viscosity) of porcine intestinal mucus at different pH (color). (D) Distributions of the diffusion coefficient of non-motile *V. cholerae* (*flrA*) after incubation in mucus at pH 8. Each distribution represents 6 replicates combining between 1,000 and 2,000 individual trajectories (~150 minutes of cumulative time). Circles: means.

Previous studies have characterized the behavior of *V. cholerae* in mucus reconstituted from purified mucin commercially available (Liu et al., 2008; Silva et al., 2003). We characterized the rheological properties of solutions of mucins from bovine sub-maxillary glands and porcine stomach purchased commercially. We used a 3% w/v concentration, which is comparable to native mucus (Allen et al., 2008; Bromberg and Barr, 2000), in phosphate saline buffer at pH 8. The beads had purely diffusive trajectories indicating that that the solutions were viscous but not elastic (Fig. 3.S1A). The storage and loss moduli of the purified mucin solutions were lower than our porcine mucus sample (Fig. 3.S1BC). Therefore, the purified mucins failed to reconstitute the gel structure of native mucus when dissolved in solution likely because they do not spontaneously crosslink. This result indicates that the physical structure of mucus reconstituted from purified mucins is not comparable to unprocessed mucus.

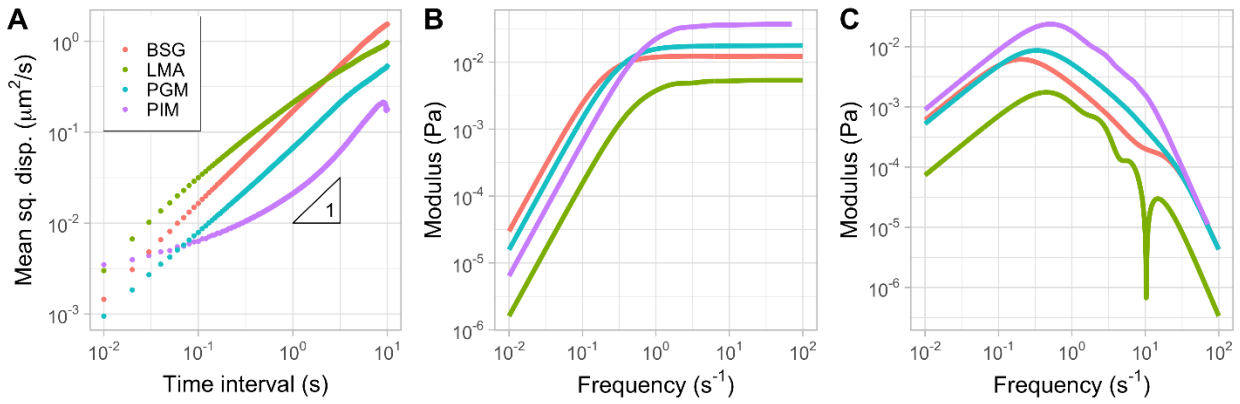

Figure 3.S1: Passive microrheology of mucin solutions. (A) Mean-squared displacement (Mean sq. disp.) of PEG-coated 1 μm polystyrene beads with respect to time in different mucin or agarose preparations (BSG: commercial bovine submaxillary gland mucin, PGM: commercial porcine gastric mucin, PIM: unprocessed porcine intestinal mucus, LMA: low-melting temperature agarose). The data points (circles) are the average of trajectories from 3 to 6 replicates (12 to 25 individual trajectories). A polynomial fit the data (line) was used to calculate the storage and loss moduli using the generalized Strokes-Einstein relation. (B) Storage moduli (elasticity) of different mucin or agarose preparations. (C) Loss moduli (viscosity) of different mucin or agarose preparations.

Alkaline pH promotes the spread of *V. cholerae* colonies in soft agar

To test the effect of pH on *V. cholerae* motility in the traditional soft agar assay, we measured the spread of colonies in M9 salts supplemented with pyruvate, tryptone, and 0.3% w/v agar (Fig. 3.4A). Both Classical 0395 and El Tor C6706 formed significantly larger colonies at alkaline pH (p-values < 10^{-4}) (Fig. 3.4B). The colony morphology of the El Tor C6706 was denser and rugged at the edge when compared to the Classical 0395. One of the differences between the two strains is that Classical does not elaborate the MshA (mannose-sensitive hemagglutinin) pilus that mediates cell attachment (Chiavelli et al., 2001; Hanne and Finkelstein, 1982; Jonson et al., 1989). We inactivated *mshA* in the El Tor background to test if MshA affects colony morphology (Fig. 3.4A). The colonies of the *mshA* mutant had

smoother edges, spread further (p-values < 10^{-4}) (Fig. 3.4B), but remained dense like the wild type. Overall, *V. cholerae* spreads further in soft agar at alkaline pH.

Colony spreading is a function of cell motility and chemotaxis to self-generated chemical gradients, but also a function of growth rate (Croze et al., 2011; Koster et al., 2012; Wolfe and Berg, 1989). *V. cholerae* growth is known to be sensitive to acidic pH (Patel et al., 1995). Therefore, we also measured growth rates in batch cultures at pH 6, 7, and 8 (Fig. 3.4C). At neutral pH, El Tor C6706 grew ~60% faster (63 minutes generation time) than Classical O395 (98 minutes generation time). pH had only a small effect on the generation time of Classical O395. El Tor C6706 grew fastest at pH 7 and 8 (63 minutes and 59 minutes generation times) but significantly slower at pH 6 (103 minutes) (p-values < 10^{-4}). The expression of MshA had a very small but measurable effect on the generation time of El Tor C6706. The effect of pH on growth rate may explain why colony spreading was reduced for El Tor C6706. However, these results do not explain why Classical O395 was similarly affected by pH and spread faster than El Tor C6706 in soft agar. Therefore, we hypothesized that pH affects *V. cholerae* flagellar motility directly.

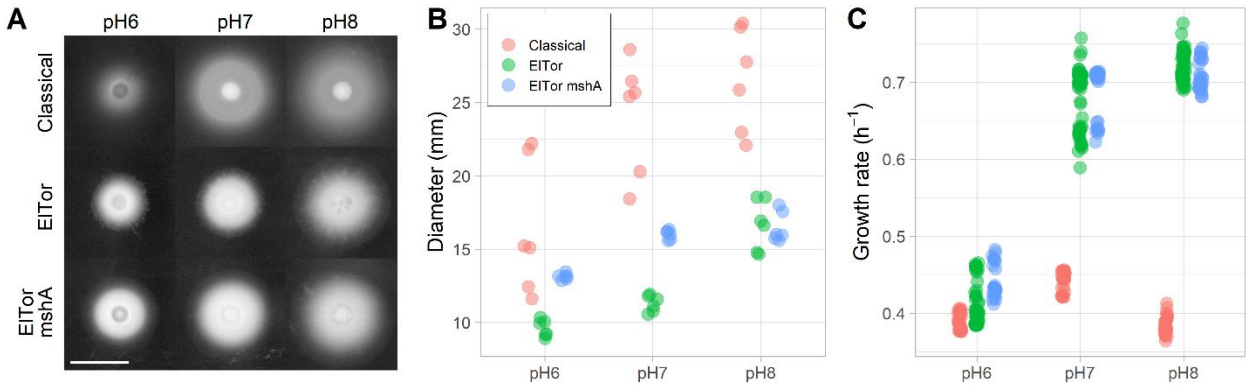

Figure 3.4: Effects of pH on the spreading of *V. cholerae* colonies in soft agar. (A) Representative colonies from the Classical O395 and El Tor C6706 (wild type and *mshA*) at different pH (white bar is 10 mm). (B) Measured colony diameters at different pH for all experimental replicates. (C) Measured growth rates in batch cultures at different pH for all experimental replicates.

***V. cholerae* swims faster at alkaline pH**

To characterize how the swimming behavior of *V. cholerae* is affected by pH more directly, we tracked single cells swimming in a liquid environment between 2 glass coverslips (~10 μm in height). The diffusion coefficient of 1 μm beads and non-motile cells (*flrA* mutant) is distributed between 0.1 and 10 $\mu m^2/s$ in liquid. Therefore, trajectories with an effective diffusion coefficient below 10 $\mu m^2/s$ were categorized as non-motile in the different conditions tested and excluded from the calculations of swimming parameters.

For Classical O395, most cells were highly motile near the end of the exponential growth phase. The diffusion coefficient and swimming speed of the motile population increased upon transfer from the spent growth medium to fresh medium at all pH (p-values < 10^{-4}) likely because of the replenishment of the energy source (addition of pyruvate to spent medium had an identical effect). In fresh medium, Classical O395 was most diffusive at alkaline pH (p-values < 10^{-4}) (Fig. 3.5A). Both swimming speed and the frequency at which cells change direction by reversing the flagellar motor rotation affects diffusion coefficient. However, analysis of the trajectories revealed that only swimming speed was affected by pH (p-values < 10^{-4}) (Fig. 3.5B). On the other hand, the directional persistence of the cell trajectories did not change substantially, indicating that the reversal frequency of the flagellar motor was not affected by pH in Classical O395.

Tracking of El Tor C6706 revealed a more complex behavioral response to change in pH. Upon transfer from the growth medium to pH 6, two third of the population became non-motile (Fig.3.5D) while at pH 7 and 8 the response was like that of Classical O395. We hypothesized that MshA-mediated surface attachment was activated in El Tor C6706 at acidic pH, so we also tracked the swimming behavior a *mshA* mutant at pH 6 and 8. The *mshA* mutant was fully motile at pH 6 (Fig. 3.5D), thus, we concluded that El Tor C6706 activates MshA-mediated attachment at acidic pH but not at neutral or alkaline pH in our growth conditions. These results are consistent with the observation that the

presence of MshA reduces the spread of colonies on soft agar (Fig. 3.4). In the absence of MshA, El Tor C6706 swimming speed at pH 8 was ~150% faster the speed at pH 6 (p-value < 10^{-4}) (Fig. 3.5E), while the directional persistence was unaffected (Fig. 3.5F).

The second messenger c-di-GMP regulates many behavioral responses in *V. cholerae*, including flagellar motility and surface attachment (Jones et al., 2015; Pursley et al., 2018; Srivastava et al., 2013). To test if the cytoplasmic c-di-GMP concentration changes after a shift in pH, we quantified the bulk c-di-GMP concentrations after transfer to buffer solution at different pH using mass spectrometry with El Tor C6706 sampled during the early stationary phase. No measurable change in the total c-di-GMP concentration could be attributed to change in pH (Fig. 3.S2). Our results cannot exclude that pH activates c-di-GMP signaling through localized pathways as previously demonstrated in *V. cholerae* (Floyd et al., 2020) or *Escherichia coli* (Sarenko et al., 2017) or that c-di-GMP changed and returned to the pre-stimulus concentrations during the incubation period (15 minutes). Overall, the increase in swimming speed in both *V. cholerae* strains is likely the main factor underlying improved motility in intestinal mucus and soft agar at alkaline pH.

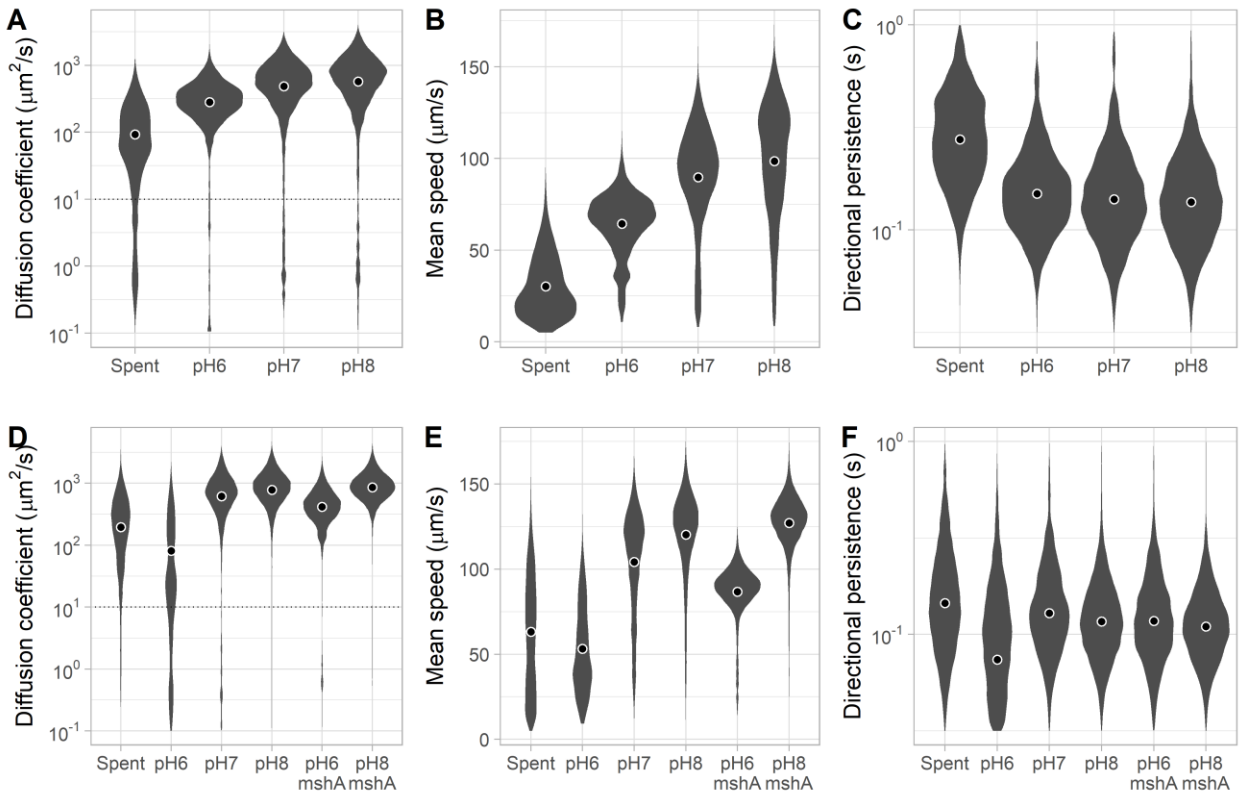

Figure 3.5: Effects of pH on *V. cholerae* flagellar motility. (A) Distributions of diffusion coefficient of Classical O395 from single-cell trajectories in spent medium (Spent) or in fresh medium at different pH. Trajectory below 10 $\mu m^2/s$ were categorized as non-motile and excluded from the remaining analyses. (B) Distributions of swimming speed from the motile cell populations. (C) Distributions of trajectory directional persistence from the motile cell populations. (D) Distributions of diffusion coefficient of El Tor C6706 from single-cell trajectories in spent medium (Spent) or in fresh medium at different pH. A *mshA* mutant was also tracked (*mshA*). (E) Distributions of swimming speed from the motile cell populations. (F) Distributions of trajectory directional persistence from the motile cell populations. Each distribution represents 3 replicates combining between 2,000 and 10,000 individual trajectories (between 100 and 500 minutes of cumulative time). Circles: means for the motile populations.

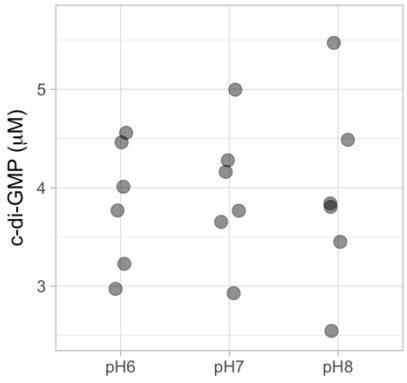

Figure 3.S2: c-di-GMP concentrations in *V. cholerae* El Tor C6706 incubated at different pH.

Inhibiting the Na^+-translocating NADH:quinone oxidoreductase (Na^+-NQR) in *V. cholerae* reduces swimming speed and hydrogel penetration.

V. cholerae uses a sodium motive force to power its flagellar motor (Kojima et al., 1999). Therefore, change in pH is unlikely to have a direct effect on the flagellar motor torque and rotation speed in *V. cholerae*. However, maintaining a strong sodium gradient across the cell membrane when the motor is rotating at high speed is energetically costly (Sowa et al., 2003). *V. cholerae* uses several sodium transporter but most of the sodium export is done by the NADH:quinone oxidoreductase (Na^+-NQR) as part of the respiratory chain (Häse and Barquera, 2001). Activity of the Na^+-NQR pump is strongest at alkaline pH while cells are respiring (Toulouse et al., 2017). Previous studies showed that *Vibrio alginolyticus* is unable to maintain a strong sodium potential across the cell membrane when the cell environment becomes acidic (Tokuda and Unemoto, 1982). Therefore, the reduction of swimming speed we observed at acidic pH is likely the result of the reduction of the Na^+-NQR pump activity.

To test if Na^+-NQR activity plays a role in the ability of *V. cholerae* to penetrate mucus, we added 2-n-Heptyl-4-hydroxyquinoline N-oxide (HQNO), a strong inhibitor of Na^+-NQR activity (Kojima et al., 1999). Unfortunately, mucus has a strong binding affinity to HQNO, which becomes unavailable to inhibit the Na^+-NQR pump. Mucus has been previously shown to bind similar small molecules with high

affinity (Witten et al., 2019). Buffer containing 100 μM HQNO recovered after incubation with porcine intestinal mucus had no effect on *V. cholerae* swimming speed or behavior.

Instead, we tested the effect of HQNO on *V. cholerae* motility in liquid and agarose gel at pH 8. Low melting temperature agarose at 0.3% w/v forms a hydrogel similar to our porcine intestinal mucus samples but with larger mesh pores and less viscosity and elasticity (Fig. 3.S1). As observed with mucus, agarose gel impaired the motility of *V. cholerae* but did not completely abolished it (as expected from the soft agar plate assays). HQNO did not appear to interact with agarose as it dramatically reduced the effective diffusion coefficients of both *V. cholerae* strains (p-values < 10^{-4}) (Fig. 3.6A). Most cells were unable to swim through the agarose gel in the presence of HQNO (diffusion coefficient < $10^{-0.5}$ $\mu m^2/s$) supporting that the ability to maintain a strong sodium gradient is required for *V. cholerae* to escape the gel matrix using flagellar motility.

To test whether HQNO blocks rotation of flagellar motors, we characterized the dose response of *V. cholerae* swimming speed at low viscosity (in liquid). The swimming speed of the motile cell population decreased in a dose-dependent manner with increasing concentration of HQNO (Fig. 3.6B). The effect was more pronounced at acidic pH, indicating a possible synergistic interaction between the effect of low pH and HQNO binding in the pump channel. Swimming speed was very low at 100 μM HQNO but both strains were still motile. Overall, our results are consistent with a model that links the reduced activity of the Na^+-NQR pump at acidic pH to the observed reduction in swimming speed and motility in porcine intestinal mucus.

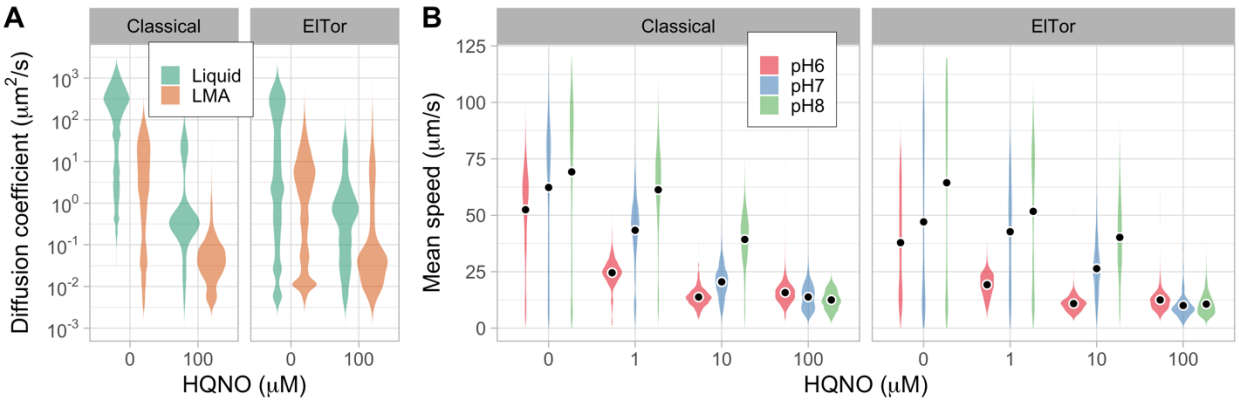

Figure 3.6: Effects of inhibiting the Na^+-NQR pump on flagellar motility in *V. cholerae*. (A) Distributions of diffusion coefficient in liquid and 0.3% w/v agarose buffered at pH 8 and with the addition of 100 µM HQNO. Each distribution represents 6 replicates combining between 1,000 and 3,000 individual trajectories (~1,000 minutes of cumulative time). (B) Distributions of swimming speed at different pH as function of HQNO concentration. Each distribution represents at least 6 replicates combining between 2,000 and 6,000 individual trajectories (between 500 and 1,000 minutes of cumulative time). Circles: means for the motile populations.

DISCUSSION

In this work, we demonstrated that *V. cholerae* can penetrate intestinal mucus using flagellar motility. We extracted mucosa from a pig small intestine and characterized its viscoelastic properties to examine the physical challenge motile bacterial pathogens have to overcome to reach the epithelial tissues from the intestinal lumen. Unprocessed intestinal mucus is a viscoelastic hydrogel with a pore size estimated to be between 200 nm and 1 µm from our microrheological analyses and previous imaging (Bajka et al., 2015; Gustafsson et al., 2012). *V. cholerae* is small enough to swim through mucus using flagellar motility. However, many cells were trapped in the mucin matrix and the effective diffusion coefficient of free-swimming cells was severely reduced when compared to swimming in liquid.

Previous studies suggested that secreted proteases help *V. cholerae* colonize the intestinal mucus layer by degrading mucins (Silva et al., 2006; Szabady et al., 2011). In the conditions we tested, incubation of *V. cholerae* in unprocessed porcine intestinal mucus did not produce measurable changes in the mucus rheological properties suggesting that secreted proteases may not be required during the initial stages of infection when the number of *V. cholerae* is low. Another study proposed that *V. cholerae* shears or loses its flagellum in the presence of bovine mucin and initiates the expression of virulence factors (Liu et al., 2008). In this study, we found that *V. cholerae* rapidly dies in bovine mucin solutions unless dissolved in rich media (likely quenching an unidentified toxic compound). Dead cells showed the expected Brownian motion consistent with previous observations (Liu et al., 2008). We found that *V. cholerae* can grow in unprocessed porcine intestinal mucus and that the motile behavior stays steady suggesting that the integrity of the flagellum is not compromised. These results indicate that, beside the physical interactions with the mucus matrix, there were no measurable biological interactions between *V. cholerae* and mucus on the timescale of our experiments.

The diffusion coefficient we observed for motile *V. cholerae* in mucus is sufficient for cells to reach epithelial tissues during infection of the human small intestine. Previous studies have indicated that directional motion controlled by chemotaxis is not required for *V. cholerae* to infect the host (Butler and Camilli, 2004; Lee et al., 2001b; Millet et al., 2014). Therefore, *V. cholerae* is likely performing a diffusive random walk through the mucosa. The typical thickness of mucus in the human small intestine is in the order of a few hundred micrometers and grows about 240 μm per hour (Gustafsson et al., 2012). The typical first-passage time of a diffusive trajectory can be calculated as the square of the distance to cross divided by twice the diffusion coefficient (Fürth, 1917). From our results, we estimate that the typical time *V. cholerae* would take to penetrate 400 μm of the small intestine mucosa at pH 8 is about 2 hours, which is comparable to the time it takes to grow mucosa of that thickness. Therefore, in the absence of factors that interfere with flagellar motility, *V. cholerae* is intrinsically capable of

overcoming the physical barrier formed by intestinal mucus using flagellar motility even without a chemotactic response.

The dynamics of infection of the human small intestine by *V. cholerae* has not been firmly established, partially because of the limitations of existing animal models (Hatton et al., 2015). The early infection steps may differ significantly between animal models and humans. Studies done on infant rabbits and mice indicate that in the early stage of infection planktonic *V. cholerae* cells are distributed throughout the small intestine. Then, the bacterial load drops in proximal and medial small intestine while the surviving cells preferentially colonize the distal small intestine (Fu et al., 2018; Millet et al., 2014). Only, a small fraction of cells is able to penetrate the mucus layer protecting epithelial tissues. In the later stage of the infection, *V. cholerae* repopulates all parts of the small intestine (Abel et al., 2015; Fu et al., 2018). Previous studies provided conflicting evidence supporting the role of flagellar motility during infection (Richardson, 1991). Some studies found that non-motile cells are less infectious (Wang et al., 2017; Watnick et al., 2001), while others reported that there is no difference and that non-motile cell can reach the epithelial crypts in infant mice (Millet et al., 2014). Therefore, the route to the epithelium may vary between experimental models.

The pH gradient along the length of the small intestine may contribute to the preferred site of infection for *V. cholerae*. In humans, the proximal small intestine is slightly acidic (pH 6.3-6.5) while the distal part is slightly alkaline (pH 7.5-7.8) (Fallingborg et al., 1989; Khutoryanskiy, 2015). *V. cholerae* is able to grow between pH 6.5 and 9, but its preferred pH is that of sea water at ~8 (Huq et al., 1984). Acidic pH regulates expression of virulence factors in *V. cholerae*. The production of cholera toxin and toxin-coregulated pili is maximal at pH 6.6 (Hung and Mekalanos, 2005; Miller and Mekalanos, 1988). Our results showed that MshA affected the motility of El Tor C6067 at acidic pH when grown on soft agar but did not have measurable effect in porcine intestinal mucus, consistent with previous observation that MshA is likely not involved during host infection (Reidl, 2002). On the other hand, high

gastrointestinal pH increases the susceptibility of *V. cholerae* infection (Bavishi and DuPont, 2011) and lactic acid producing bacteria, such as *Lactococcus lactis*, provide some protection against *V. cholerae* infections (Mao et al., 2018).

Our results showed that alkaline pH increases swimming speed and improves the ability of *V. cholerae* to penetrate intestinal mucus. Because *V. cholerae*'s flagellar rotation is powered by the transmembrane sodium gradient, the effect of environmental pH on flagellar motility is likely indirect. The main sodium pump of *V. cholerae*, Na^+-NQR, has increased activity at alkaline pH and no activity at acidic pH, thereby, affecting the sodium potential across the membrane (Tokuda and Unemoto, 1982; Toulouse et al., 2017). In this study, inhibiting Na^+-NQR with HQNO had the same effect as reducing pH on motility, presumably because the sodium motive force is weakened. In addition, a previous study reported that mutant strain lacking NqrA (a subunit of the Na^+-NQR complex) is defective at colonizing infant mice (Merrell et al., 2002) and inhibiting Na^+-NQR activity decreased the production of cholera toxin (Minato et al., 2014). Our model is that *V. cholerae* has difficulty maintaining a strong sodium motive force at acidic pH, reducing the cells capacity to penetrate mucus and reach the epithelium. In addition, acidic pH reduces the production of cholera toxin, which is essential to disrupt the normal function of the small intestine to provide a competitive advantage to *V. cholerae*. Therefore, the preferred site of infection of *V. cholerae* in the human small intestine is likely in the in ileum where the pH is alkaline.

REFERENCES

REFERENCES

Abel, S., Abel zur Wiesch, P., Chang, H.-H., Davis, B.M., Lipsitch, M., and Waldor, M.K. (2015). Sequence tag–based analysis of microbial population dynamics. Nat. Methods *12*, 223–226.

Ali, M., Nelson, A.R., Lopez, A.L., and Sack, D.A. (2015). Updated Global Burden of Cholera in Endemic Countries. PLoS Negl. Trop. Dis. *9*, e0003832.

Allen, A., Hutton, D.A., Pearson, J.P., and Sellers, L.A. (2008). Mucus Glycoprotein Structure, Gel Formation and Gastrointestinal Mucus Function. In Mucus and Mucosa, pp. 137–156.

Anthouard, R., and DiRita, V.J. (2013). Small-Molecule Inhibitors of toxT Expression in Vibrio cholerae. MBio *4*, 00403-13

Atuma, C., Strugala, V., Allen, A., and Holm, L. (2001). The adherent gastrointestinal mucus gel layer: thickness and physical state in vivo. Am. J. Physiol. Liver Physiol. *280*, G922–G929.

Baine, W., Mazzotti, M., Greco, D., Izzo, E., Zampieri, A., Angioni, G., Di Gioia, M., Gangarosa, E., and Pocchiari, F. (1974). EPIDEMIOLOGY OF CHOLERA IN ITALY IN 1973. Lancet *304*, 1370–1374.

Bajka, B.H., Rigby, N.M., Cross, K.L., Macierzanka, A., and Mackie, A.R. (2015). The influence of small intestinal mucus structure on particle transport ex vivo. Colloids Surfaces B Biointerfaces *135*, 73–80.

Bansil, R., Celli, J., Chasan, B., Erramilli, S., Hong, Z., Afdhal, N.H., Bhaskar, K.R., and Turner, B.S. (2005). pH-dependent Gelation of Gastric Mucin. MRS Proc. *897*, 0897-J02-04.

Bansil, R., Celli, J.P., Hardcastle, J.M., and Turner, B.S. (2013). The Influence of Mucus Microstructure and Rheology in Helicobacter pylori Infection. Front. Immunol. *4*, 310.

Bavishi, C., and DuPont, H.L. (2011). Systematic review: the use of proton pump inhibitors and increased susceptibility to enteric infection. Aliment. Pharmacol. Ther. *34*, 1269–1281.

Beyhan, S., Tischler, A.D., Camilli, A., and Yildiz, F.H. (2006). Differences in Gene Expression between the Classical and El Tor Biotypes of Vibrio cholerae O1. Infect. Immun. *74*, 3633–3642.

Bi, Q., Ferreras, E., Pezzoli, L., Legros, D., Ivers, L.C., Date, K., Qadri, F., Digilio, L., Sack, D.A., Ali, M., et al. (2017). Protection against cholera from killed whole-cell oral cholera vaccines: a systematic review and meta-analysis. Lancet Infect. Dis. *17*, 1080–1088.

Bromberg, L.E., and Barr, D.P. (2000). Self-Association of Mucin. Biomacromolecules *1*, 325–334.

Bürkner, P.-C. (2017). brms : An R Package for Bayesian Multilevel Models Using Stan. J. Stat. Softw. *80*.

Bürkner, P.-C. (2018). Advanced Bayesian Multilevel Modeling with the R Package brms. R J. *10*, 395.

Butler, S.M., and Camilli, A. (2004). Both chemotaxis and net motility greatly influence the infectivity of Vibrio cholerae. Proc. Natl. Acad. Sci. *101*, 5018–5023.

Calia, K.E., Murtagh, M., Ferraro, M.J., and Calderwood, S.B. (1994). Comparison of Vibrio cholerae O139 with V. cholerae O1 classical and El Tor biotypes. Infect. Immun. *62*, 1504–1506.

Cameron, D.E., Urbach, J.M., and Mekalanos, J.J. (2008). A defined transposon mutant library and its use in identifying motility genes in Vibrio cholerae. Proc. Natl. Acad. Sci. *105*, 8736–8741.

Chatterjee, S.N., and Chaudhuri, K. (2003). Lipopolysaccharides of Vibrio cholerae. Biochim. Biophys. Acta - Mol. Basis Dis. *1639*, 65–79.

Chiavelli, D.A., Marsh, J.W., and Taylor, R.K. (2001). The Mannose-Sensitive Hemagglutinin ofVibrio cholerae Promotes Adherence to Zooplankton. Appl. Environ. Microbiol. *67*, 3220–3225.

Croze, O.A., Ferguson, G.P., Cates, M.E., and Poon, W.C.K. (2011). Migration of Chemotactic Bacteria in Soft Agar: Role of Gel Concentration. Biophys. J. *101*, 525–534.

Dalia, A.B. (2018). Natural Cotransformation and Multiplex Genome Editing by Natural Transformation (MuGENT) of Vibrio cholerae. In Methods in Molecular Biology, pp. 53–64.

Dufour, Y.S., Gillet, S., Frankel, N.W., Weibel, D.B., and Emonet, T. (2016). Direct Correlation between Motile Behavior and Protein Abundance in Single Cells. PLoS Comput. Biol. *12*, e1005041.

Engevik, M.A., Luk, B., Chang-Graham, A.L., Hall, A., Herrmann, B., Ruan, W., Endres, B.T., Shi, Z., Garey, K.W., Hyser, J.M., et al. (2019). Bifidobacterium dentium Fortifies the Intestinal Mucus Layer via Autophagy and Calcium Signaling Pathways. MBio *10*, 01087-19.

Fallingborg, J., Christensen, L.A., Ingeman-Nielsen, M., Jacobsen, B.A., Abildgaard, K., and Rasmussen, H.H. (1989). pH-profile and regional transit times of the normal gut measured by a radiotelemetry device. Aliment. Pharmacol. Ther. *3*, 605–613.

Figueroa-Morales, N., Dominguez-Rubio, L., Ott, T.L., and Aranson, I.S. (2019). Mechanical shear controls bacterial penetration in mucus. Sci. Rep. *9*, 9713.

Floyd, K.A., Lee, C.K., Xian, W., Nametalla, M., Valentine, A., Crair, B., Zhu, S., Hughes, H.Q., Chlebek, J.L., Wu, D.C., et al. (2020). c-di-GMP modulates type IV MSHA pilus retraction and surface attachment in Vibrio cholerae. Nat. Commun. *11*, 1–16.

Fu, Y., Ho, B.T., and Mekalanos, J.J. (2018). Tracking Vibrio cholerae Cell-Cell Interactions during Infection Reveals Bacterial Population Dynamics within Intestinal Microenvironments. Cell Host Microbe *23*, 274-281.e2.

Fürth, R. (1917). Einige Untersuchungen über Brownsche Bewegung an einem Einzelteilchen. Ann. Phys. *358*, 177–213.

Green, M.S. (1954). Markoff Random Processes and the Statistical Mechanics of Time-Dependent Phenomena. II. Irreversible Processes in Fluids. J. Chem. Phys. *22*, 398–413.

Guentzel, M.N., and Berry, L.J. (1975). Motility as a virulence factor for Vibrio cholerae. Infect. Immun. *11*, 890–897.

Gustafsson, J.K., Ermund, A., Johansson, M.E.V. V., Schütte, A., Hansson, G.C., and Sjövall, H. (2012). An ex vivo method for studying mucus formation, properties, and thickness in human colonic biopsies and mouse small and large intestinal explants. Am. J. Physiol. Liver Physiol. *302*, G430–G438.

Hammer, B.K., and Bassler, B.L. (2009). Distinct Sensory Pathways in Vibrio cholerae El Tor and Classical Biotypes Modulate Cyclic Dimeric GMP Levels To Control Biofilm Formation. J. Bacteriol. *191*, 169–177.

Hanne, L.F., and Finkelstein, R.A. (1982). Characterization and distribution of the hemagglutinins produced by Vibrio cholerae. Infect. Immun. *36*, 209–214.

Häse, C.C., and Barquera, B. (2001). Role of sodium bioenergetics in Vibrio cholerae. Biochim. Biophys. Acta - Bioenerg. *1505*, 169–178.

Hatton, G.B., Yadav, V., Basit, A.W., and Merchant, H.A. (2015). Animal Farm: Considerations in Animal Gastrointestinal Physiology and Relevance to Drug Delivery in Humans. J. Pharm. Sci. *104*, 2747–2776.

Hu, D., Liu, B., Feng, L., Ding, P., Guo, X., Wang, M., Cao, B., Reeves, P.R., and Wang, L. (2016). Origins of the current seventh cholera pandemic. Proc. Natl. Acad. Sci.*113*, E7730-E7739

Hung, D.T., and Mekalanos, J.J. (2005). Bile acids induce cholera toxin expression in Vibrio cholerae in a ToxT-independent manner. Proc. Natl. Acad. Sci. *102*, 3028–3033.

Huq, A., Small, E.B., West, P.A., Huq, M.I., Rahman, R., and Colwell, R.R. (1983). Ecological relationships between Vibrio cholerae and planktonic crustacean copepods. Appl. Environ. Microbiol. *45*, 275–283.

Huq, A., West, P.A., Small, E.B., Huq, M.I., and Colwell, R.R. (1984). Influence of water temperature, salinity, and pH on survival and growth of toxigenic Vibrio cholerae serovar 01 associated with live copepods in laboratory microcosms. Appl. Environ. Microbiol. *48*, 420–424.

Jaqaman, K., Loerke, D., Mettlen, M., Kuwata, H., Grinstein, S., Schmid, S.L., and Danuser, G. (2008). Robust single-particle tracking in live-cell time-lapse sequences. Nat. Methods *5*, 695–702.

Johansson, M.E.V. V, Phillipson, M., Petersson, J., Velcich, A., Holm, L., and Hansson, G.C. (2008). The inner of the two Muc2 mucin-dependent mucus layers in colon is devoid of bacteria. Proc. Natl. Acad. Sci. *105*, 15064–15069.

Jones, C.J., Utada, A., Davis, K.R., Thongsomboon, W., Zamorano Sanchez, D., Banakar, V., Cegelski, L., Wong, G.C.L., and Yildiz, F.H. (2015). C-di-GMP Regulates Motile to Sessile Transition by Modulating MshA Pili Biogenesis and Near-Surface Motility Behavior in Vibrio cholerae. PLOS Pathog. *11*, e1005068.

Jonson, G., Sanchez, J., and Svennerholm, A.M. (1989). Expression and detection of different biotype-associated cell-bound haemagglutinins of Vibrio cholerae O1. J. Gen. Microbiol. *135*, 111–120.

Kay, M. (2019). tidybayes: Tidy Data and Geoms for Bayesian Models. R Packag. Version 1.1.0.

Khutoryanskiy, V. V. (2015). Supramolecular materials: Longer and safer gastric residence. Nat. Mater. *14*, 963–964.

Kojima, S., Yamamoto, K., Kawagishi, I., and Homma, M. (1999). The Polar Flagellar Motor of Vibrio

cholerae Is Driven by an Na+ Motive Force. J. Bacteriol. *181*, 1927–1930.

Koster, D.A., Mayo, A., Bren, A., and Alon, U. (2012). Surface Growth of a Motile Bacterial Population Resembles Growth in a Chemostat. J. Mol. Biol. *424*, 180–191.

Krebs, S.J., and Taylor, R.K. (2011). Protection and Attachment of Vibrio cholerae Mediated by the Toxin-Coregulated Pilus in the Infant Mouse Model. J. Bacteriol. *193*, 5260–5270.

Kubo, R. (1957). Statistical-Mechanical Theory of Irreversible Processes. I. General Theory and Simple Applications to Magnetic and Conduction Problems. J. Phys. Soc. Japan *12*, 570–586.

Lai, S.K., O'Hanlon, D.E., Harrold, S., Man, S.T., Wang, Y.-Y., Cone, R., and Hanes, J. (2007). Rapid transport of large polymeric nanoparticles in fresh undiluted human mucus. Proc. Natl. Acad. Sci. *104*, 1482–1487.

Lauga, E. (2016). Bacterial Hydrodynamics. Annu. Rev. Fluid Mech. *48*, 105–130.

Lee, S.H., Hava, D.L., Waldor, M.K., and Camilli, A. (1999). Regulation and Temporal Expression Patterns of Vibrio cholerae Virulence Genes during Infection. Cell *99*, 625–634.

Lee, S.H., Butler, S.M., and Camilli, A. (2001a). Selection for in vivo regulators of bacterial virulence. Proc. Natl. Acad. Sci. *98*, 6889–6894.

Lee, S.H., Butler, S.M., and Camilli, A. (2001b). Selection for in vivo regulators of bacterial virulence. Proc. Natl. Acad. Sci. *98*, 6889–6894.

Lee, S.H.H., Butler, S.M., Camilli, A., Hsiao, A., Goulian, M., and Zhu, J. (2002). Selection for in vivo regulators of bacterial virulence. Proc. Natl. Acad. Sci. *98*, 6889–6894.

Leitch, G.J. (1988). Cholera enterotoxin-induced mucus secretion and increase in the mucus blanket of the rabbit ileum in vivo. Infect. Immun. *56*, 2871–2875.

Lertsethtakarn, P., Ottemann, K.M., and Hendrixson, D.R. (2011). Motility and Chemotaxis in Campylobacter and Helicobacter. Annu. Rev. Microbiol. *65*, 389–410.

Liu, Z., Miyashiro, T., Tsou, A., Hsiao, A., Goulian, M., and Zhu, J. (2008). Mucosal penetration primes Vibrio cholerae for host colonization by repressing quorum sensing. Proc. Natl. Acad. Sci. *105*, 9769–9774.

Lombardo, M.-J., Michalski, J., Martinez-Wilson, H., Morin, C., Hilton, T., Osorio, C.G., Nataro, J.P., Tacket, C.O., Camilli, A., and Kaper, J.B. (2007). An in vivo expression technology screen for Vibrio cholerae genes expressed in human volunteers. Proc. Natl. Acad. Sci. *104*, 18229–18234.

Mao, N., Cubillos-Ruiz, A., Cameron, D.E., and Collins, J.J. (2018). Probiotic strains detect and suppress cholera in mice. Sci. Transl. Med. *10*, eaao2586.

Mason, T.G. (2000). Estimating the viscoelastic moduli of complex fluids using the generalized Stokes-Einstein equation. Rheol. Acta *39*, 371–378.

Massie, J.P., Reynolds, E.L., Koestler, B.J., Cong, J.-P., Agostoni, M., and Waters, C.M. (2012). Quantification of high-specificity cyclic diguanylate signaling. Proc. Natl. Acad. Sci. *109*, 12746–12751.

Merrell, D.S., Hava, D.L., and Camilli, A. (2002). Identification of novel factors involved in colonization and acid tolerance of Vibrio cholerae. Mol. Microbiol. *43*, 1471–1491.

Miller, V.L., and Mekalanos, J.J. (1988). A novel suicide vector and its use in construction of insertion mutations: osmoregulation of outer membrane proteins and virulence determinants in Vibrio cholerae requires toxR. J. Bacteriol. *170*, 2575–2583.

Millet, Y.A., Alvarez, D., Ringgaard, S., von Andrian, U.H., Davis, B.M., and Waldor, M.K. (2014). Insights into Vibrio cholerae Intestinal Colonization from Monitoring Fluorescently Labeled Bacteria. PLoS Pathog. *10*, e1004405.

Minato, Y., Fassio, S.R., Reddekopp, R.L., and Häse, C.C. (2014). Inhibition of the sodium-translocating NADH-ubiquinone oxidoreductase [Na+-NQR] decreases cholera toxin production in Vibrio cholerae O1 at the late exponential growth phase. Microb. Pathog. *66*, 36–39.

Miyata, S.T., Kitaoka, M., Wieteska, L., Frech, C., Chen, N., and Pukatzki, S. (2010). The Vibrio Cholerae Type VI Secretion System: Evaluating its Role in the Human Disease Cholera. Front. Microbiol. *1*, 117.

Patel, M., Isaäcson, M., and Gouws, E. (1995). Effect of iron and pH on the survival of Vibrio cholerae in water. Trans. R. Soc. Trop. Med. Hyg. *89*, 175–177.

Pursley, B.R., Maiden, M.M., Hsieh, M.-L., Fernandez, N.L., Severin, G.B., and Waters, C.M. (2018). Cyclic di-GMP Regulates TfoY in Vibrio cholerae To Control Motility by both Transcriptional and Posttranscriptional Mechanisms. J. Bacteriol. *200*, e00578-17.

R Core Team (2019). R: A Language and Environment for Statistical Computing. Vienna, Austria.

Reidl, J. (2002). Vibrio cholerae and cholera: out of the water and into the host. FEMS Microbiol. Rev. *26*, 125–139.

Richardson, K. (1991). Roles of motility and flagellar structure in pathogenicity of Vibrio cholerae: analysis of motility mutants in three animal models. Infect. Immun. *59*, 2727–2736.

Sack, D.A., Sack, R.B., Nair, G.B., and Siddique, A. (2004). Cholera. Lancet *363*, 223–233.

Sarenko, O., Klauck, G., Wilke, F.M., Pfiffer, V., Richter, A.M., Herbst, S., Kaever, V., and Hengge, R. (2017). More than Enzymes That Make or Break Cyclic Di-GMP—Local Signaling in the Interactome of GGDEF/EAL Domain Proteins of Escherichia coli. MBio *8*, 01639-17.

Schild, S., Tamayo, R., Nelson, E.J., Qadri, F., Calderwood, S.B., and Camilli, A. (2007). Genes Induced Late in Infection Increase Fitness of Vibrio cholerae after Release into the Environment. Cell Host Microbe *2*, 264–277.

Shen, Y., Chen, L., Wang, M., Lin, D., Liang, Z., Song, P., Yuan, Q., Tang, H., Li, W., Duan, K., et al. (2017). Flagellar Hooks and Hook Protein FlgE Participate in Host Microbe Interactions at Immunological Level. Sci. Rep. *7*, 1433.

Silva, A.J., and Benitez, J.A. (2016). Vibrio cholerae Biofilms and Cholera Pathogenesis. PLoS Negl. Trop. Dis. *10*, e0004330.

Silva, A.J., Pham, K., and Benitez, J.A. (2003). Haemagglutinin/protease expression and mucin gel penetration in El Tor biotype Vibrio cholerae. Microbiology *149*, 1883–1891.

Silva, A.J., Leitch, G.J., Camilli, A., and Benitez, J.A. (2006). Contribution of Hemagglutinin/Protease and Motility to the Pathogenesis of El Tor Biotype Cholera. Infect. Immun. *74*, 2072–2079.

Son, M.S., Megli, C.J., Kovacikova, G., Qadri, F., and Taylor, R.K. (2011). Characterization of Vibrio cholerae O1 El Tor Biotype Variant Clinical Isolates from Bangladesh and Haiti, Including a Molecular Genetic Analysis of Virulence Genes. J. Clin. Microbiol. *49*, 3739–3749.

Sowa, Y., Hotta, H., Homma, M., and Ishijima, A. (2003). Torque–speed Relationship of the Na+-driven Flagellar Motor of Vibrio alginolyticus. J. Mol. Biol. *327*, 1043–1051.

Squires, T.M., and Mason, T.G. (2010). Fluid Mechanics of Microrheology. Annu. Rev. Fluid Mech. *42*, 413–438.

Srivastava, D., Hsieh, M.-L., Khataokar, A., Neiditch, M.B., and Waters, C.M. (2013). Cyclic di-GMP inhibits Vibrio cholerae motility by repressing induction of transcription and inducing extracellular polysaccharide production. Mol. Microbiol. *90*, 1262–1276.

Stan Development Team (2019). RStan: the R interface to Stan.

Szabady, R.L., Yanta, J.H., Halladin, D.K., Schofield, M.J., and Welch, R.A. (2011). TagA is a secreted protease of Vibrio cholerae that specifically cleaves mucin glycoproteins. Microbiology *157*, 516–525.

Taylor, D.L., Kahawita, T.M., Cairncross, S., and Ensink, J.H.J. (2015). The Impact of Water, Sanitation and Hygiene Interventions to Control Cholera: A Systematic Review. PLoS One *10*, e0135676.

Thelin, K.H., and Taylor, R.K. (1996). Toxin-coregulated pilus, but not mannose-sensitive hemagglutinin, is required for colonization by Vibrio cholerae O1 El Tor biotype and O139 strains. Infect. Immun. *64*, 2853–2856.

Tokuda, H., and Unemoto, T. (1982). Characterization of the respiration-dependent Na+ pump in the marine bacterium vibrio alginolyticus. J. Biol. Chem. *257*, 10007–10014.

Toulouse, C., Claussen, B., Muras, V., Fritz, G., and Steuber, J. (2017). Strong pH dependence of coupling efficiency of the Na+ – translocating NADH:quinone oxidoreductase (Na+-NQR) of Vibrio cholerae. Biol. Chem. *398*, 251–260.

Varum, F.J.O., Veiga, F., Sousa, J.S., and Basit, A.W. (2012). Mucus thickness in the gastrointestinal tract of laboratory animals. J. Pharm. Pharmacol. *64*, 218–227.

Wang, Z., Lazinski, D.W., and Camilli, A. (2017). Immunity Provided by an Outer Membrane Vesicle Cholera Vaccine Is Due to O-Antigen-Specific Antibodies Inhibiting Bacterial Motility. Infect. Immun. *85*, 1–9.

Watnick, P.I., Lauriano, C.M., Klose, K.E., Croal, L., and Kolter, R. (2001). The absence of a flagellum leads to altered colony morphology, biofilm development and virulence in Vibrio cholerae O139. Mol. Microbiol. *39*, 223–235.

Wickham, H. (2009). ggplot2 (New York, NY: Springer New York).

Witten, J., Samad, T., and Ribbeck, K. (2019). Molecular Characterization of Mucus Binding. Biomacromolecules *20*, 1505–1513.

Wolfe, A.J., and Berg, H.C. (1989). Migration of bacteria in semisolid agar. Proc. Natl. Acad. Sci. *86*, 6973–6977.

Zhu, J., and Mekalanos, J.J. (2003). Quorum Sensing-Dependent Biofilms Enhance Colonization in Vibrio cholerae. Dev. Cell *5*, 647–656.

Zhu, J., Miller, M.B., Vance, R.E., Dziejman, M., Bassler, B.L., and Mekalanos, J.J. (2002). Quorum-sensing regulators control virulence gene expression in Vibrio cholerae. Proc. Natl. Acad. Sci. *99*, 3129–3134.

Chapter 4: CURVATURE IMPROVES THE SWIMMING SPEED AND DIFFUSION OF *VIBRIO CHOLERAE* IN LIQUID AND SOFT AGAR

Some results from this chapter have been published in Fernandez, N.L., Hsueh, B., Nhu, N.T.Q., Franklin, J.L., Dufour, Y.S., Waters, C.M. (2020). Vibrio cholerae adapts to sessile and motile lifestyles by cyclic-di-GMP regulation of cell shape. PNAS. These results include the cell metrics in liquid and *V. cholerae* near-surface motility.

INTRODUCTION

Shape was one of the first characteristics used to classify bacteria since the inception of microbiology. The cell shape is formed and supported by the cell wall and the cytoskeleton. The deletion of cytoskeleton proteins or peptidoglycan can result in cell shape modification (Frirdich et al., 2012, 2014; Jiang et al., 2011; Shi et al., 2018). The shape of bacteria is under selective forces imposed by the environment bacteria live in. However, little is known about why bacteria acquire certain cell shapes and what their functional significance is.

The shape of bacteria satisfies the primary needs of nutrient uptake, cell division and escaping from predators (Young, 2006). Most observed bacterial cells are symmetrical, convenient for cell division and ensure that materials are equally distributed to daughter cells. In terms of physics, the size and shape of bacteria are constrained by the diffusion of nutrients. First, the size must be big enough to store all the components and small enough to allow efficient nutrient diffusion in the cytosol. Secondly, to satisfy nutrient acquisition and growth, bacteria need to reside in the best food source and niches. Some of these needs are translated into functions such as motility or cell attachment. These functions can be optimized by changing the cell shape. Some of the findings are that curved *C. crescentus* has an increased resistance to flow so that it can stick to its preferred surface (Persat et al., 2014). Another includes *E. coli* swarm cells that are longer than its swimming counterparts. The long cells are better for maintaining direction to swarm outward (Damton et al., 2010).

Cell shape can affect swimming performance. Bacteria are propelled forward by the rotation of their flagella and cell body (Magariyama et al., 1995). The rotation provides torque which results in forward thrust. Although the cell body provides less propulsion than the flagellum, changes in its shape can affect thrust. It was shown that the curved shape of *Caulobacter crescentus* produces an additional thrust when swimming in a helical trajectory (Liu et al., 2014; Magariyama et al., 1995). In fact, the contribution of curvature to swimming speed has been shown in *H. pylori* and *C. crescentus* (Constantino et al., 2016a). The studies by Constanino et al. showed that the spiral shape increases the swimming speed of *H. pylori* in buffer and porcine gastric mucin to ~15% compared to its rod counterpart. In addition, theoretical research by Schuech et al. found that a Pareto optimum for construction cost, chemotaxis, and swimming speed is achieved in curved shape bacteria (Schuech et al., 2019). Overall, the curvature is likely to improve swimming performance and chemotaxis.

Vibrio cholerae, as a member of *Vibrio* genus lives in marine and brackish environment. It regulates its lifestyle between a sessile and motile states. *V. cholera* is mono-flagellated. Counter-clockwise rotation of the flagella results in clockwise rotation of the cell body to go forward (Homma et al., 1996). When swimming in liquid, *Vibrio* changes direction by a "reverse and flick" model. A reversion in direction happens as a result of changing the rotation direction of flagella. Right after the reversion, a 90^{o} "flick" helps *V. cholerae* to reorient and continue to swim forward (Stocker, 2011). How the curved shape of *V. cholerae* impacts swimming performance is still unknown.

While *V. cholerae* predominantly exists as a free-living microbe, it can be pathogenic when it colonizes a susceptible host (e.g. humans). Cell shape is thought to contribute successful *V. cholerae* pathogenesis, as flagellar motility is required for infection. Recently, it was discovered that the deletion of *crv*AB (Bartlett et al., 2017) resulted in a rod shape *V. cholerae* without noticeable pleotropic effects. The gene has a role in inhibiting the insertion of peptidoglycan on one side of the cell wall making the cell curved. It was reported that the rod-shaped *V. cholerae* produces a smaller colony on Luria-Bertani

(LB) swim plates. In terms of pathogenesis, colonization success of rod-shaped *V. cholerae* was decreased compared to WT (curved *V. cholerae*) in mice and rabbit distal gut. These results suggest that the curvature might promote motility in hydrogels, such as mucin. However, the results on swim plates and mice guts are difficult to interpret since it might be the results of many factors such as growth, chemotaxis, and motility regulation. Therefore, I used single cell tracking to decipher the role of curvature in *V. cholerae* swimming motility. In this study, I investigated if the curved shape provides an advantage in navigating through liquid and visco-elastic environments (hydrogels).

METHODS

Bacterial strains

In this study, I used *V. cholerae* El Tor C6706str2 and its Δ*crvA* mutant (Fernandez et al., 2020). Except for when tracked in buffer, *V. cholerae* strains were fluorescently labelled with the expression of the green fluorescent protein expressed from a constitutive cytochrome c *V. cholerae* promoter on a p15a plasmid derivative, pCMW5 (gift from Dr. Christopher Waters). All the strains were grown in M9 minimal media (52 mM Na_2HPO_4, 18 mM K_2HPO_4, 18.69 mM NH_4Cl, 2 mM $MgSO_4$) supplemented with 10 µM $FeSO_4$, 20 µM $C_6H_9Na_3O_9$ and 36.4 mM Sodium pyruvate (M9P) until it reached early stationary phase (1.9×10^9 c.f.u./mL).

Swim plates

Swim plates were prepared with M9 minimal salts with the addition of 0.1% w/v tryptone (BD) and 0.4% w/v Bacto agar (BD). For cell tracking, agar was poured into a µ-Slide 2 Well (cat 80281, ibidi). Agar plates and slides were kept at room temperature for 15 hours before inoculation. To set up the swim plates and slides, a 10 µl-pipette tip covered with motile cells were stabbed into the agar. The swim plates/slides were incubated at 37°C for 24 hours before measuring the cell metrics and 10 hours before tracking.

Cell metrics

V. cholerae cells were obtained from M9 minimal salts supplemented with 0.4% w/v sodium pyruvate at exponential and early stationary phase. To measure *V. cholerae* cells from agar, a plug of agar from the swim colony edge was pipetted to M9 minimal media and shaken to extract the cells. Two µl of cell suspension was dropped on a 1% w/v agarose pad. The drop was covered by a coverslip. Pictures of *V. cholerae* was taken at phase contrast with magnification 100X. The segmentation of *V. cholerae* cell shape was done by SuperSegger (Stylianidou et al., 2016). The cell size is measured by mesh analysis (Sliusarenko et al., 2011). Data were visualized using R and ggplot2.

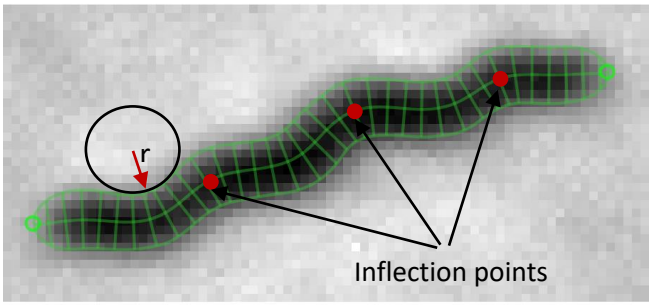

Figure 4.1: Mesh analysis to measure cell shape parameters. The curvature is calculated as the reciprocal of cell radius (r) (μm^{-1}). The number of inflections per cell is the number of inflection points (filled red circle)

Visco-elastic materials preparation

1% w/v methylcellulose (MC) (M352-500, Fisher Scientific) was prepared one night before experimentation and stored at 4°C before tracking so that it was dissolved completely. Agarose (LMA) was made by heating 0.3% (w/v) low-melting agarose (BP165-25, Fisher Scientific) to 70 °C. MC and LMA were made in bacterial motility buffer. To make MCLMA, 2% MC and 0.6% LMA are first prepared separately. Later, half the volume of each material is incubated at 37°C before being mixed. Mucus was

prepared by hydrating 100 µg of pig intestinal mucus with 50 µl M9 minimal buffer and incubating at 37°C for 1 hour. Before used for tracking, hydrated mucus was briefly centrifuged and excessive liquid removed. All materials are incubated at 37°C at least 15 minutes before inoculating bacteria.

Growth rate analysis

The growth rates of bacterial cultures were calculated by recording the change in optical density at 590 nm of 200 µL cultures in 96-well plates (Corning, CLS3595) using a Sunrise plate reader (Tecan Trading AG, Switzerland). Cultures were inoculated with 1.6 x 10^6 c.f.u./mL cells in the exponential growth phase and incubated at 37°C with intermittently shaking every 10 mins for 24 hours. Precautions were taken to limit evaporation.

Single cell tracking

Bacterial cells were tracked in liquid following a previously described protocol (Dufour et al., 2016). *S. enterica* grown in VB2Y was washed and tracked in VB supplemented with 0.5% glucose. *V. cholerae* were tracked in M9P at pH 8.0. For optimal tracking, bacterial cells were diluted to 1.9 x 10^7 cells/mL in motility buffer. Cells were incubated at 37° C for 15 minutes before tracking to allow for adaptation of the chemotaxis response. Polyvinylpyrrolidone (PVP, BP431-100, Fisher Scientific) was added at 0.05% w/v to the samples to prevent attachment on the glass slide. 6 µl of each sample dropped on a glass slide and trapped under a 22 x 22 mm, #1.5 coverslip sealed with wax and paraffin to create a thin water film (10±2 µm) for video microscopy. For tracking in mucus, MC, and LMA, a 130 µm spacer was added between the slide and the coverslip and fluorescently labelled cells were used. LMA slides were kept at room temperature for 30 minutes to allow solidification. The samples were kept at 37°C during tracking. Images of swimming cells were recorded using a sCMOS camera (Andor Zyla 4.2, Oxford Instruments) at 20 frames per second using a 40X objective (Plan Fluor 40x, Nikon Instruments, Inc.) mounted on an inverted microscope (Eclipse Ti-E, Nikon Instruments, Inc.). Cell were illuminated using phase contrast in liquid or epifluorescence in mucus and agarose. Images were analyzed to detect

and localize cells using custom scripts (Dufour et al., 2016) and cell trajectories were reconstructed using the μ-track package (Jaqaman et al., 2008). The analysis and plots of the cell trajectory statistics were done in MATLAB (The Mathworks, Inc.) as previously described (Dufour et al., 2016).

RESULTS

*crv*A expression imposes a metabolism cost on *V. cholerae*.

V. cholerae shape is twisted (Fig. 4.2A). The deletion of *crv*A gene results in the loss of *V. cholerae* curvature. I obtained the *V. cholerae* El Tor C6706str2 WT and Δ*crv*A mutant from Dr. Chris Waters. To measure the effect of *crv*A expression on the growth of *V. cholerae*, I grew *V. cholerae* in minimal media supplemented with 0.4% w/v sodium pyruvate as the carbon source. I calculated the generation time of each strain from the early log phase when the cell density is still low. I found that *V. cholerae* Δ*crv*A mutant has a shorter generation time comparing to WT (57.5 vs 58.5 mins) (p-value = 0.02). This result suggests a metabolism cost of ~1.5% to WT to produce the curvature.

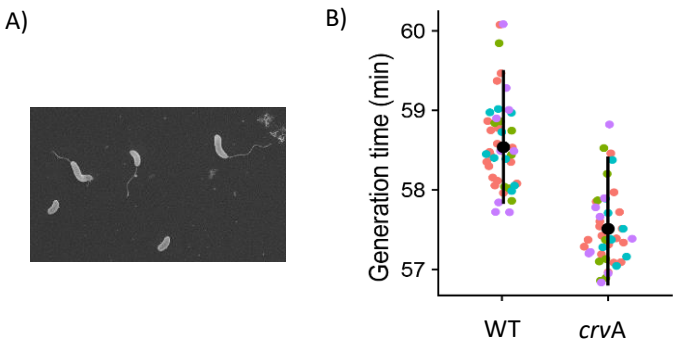

Figure 4.2: *crv*A has a negative effect on the generation time *of V. cholerae*. A) Scanning electron microscope (SEM) picture of *V. cholerae* El Tor C6706str2 WT. The cells were retrieved from M9 minimal culture at stationary phase. Photo was taken by John Lee. B) Comparison of generation time between WT and ΔcrvA mutant. The differences in generation time between two strains was evaluated from a

Figure 4.2 (cont'd)

linear mixed-effect model. The vertical line represents for the 95% credible intervals of the mean. The results are from four biological replicates.

Curvature improves *V. cholerae* swimming speed and diffusion in liquid

V. cholerae lives in aquatic environments, including sea, brackish, and river water. It has been reported that the spiral and curved shape increase *H. pylori* and *C. crescentus* swimming speed compared to rod shape mutants (Constantino et al., 2016b; Liu et al., 2014). I hypothesize that the curvature improves *V. cholerae* swimming motility in liquid. To test this hypothesis, I tracked *V. cholerae* El Tor C6706str2 WT and Δ*crv*A mutant in M9 minimal salts supplemented with sodium pyruvate. The medium was adjusted to pH 8.0 to mimic the pH of sea water (chapter 3). I took videos of swimming *V. cholerae* at near (~1 μm) and far (~40 μm) from the glass surface. When comparing between the two cell shapes, *V. cholerae* WT had higher motile population comparing to Δ*crv*A mutant (7-9.0%) in both distances (p-values < 10^{-4}) (Fig. 4.3C). In addition, *V. cholerae* WT had a higher swimming speed comparing to rod shape mutant, around 5.5% at near surface and 11.0% at far surface (p-values < 10^{-4}) (Fig. 4.3D). I also observed that Δ*crv*A mutant had higher directional persistence time and lower speed variance than WT at far surface. There was no significant difference in these parameters at near surface motility between the two strains (Fig. 4.3EF). In the end, WT has higher mean diffusion coefficient than Δ*crv*A mutant, 3.0% and 12.0% at near and far surface, respectively (p-values < 10^{-4}). Overall, the most notable effect of *crv*A expression is on *V. cholerae* swimming speed with up to 11.0% increment. Our finding agrees with a research on *H. pylori* in which the helical morphology increases the motile population and swimming speed (Martínez et al., 2016). More interesting, they also observe the same increment in speed (7-11%) when tracking *H. pylori* in broth.

In addition, I found that the swimming speed of WT increase 7.9% when swimming at near surface (105.0 vs 96.7 um/s) (p-value < 10^{-4}) (Fig. 4.3D). *V. cholerae* cells swim straight longer near the surface with longer directional persistence time (Fig. 4.3E). Our tracking results agree with a study on *V. alginolyticus* in which cells have faster swimming speed when swimming near glass surface due to the wall effect (Magariyama et al., 2005; Ramia et al., 1993).

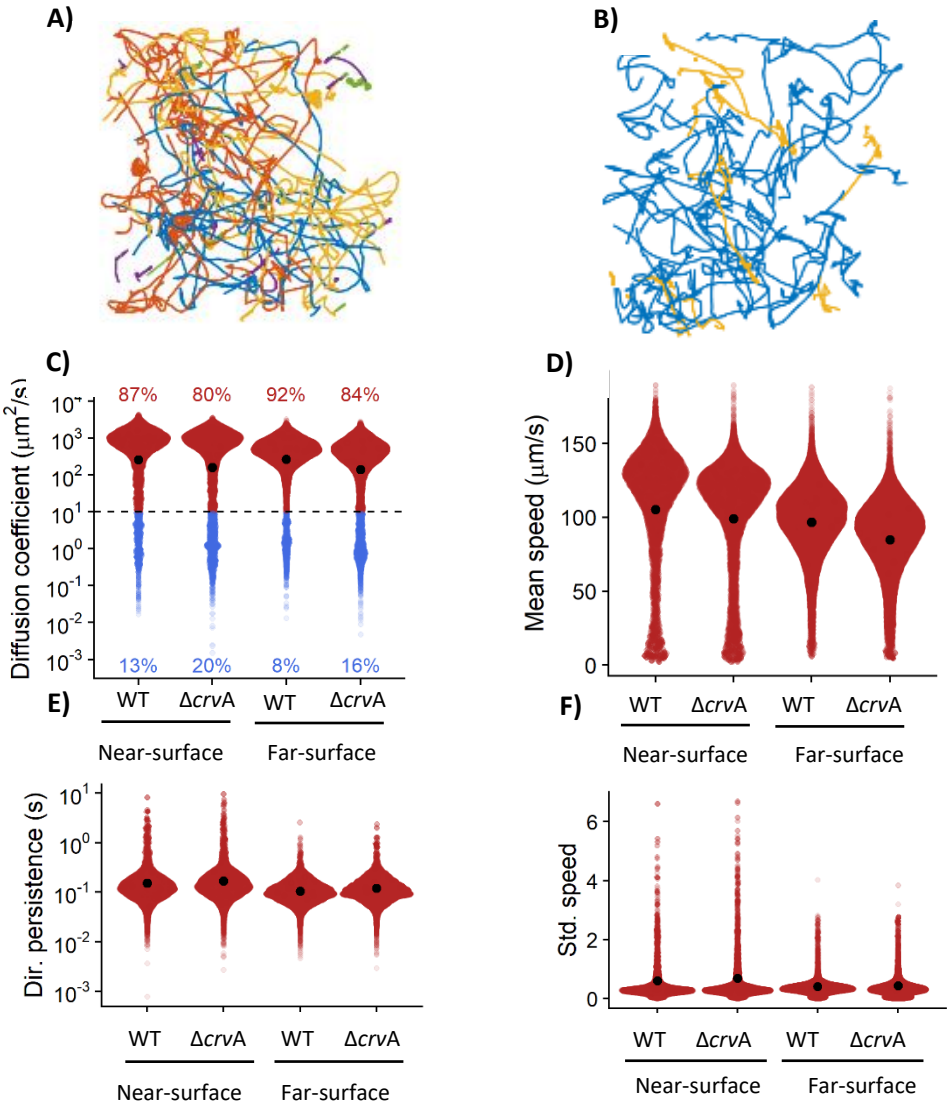

Figure 4.3: *V. cholerae* motility in M9 minimal media. *V. cholerae* WT swimming trajectories at A) near – and B) far – surface motility. Distribution of C) diffusion coefficients, D) swimming speed, E) directional

Figure 4.3 (cont'd)

persistence time, and F) speed variance of V. cholerae WT and ΔcrvA mutant from trajectories at near and far from the glass surface. Trajectory with diffusion coefficients below 10 $\mu m^2/s$ were categorized as non-motile (blue) and excluded from the remaining analyses. The black dot represents the mean. Data is calculated from 11,000 to 25,000 trajectories collected from four to five biological replicates.

Curvature improves *V. cholerae* penetration in mucus

V. cholerae infects the human small intestine. Genetics and in vivo studies suggest that flagellar motility is important for gut colonization (Guentzel and Berry, 1975; Lee et al., 2001; Martinez et al., 2009). A previous study has shown that WT *V. cholerae* was better than the Δ*crv*A mutant in infecting mice and rabbit ileum models (Bartlett et al., 2017). In addition, it has been reported that the spiral shape increases *H. pylori* swimming speed in porcine gastric mucin (Martínez et al., 2016). I hypothesize that the curvature promotes *V. cholerae* motility through mucus. I tracked *V. cholerae* WT and Δ*crv*A mutant in raw, unprocessed mucus collected from pig small intestine. By tracking on a glass slide, I directly related cell shape to swimming ability and avoided confounding factors such as growth, chemotaxis, and gene mutation which are normally present in in vivo models. In brief, motile *V. cholerae* cells from liquid culture were transferred to mucus and incubated for a short time (15 mins) before tracking. To evaluate the role of curvature in motility, I compare the diffusion coefficients between WT and Δ*crv*A mutant. Our results suggest that there is a small difference in diffusion and swimming performance in mucus between two strains (Fig. 4.4). I found that WT has the same speed as the Δ*crv*A mutant but longer directional persistence time, resulting in higher diffusion coefficients (1.55 vs 1.2$\mu m^2/s$) (p-value < 10^{-4}). The result suggests that curvature affects the ability to change direction of *V. cholerae* in mucus. These results contrast what I observed in liquid, where WT has higher speed and lower directional persistence time than Δ*crv*A mutant. Overall, the additive value of curvature to *V.*

cholerae motility in mucus is different from that in liquid with its effect on helping *V. cholerae* to maintain direction.

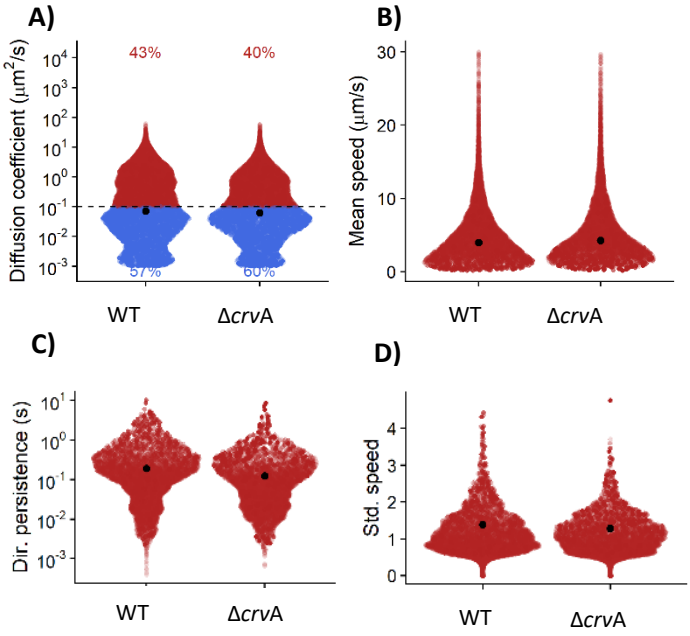

Figure 4.4: *V. cholerae* motility in mucus. Distributions of A) diffusion coefficient, B) swimming speed, C) directional persistence time and D) speed variance of the WT and Δ*crv*A mutant extracted from trajectories when swimming in mucus. Trajectory with diffusion coefficients below 10^{-1} μm^2/s were categorized as non-motile (blue) and excluded from the remaining analyses. The black dot represents the mean. Data is calculated from 6,000 to 7,000 trajectories collected from three biological replicates. The results were statistically tested by a linear mixed-effect model.

Migrating *V. cholerae* WT has higher swimming speed and diffusion in agar than Δ*crv*A mutant.

It was previously reported that *V. cholerae* WT has larger swimming colonies compared to Δ*crv*A mutant in LB soft agar (Bartlett et al., 2017). In our lab, I reproduced these result in 0.4% agar plates buffered with M9 minimal salts supplemented with 0.4% sodium pyruvate, and 0.1% tryptone. The swim colony on the agar plate is the net result of many factors such as visco-elasticity, motility, growth,

chemotaxis, signaling, and mutation. I took videos of *V. cholerae* at the edge of swim colonies with phase contrast. At 10X magnification, the WT colony appeared round and evenly spread out. On the other hand, Δ*crv*A mutant colony has clumps of bacteria at the edge (Fig. 4.5). To avoid incorrect detection of nonmotile cells with the agar background, I tracked the movement of motile cells only. Even though Δ*crv*A mutant has higher growth rate than WT, tracking results revealed that WT had more motile cells than Δ*crv*A mutant (~3,500 vs 1,200 trajectories). Among the motile cells, the mean speed of WT is 18.3% faster than that of Δ*crv*A mutant (6.92 vs 5.85 μm/s) (p-value < 10^{-4}), resulting in a higher diffusion coefficient. I did not find significant differences in directional persistence time and speed variance (Fig. 4.6)

Overall, our results suggest that WT can navigate through the porous environment of agar better than Δ*crv*A mutant. Thus, the tracking result is compatible with the colony size on swim plates.

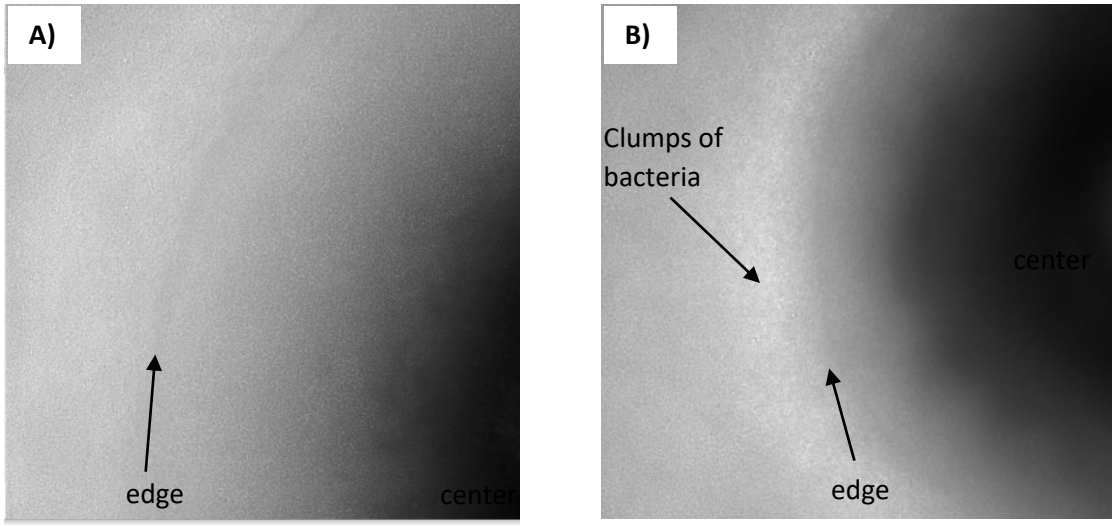

Figure 4.5: The edge of swim colony by A) WT and B) Δ*crv*A mutant. Pictures were taken at Phase contrast, 10X.

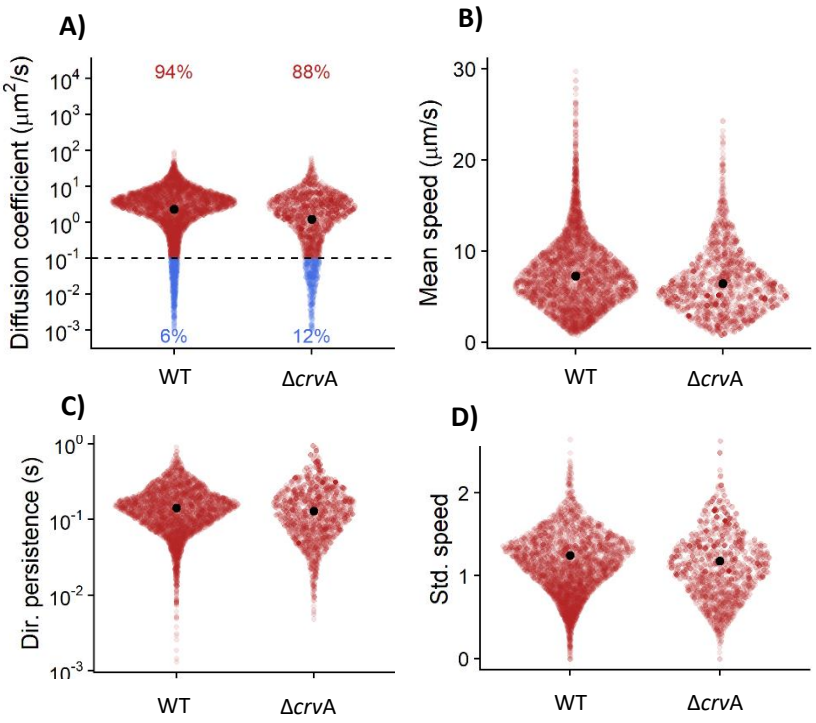

Figure 4.6: Comparison of the motility of WT and Δ*crv*A mutant in agar. Distributions of A) diffusion coefficient, B) swimming speed, C) directional persistence time and D) speed variance of the WT and Δ*crv*A mutant extracted from trajectories when swimming in 0.4% agar. Trajectory with diffusion coefficients below 10^{-1} μm^2/s were categorized as being trapped (blue) and excluded from the remaining analyses. The dot represents the mean. Data is calculated from 1,200 to 3,500 trajectories collected from three biological replicates. The results were statistically tested by a linear mixed-effect model.

Curvature improves *V. cholerae* diffusion in highly visco-elastic agarose.

Swim plate is a complex environment where the motility is affected by many factors, such as chemotaxis and growth. I aimed to track the motility of *V. cholerae* in agar on a microscope slide to avoid these confounding factors. However, agar solidifies quickly at 32 to 40°C, making the handling at room temperature difficult. Agar is made of agarose and agaropectin. Agarose provides the elasticity while agaropectin provides the viscosity. In the lab, low-melting agarose allows for handling at low

temperature. Methyl cellulose is a highly viscous material. I mixed 1.0% w/v MC and 0.3% w/v LMA (MCLMA) to imitate the condition on an agar plate. This mixture was made in M9 minimal salts supplemented with 0.4% sodium pyruvate and 0.1% tryptone. On the swim plate made by MCLMA, WT colony looks bigger than Δ*crv*A mutant colony, similar to the results on LB soft agar (Fig. 4.7A). Thus, MCLMA can reproduce the results on agar plate while it allows for real-time tracking and avoids confounding factors. I inoculated *V. cholerae* from liquid culture to MCLMA supplemented with minimal salts and 0.4% sodium pyruvate. In this condition, *V. cholerae* WT has higher speed and diffusion coefficients in MCLMA compared to the Δ*crv*A mutant (Fig. 4.8AB) (p-values < 10^{-4}). This result might explain why *V. cholerae* WT is able to spread faster than Δ*crv*A mutant on the swim plate made of MCLMA. However, WT has less proportion of motile cells and lower speed variance than Δ*crv*A mutant, in contrast to the results on swim plates (Fig. 4.6AD and 4.8AD).

On the swim plate made by LMA only, the colonies of two strains were small after 24 hours of incubation (Fig. 4.7B). The difference in colony size between two strains was negligible. When tracking on the microscope slide, neither strain diffused well in 0.3% LMA, with most cells being trapped in agarose mesh (Fig. 4.8E). Their speed variance is higher compared to that in M9 minimal media and MCLMA, suggesting that *V. cholerae* is trapped and changes direction frequently in a porous environment. In this condition, WT had higher swimming speed but lower motile population comparing to Δ*crv*A mutant (5.0 vs 17.0%) (p-values < 10^{-4}).

Thus, the curvature improves the swimming speed and diffusion of WT in MCLMA, an agar-like material. The curvature appears to be not beneficial to motility in LMA. In addition, MCLMA tracking results also reveal some divergence with agar tracking such as the motile population and speed variance. This difference might stem from the effect of growth and chemotaxis which is not present on the microscope slides.

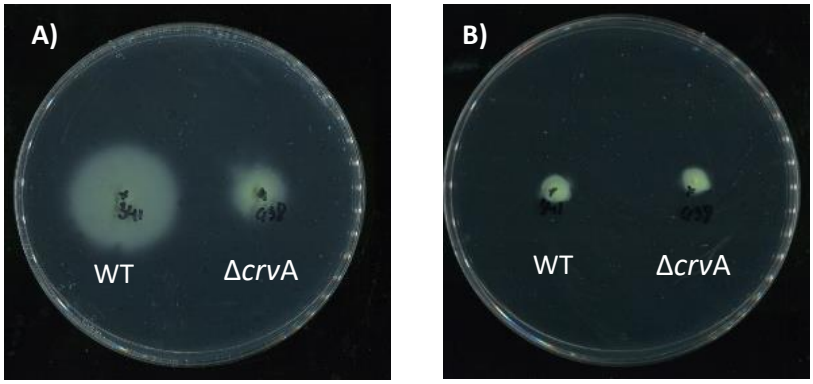

Figure 4.7: Picture shows the colonies of *V. cholerae* WT and Δ*crv*A mutant on swim plates made with A) MCLMA and B) LMA.

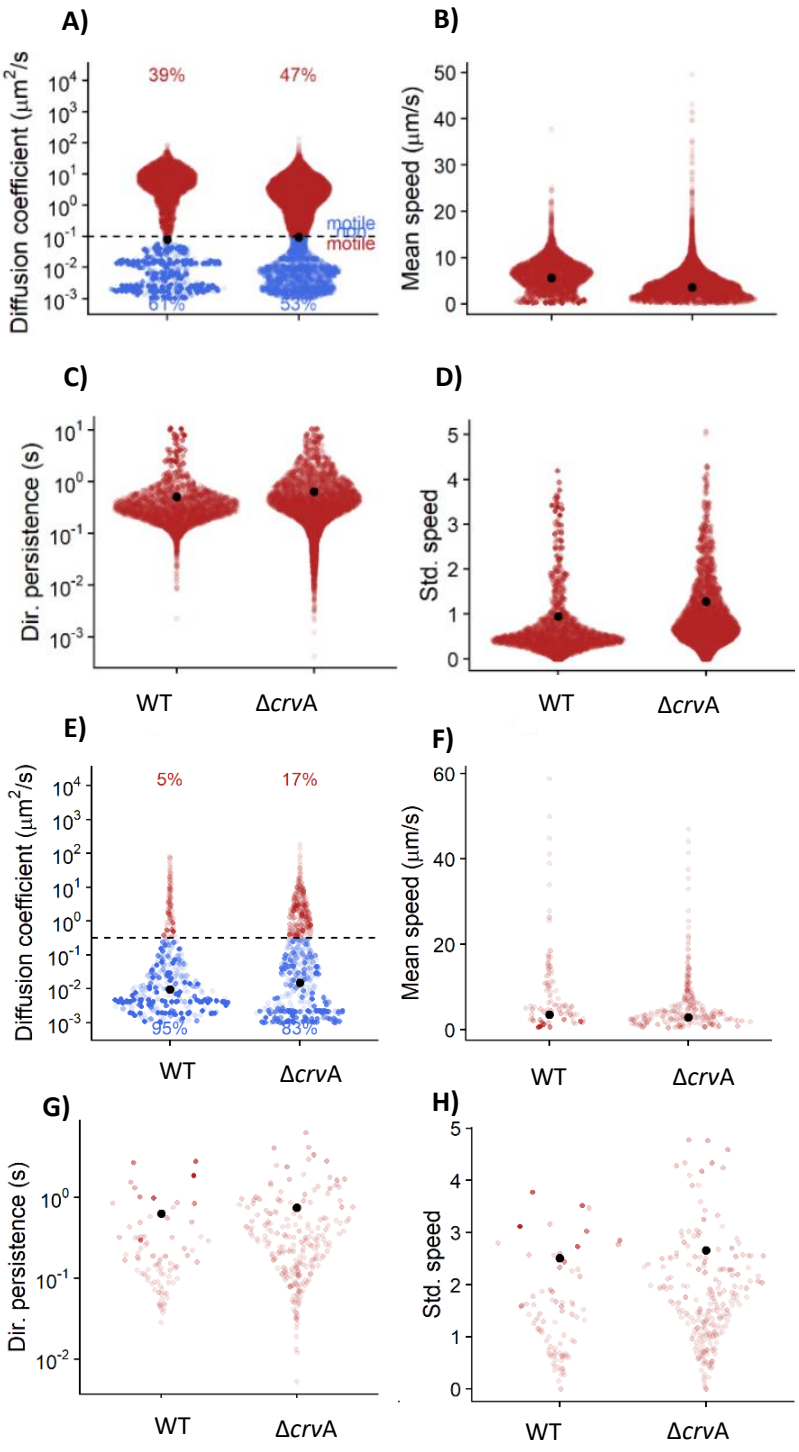

Figure 4.8: Comparison of the motility of WT and Δ*crv*A mutant in MCLMA and LMA. Distributions of A) diffusion coefficient, B) swimming speed, C) directional persistence time and D) speed variance of the

Figure 4.8 (cont'd)

WT and Δ*crv*A mutant extracted from trajectories when swimming in MCLMA. Data is calculated from approximately *3,0*00 *to 6,000* trajectories collected from three biological replicates. Distributions of E) diffusion coefficient, F) swimming speed, G) directional persistence time and H) speed variance of the WT and Δ*crv*A mutant extracted from trajectories when swimming in LMA. Data is calculated from approximately *1*700 trajectories collected from three biological replicates. The results were statistically tested by a linear mixed-effect model. The black dot represents the mean.

Migrating *V. cholerae* cells in agar have decreased curvature but increased inflection comparing to cells in liquid

Agar is a hydrogel which imposes different constraints than liquid environments. I tested if *V. cholerae* retains its curvature when migrating in agar. After incubating for 24 hours, cells were extracted from the edge of a swim colony and fixed on an agarose pad to take pictures at 100X. On a two-dimensional surface, *V. cholerae* twisted shape is seen as a comma (Fig. 4.9). I measured the metrics of cells collected from agar and compared with cells collected from a liquid culture at the stationary phase.

In liquid, *V. cholerae* WT has equal width with Δ*crv*A mutant (0.57 µm). However, its length is 8.38% shorter (1.64 vs 1.79 µm) (Fig. 4.10). I think that the difference stems from cell curvature which appears shorter when projected on a two-dimensional surface. In fact, the higher sinuosity of WT strain supports our hypothesis. As expected, *V. cholerae* WT has a higher degree of curvature comparing to Δ*crv*A mutant, (0.58 vs 0.16 μm^{-1}). The differences between WT and Δ*crv*A mutant are repeated in agar with WT cells having a higher curvature and shorter length comparing to Δ*crv*A mutant.

Comparing between two conditions, migrating cells from agar have ~150% larger volume than cells collected from liquid. I found that *V. cholerae* WT decreases its curvature in 0.4% agar whereas Δ*crv*A mutant retains the same curvature. When compared with cells collected from liquid, *V. cholerae*

WT from agar has more inflection with a higher proportion of cells having two to three inflections. It was reported that the cells at the edge of a colony are growing cells (Shao et al., 2017). In fact, these cells are more alike *V. cholerae* cells at exponential phase in liquid (Fig. 4.11). To compare the curvature between cells in agar and liquid, I focused on the cells with one inflection. Although cells from the colony edge have a similar length to exponential cells, their curvature is lower (Fig. 4.11). The result is also true when comparing between cells from the colony center and stationary cells in liquid (Fig. 4.S1).

Overall, our results suggest that the curvature is exploited differently in liquid and agar to satisfy the same need, diffusion. In liquid, the highly curved, one inflection shape increases the swimming speed. In agar, the low curvature, high inflection shape promotes the speed and expansion.

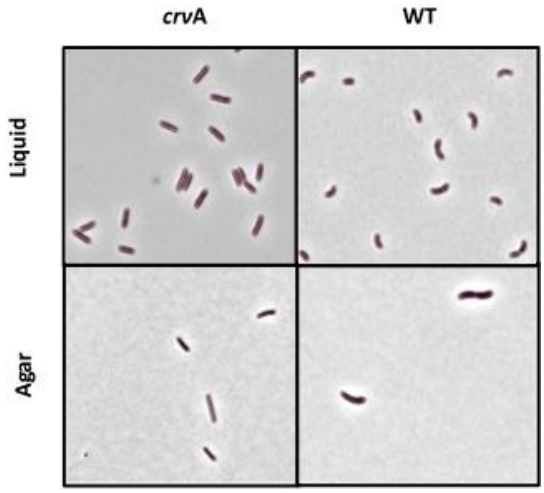

Figure 4.9: Phase-contrast photograph of *V. cholerae* cells collected from liquid and agar. Pictures were taken at 100X.

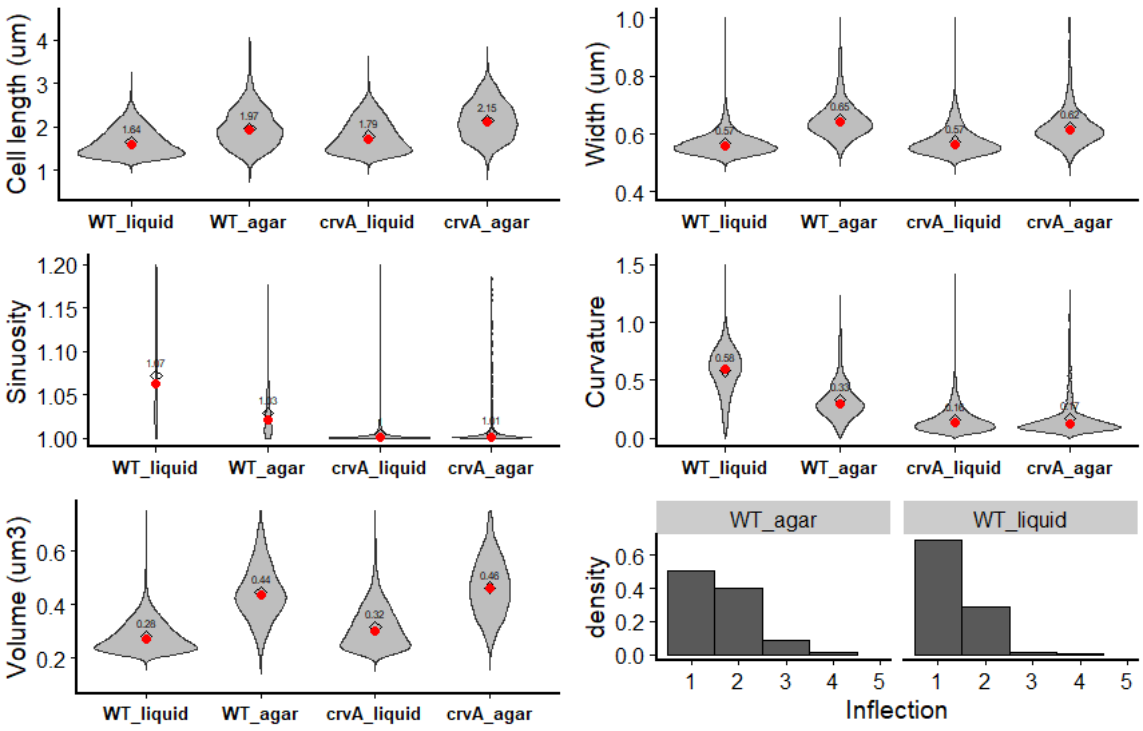

Figure 4.10: *V. cholerae* cell metrics. The results are from three biological replicates.

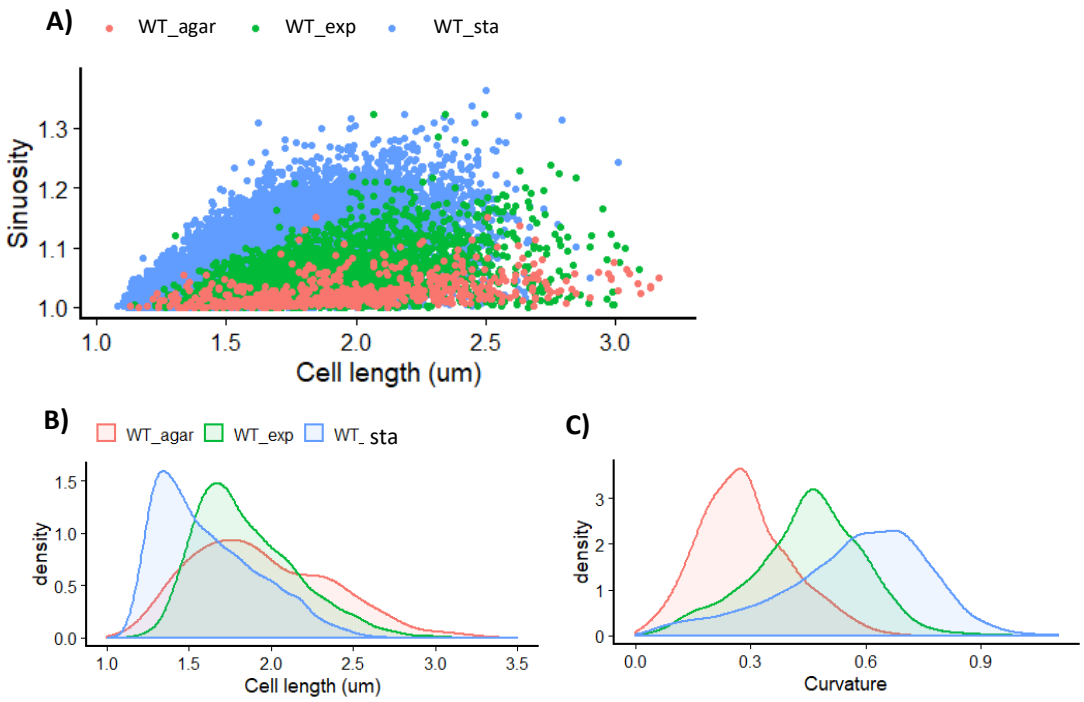

Figure 4.11: Comparison of *V. cholerae WT* cells grown in swim plate and liquid culture. A) V. cholerae from the edge of swim colony is more like exponential cells in liquid culture. Comparison of the B) length and C) curvature between one-inflection cells. The cells are from three conditions, the edge of swim colony (WT_agar), liquid culture at exponential phase (WT_exp), and liquid culture at stationary phase (WT_sta).

To test if the low curvature, high inflection shape retains its function when being switched to a different environment, I extracted cells from agar and transferred them to M9 minimal media. I used low-viscosity M9 minimal media so I could study motility without chemotaxis. In this condition, WT seems to swim faster than Δ*crv*A mutant with higher mean speed (65.6 vs 53.3 µm/s). However, this difference is not statistically significant. I also did not see a significant difference in directional persistence time and diffusion coefficients between two strains. In addition, the tracking revealed that most of the cells are non-motile (~96.0%) (Fig. 4.12). There is no difference in the proportion of motile

cells between two strains. This result is different from agar tracking where WT has around three times more motile cells than Δ*crv*A mutant, suggesting that most of motile Δ*crv*A cells were trapped in agar.

In general, the low curvature, high inflection shape might help *V. cholerae* to escape the porous agar and spread outward. This result suggests that *V. cholerae* motility adapts to its environment, in this case, by adjusting the shape. Whether this shape benefits *V. cholerae* motility in liquid still needs to be verified by a larger sample size.

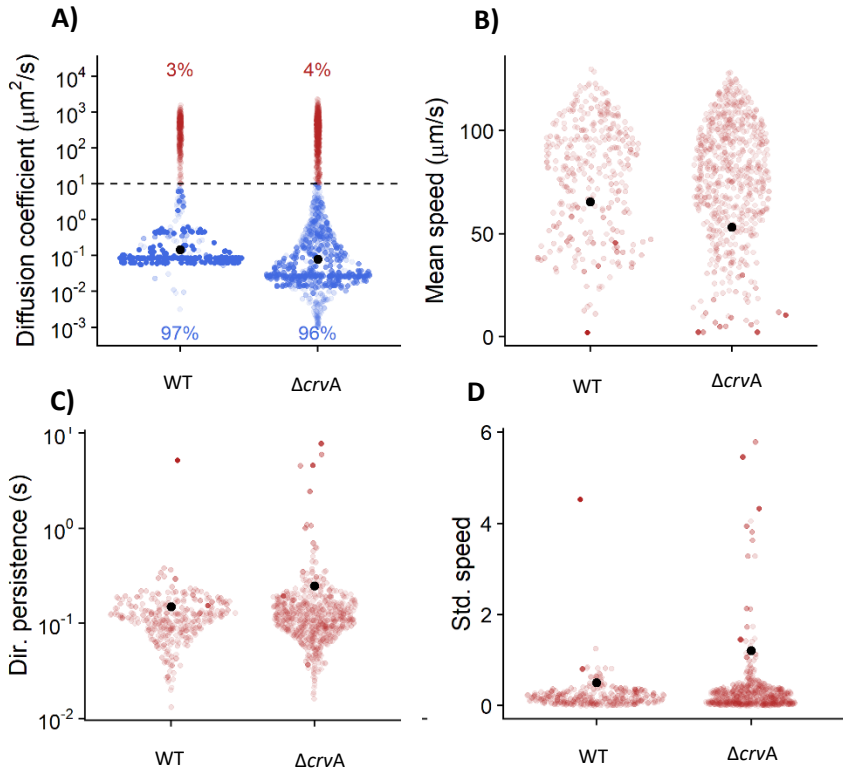

Figure 4.12: Swimming behavior of agar-grown *V. cholerae* in liquid. Distributions of A) diffusion coefficient, B) swimming speed, C) directional persistence time and D) speed variance of the agar-grown WT and Δ*crv*A mutant in liquid. Trajectory with diffusion coefficients below 10 μm^2/s were categorized as non-motile (blue) and excluded from the remaining analyses. The dot represents the mean. Data is calculated from 300 to 700 trajectories collected from three biological replicates. The results were statistically tested by a linear mixed-effect model.

DISCUSSION

V. cholerae is an opportunistic pathogen. It was not known how the curved shape benefits its life in the two environments where it is found, the aquatic habitats, and the human gut. These environments are characterized by very different physical parameters. Whereas sea water has low viscosity, mucus is a viscoelastic hydrogel. How the curved shape satisfies the need for diffusion in both environments has never been investigated before. Our main finding is that curvature improves *V. cholerae* motility in both liquid and mucus, but in different ways. Another finding is that *V. cholerae* curvature changes with the environments they live in. In the end, the curvature was exploited to improve the speed and diffusion of *V. cholerae* in both liquid and agar.

Nutrient molecules are highly dispersed in the marine environment. Therefore, *V. cholerae* must swim fast to reach to its food source. The 11.0% increment in speed of the curved cell compared to rod shape allows it to swim in water more efficiently and increases the chance to find food. The increment in speed is higher far from surfaces suggesting that the curved shape is more necessary for navigation through the sea water than roaming on a surface. In addition, it was reported that the high speed increases the chemotactic response in *V. alginolyticus* by increasing the frequency of flick (Son et al., 2016). In fact, our results are compatible with a model proposed by (Schuech et al., 2019) in which the curved shape is optimal for swimming speed, chemotaxis, and construction cost.

Mucus is a high visco-elastic environment. Curvature promotes *V. cholerae* motility in mucus by helping it maintain direction. I speculate that the curvature might help WT to drill through mucus using a corkscrew motion. Nevertheless, the difference in diffusion is small (~0.35 $\mu m^2/s$), making the interpretation about the role of curvature in mucus difficult. When compared to the role of strong flagellar rotation as shown in chapter 3, the role of curvature to *V. cholerae* motility in raw mucus seems small. The role of curvature may be more important for penetrating through the inner mucus layer or the fluid streams in mucus.

Lastly, I found that *V. cholerae* WT is the better swimmer in agar with higher swimming speed and diffusion coefficients. However, WT from agar has lower curvature compering to liquid-grown WT. On the other hand, migrating *V. cholerae* cells have more inflections than cells from liquid. More inflections make *V. cholerae* become spiral. Our data suggests that the low curvature and high inflection shape might help *V. cholerae* to escape the mesh structure of agar. Future studies should investigate the role of spiral *V. cholerae* in penetrating through the gel. The diffusion strategy of *V. cholerae* in agar might suggest how *V. cholerae* penetrates through the dense inner mucus layer.

Overall, our results show that the advantage of cell shape on motile performance dependent on the environmental context. In addition, the curvature of *V. cholerae* is not fixed but changing depending on the environments. I propose a model in which the highly curved shape might help *V. cholerae* to navigate through the lumen, loose mucus layer and against the fluid flow in the gut. When *V. cholerae* got stuck at the dense mucus portion, the cell is starting to grow and becomes less curved and spiral. This shape helps *V. cholerae* to improve the motility through mucus.

APPENDIX

APPENDIX

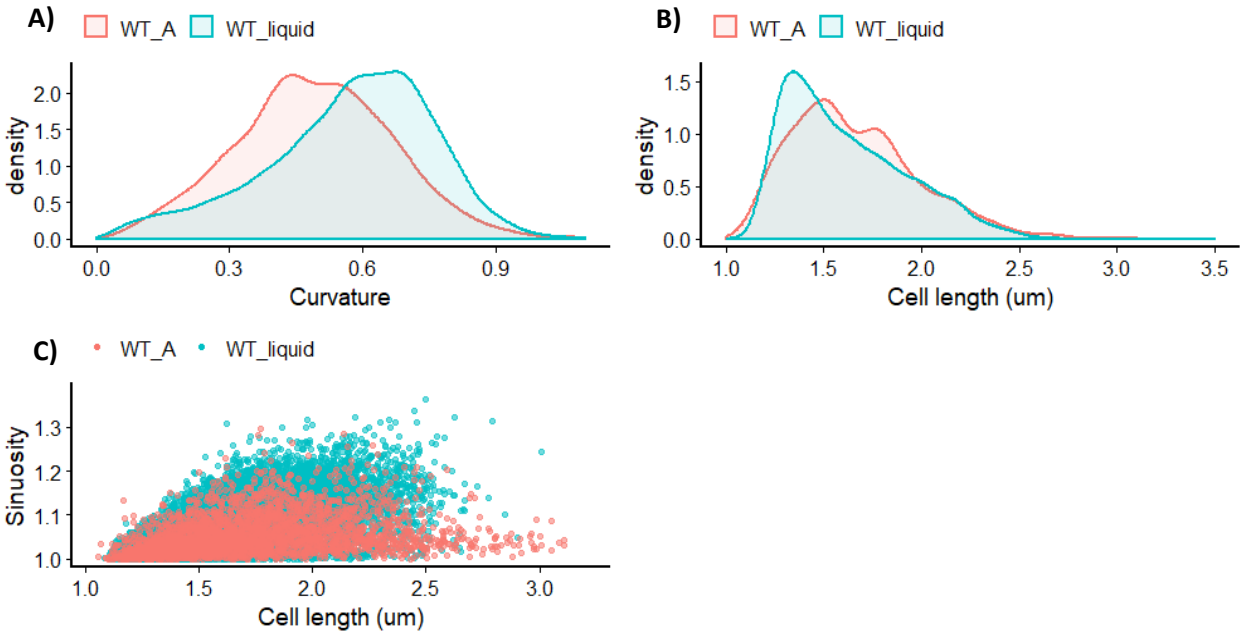

Figure 4.S1: Comparison of *V. cholerae* WT cells grown in swim plate and stationary culture.

Comparison of the A) curvature and B) curvature between one-inflection cells. C) Comparison of the cells collected from the center of swim colony and stationary cells.

REFERENCES

REFERENCES

Bartlett, T.M., Bratton, B.P., Duvshani, A., Miguel, A., Sheng, Y., Martin, N.R., Nguyen, J.P., Persat, A., Desmarais, S.M., VanNieuwenhze, M.S., et al. (2017). A Periplasmic Polymer Curves Vibrio cholerae and Promotes Pathogenesis. Cell *168*, 172-185.e15.

Constantino, M.A., Jabbarzadeh, M., Fu, H.C., and Bansil, R. (2016b). Helical and rod-shaped bacteria swim in helical trajectories with little additional propulsion from helical shape. Sci. Adv. *2*, e1601661.

Damton, N.C., Turner, L., Rojevsky, S., and Berg, H.C. (2010). Dynamics of bacterial swarming. Biophys. J. *98*, 2082–2090.

Dufour, Y.S., Gillet, S., Frankel, N.W., Weibel, D.B., and Emonet, T. (2016). Direct Correlation between Motile Behavior and Protein Abundance in Single Cells. PLoS Comput. Biol. *12*, e1005149.

Fernandez, N.L., Hsueh, B.Y., Nhu, N.T.Q., Franklin, J.L., Dufour, Y.S., and Waters, C.M. (2020). Vibrio cholerae adapts to sessile and motile lifestyles by cyclic di-GMP regulation of cell shape. Proc. Natl. Acad. Sci. e00578-17.

Frirdich, E., Biboy, J., Adams, C., Lee, J., Ellermeier, J., Gielda, L.D., DiRita, V.J., Girardin, S.E., Vollmer, W., and Gaynor, E.C. (2012). Peptidoglycan-modifying enzyme Pgp1 is required for helical cell shape and pathogenicity traits in campylobacter jejuni. PLoS Pathog. *8*, e1002602.

Frirdich, E., Vermeulen, J., Biboy, J., Soares, F., Taveirne, M.E., Johnson, J.G., DiRita, V.J., Girardin, S.E., Vollmer, W., and Gaynor, E.C. (2014). Peptidoglycan LD-carboxypeptidase Pgp2 influences Campylobacter jejuni helical cell shape and pathogenic properties and provides the substrate for the DL-carboxypeptidase Pgp1. J. Biol. Chem. *289*, 8007–8018.

Guentzel, M.N., and Berry, L.J. (1975). Motility as a virulence factor for Vibrio cholerae. Infect. Immun. *11*, 890–897.

Homma, M., Oota, H., Kojima, S., Kawagishi, I., and Imae, Y. (1996). Chemotactic responses to an attractant and a repellent by the polar and lateral flagellar systems of Vibrio alginolyticus. Microbiology *142*, 2777–2783.

Jaqaman, K., Loerke, D., Mettlen, M., Kuwata, H., Grinstein, S., Schmid, S.L., and Danuser, G. (2008). Robust single-particle tracking in live-cell time-lapse sequences. Nat. Methods. *5*, 695-702.

Jiang, H., Si, F., Margolin, W., and Sun, S.X. (2011). Mechanical control of bacterial cell shape. Biophys. J. *101*, 327–335.

Lee, S.H., Butler, S.M., and Camilli, A. (2001). Selection for in vivo regulators of bacterial virulence. Proc. Natl. Acad. Sci. *98*, 6889–6894.

Liu, B., Gulino, M., Morse, M., Tang, J.X., Powers, T.R., and Breuer, K.S. (2014). Helical motion of the cell body enhances Caulobacter crescentus motility. Proc. Natl. Acad. Sci. U. S. A. *111*, 11252–11256.

Magariyama, Y., Sugiyama, S., Muramoto, K., Kawagishi, I., Imae, Y., and Kudo, S. (1995). Simultaneous measurement of bacterial flagellar rotation rate and swimming speed. Biophys. J. *69*, 2154–2162.

Magariyama, Y., Ichiba, M., Nakata, K., Baba, K., Ohtani, T., Kudo, S., and Goto, T. (2005). Difference in bacterial motion between forward and backward swimming caused by the wall effect. Biophys. J. *88*, 3648–3658.

Martinez, R.M., Dharmasena, M.N., Kirn, T.J., and Taylor, R.K. (2009). Characterization of two outer membrane proteins, FlgO and FlgP, that influence vibrio cholerae motility. J. Bacteriol. *191*, 5669–5679.

Martínez, L.E., Hardcastle, J.M., Wang, J., Pincus, Z., Tsang, J., Hoover, T.R., Bansil, R., and Salama, N.R. (2016). Helicobacter pylori strains vary cell shape and flagellum number to maintain robust motility in viscous environments. Mol. Microbiol. *99*, 88–110.

Persat, A., Stone, H.A., and Gitai, Z. (2014). The curved shape of caulobacter crescentus enhances surface colonization in flow. Nat. Commun. *5*, 3824.

Ramia, M., Tullock, D.L., and Phan-Thien, N. (1993). The role of hydrodynamic interaction in the locomotion of microorganisms. Biophys. J. *65*, 755-778.

Schuech, R., Hoehfurtner, T., Smith, D.J., and Humphries, S. (2019). Motile curved bacteria are Pareto-optimal. Proc. Natl. Acad. Sci. U. S. A. *116*, 14440–14447.

Shao, X., Mugler, A., Kim, J., Jeong, H.J., Levin, B.R., and Nemenman, I. (2017). Growth of bacteria in 3-d colonies. PLoS Comput. Biol. *13*, e1005679.

Shi, H., Bratton, B.P., Gitai, Z., and Huang, K.C. (2018). How to Build a Bacterial Cell: MreB as the Foreman of E. coli Construction. Cell *172*, 1294–1305.

Sliusarenko, O., Heinritz, J., Emonet, T., and Jacobs-Wagner, C. (2011). High-throughput, subpixel precision analysis of bacterial morphogenesis and intracellular spatio-temporal dynamics. Mol. Microbiol. *80*, 612–627.

Son, K., Menolascina, F., and Stocker, R. (2016). Speed-dependent chemotactic precision in marine bacteria. Proc. Natl. Acad. Sci. 201602307.

Stocker, R. (2011). Reverse and flick: Hybrid locomotion in bacteria. Proc. Natl. Acad. Sci. U. S. A. *108*, 2635–2636.

Stylianidou, S., Brennan, C., Nissen, S.B., Kuwada, N.J., and Wiggins, P.A. (2016). SuperSegger : robust image segmentation, analysis and lineage tracking of bacterial cells. Mol. Microbiol. *102*, 690–700.

Young, K.D. (2006). The Selective Value of Bacterial Shape. Microbiol. Mol. Biol. Rev. *70*, 660–703.

Chapter 5: FLAGELLAR NUMBER AFFECTS THE SWIMMING SPEED AND SPREADING OF *SALMONELLA ENTERICA* IN LIQUID AND HYDROGELS

This chapter is part of a project partnered with Josh Franklin to investigate the role of flagellar number in *Salmonella enterica* motility.

INTRODUCTION

Salmonella is a common cause of enteric infection in the U.S.A. Every year, 1.35 million Americans are infected, resulting in approximately 420 deaths (CDC). The main source of infection is from raw and undercooked poultry, raw eggs, or unpasteurized dairy products. *Salmonella* can also be found on fruit and vegetables (CDC). Once *Salmonella* is in the intestine, it can invade the epithelial cells and trigger an inflammatory response (Patel and McCormick, 2014). The common symptoms of *Salmonella* infection are diarrhea, fever, and stomach cramp (CDC).

It was reported that the flagellar motility is necessary for infection. In fact, non-motile *S. enterica* have reduced colonization success in a chicken model (Parker and Guard-Petter, 2001). *Salmonella* flagella were found to play a role in attachment to host cells (Salehi et al., 2017) and biofilm formation on abiotic surfaces (Wang et al., 2020). In the human host, the mucus layer acts as a physical barrier to bacterial penetration to the epithelial tissue (Gustafsson et al., 2012). However, it was demonstrated that flagella can help *S. enterica* move toward nutrients in the loose outer mucus layer (Stecher et al., 2004, 2008). Nevertheless, it was found that *S. enterica* cannot penetrate the inner mucus layer. *Salmonella*'s strategy is to avoid this layer by infecting the exposed epithelial cells in the colon, such as non-mucin producing M cells, or swimming through fluid streams in mouse mucus (Furter et al., 2019). These factors are strong evidence that *Salmonella* relies on motility to initiate its infection.

S. enterica is peritrichous with three to four flagella (Iino, 1969; Partridge and Harshey, 2013). The production of flagella in *S. enterica* is regulated by a cascade of gene expression with the master *flh*DC operon regulating the downstream genes (Erhardt and Hughes, 2010; Liu and Matsumura, 1994). *S. enterica* swims with a "run and tumble" model (Nakamura and Minamino, 2019). It changes direction

when the flagella change rotation direction. However, the role of number of flagella in *S. enterica* motility is not known. Compared to other enteric pathogens such as *V. cholerae* and *C. jejuni*, *Salmonella* flagellar motors have a weaker torque (Beeby et al., 2016). Having multiple flagella could be a strategy to increase the sum of thrust in *Salmonella*. In fact, in *H. pylori*, having more flagella correlates with higher speed and motility in porcine gastric mucin (Martínez et al., 2016). Thus, having more flagella seems to benefit to the swimming behaviors in terms of speed at high viscosity.

Flagellar production costs ~2% of metabolism expenditure (Moens and Vanderleyden, 1996). Therefore, it is not metabolically sustainable to produce more than necessary. In addition, *Samonella* flagellin can be an antigen to TLR-5 (St. Paul et al., 2013) and trigger inflammatory response (Miao and Rajan, 2011). In fact, *Salmonella* virulence decreases when it overexpresses flagellin proteins (Yang et al., 2012). These findings suggest that *Salmonella* must limit the expression of flagella to balance efficient motility with the metabolic costs of producing flagella and the benefit of evading the host immune defense. Therefore, the costs and benefits of having more or less flagella must be clarified.

Some enteric pathogens are peritrichous. The role of flagellar number in these bacteria has never been investigated before. Understanding the role of flagellar number in penetrating the mucus layer will help elucidate the colonization strategy of these bacteria. Moreover, it will help answer why there is the difference in virulence between strains. In this chapter, I used single cell tracking to investigate the benefits of having more flagella in *S. enterica* motility and diffusion in liquid and hydrogels. I tracked an inducible *flh*DC strain that can produce a population with a desired average number of flagella. By changing the inducer concentration, I investigated the motility of *S. enterica* cells that harbored one to five flagella on average.

METHODS

Bacterial strains

The strains used in this study were *S. enterica* LT2. The strain was fluorescently labelled with green fluorescent protein expressed from a constitutive cytochrome c promoter on a p15a plasmid derivative, pCMW5 (gift from Dr. Christopher Waters).

Growth conditions

S. enterica was grown in Vogel-Bonner medium supplemented with 2% (w/v) yeast extract (VB2Y) (Koirala et al., 2014) until it reached OD_{600nm} ~1.0. *S. enterica* were started at the same OD, 0.01. All cultures were grown at 37°C, and liquid cultures were shaken at 200RPM. Kanamycin was added to 50 μg/ml when needed.

Raw pig intestinal mucus preparation

Pig intestines were obtained from pigs slaughtered at the Michigan State University meat laboratory with approval from the United States Department of Agriculture. Crude mucus was freshly collected by scraping the small intestines. Mucus was frozen in liquid nitrogen, then stored at -80° C. Raw mucus were hydrated in 1ml of VB. Mucus was incubated at 37° C for ~1 hour. Before tracking, excess liquid was removed by centrifugation at 21,000 g for 40 s.

Inducing *S. enterica* to produce different flagella number

S. enterica LT2 with an inducible flhDC operon (TH 4872) was used (Dr. Marc Erhardt). The operon is under the control of a pTet promoter. Anhydrotetracycline (AnTc) was used as an inducer. By changing the concentration of AnTc, I can obtain *S. enterica* with different flagellar number on average with a negative binomial distribution. The concentrations of AnTc used for inducing extracted from a fitting curved built by my work colleague Josh Franklin based on his calculation of the flagellar number as a function of inducer concentration (Fig. 5.S1). However, I grew *S. enterica* at 37°C instead of at 32°C as per his research. The number of flagella presented in this study is the mean number of a population

induced by an AnTc concentration. It was determined that AnTc concentrations of 0.73, 1.63, 2.92, 5.05, and 9.68 ng/ml were needed to achieve *S. enterica* with 1, 2, 3, 4, or 5 flagella on average, respectively. Salmonella was cultured in VB2Y medium containing desired AnTc concentrations and incubated with shaking until the OD_{600} reached ~1.0 (~10^9 CFU/ml).

Single-cell tracking

S. enterica cells were tracked in liquid following a previously described protocol (Dufour et al., 2016). *S. enterica* grown in VB2Y was washed and tracked in VB supplemented with 0.5% glucose. Cells were incubated at 37° C for 15 minutes before tracking to allow for adaptation of the chemotaxis response. Polyvinylpyrrolidone (PVP, BP431-100, Fisher Scientific) was added at 0.05% w/v to the samples to prevent attachment on the glass slide. 6 µl of each sample dropped on a glass slide and trapped under a 22 x 22 mm, #1.5 coverslip sealed with wax and paraffin to create a thin water film (10±2 µm) for video microscopy. For tracking in mucus, and LMA, a 130 µm spacer was added between the slide and the coverslip and fluorescently labelled cells were used. LMA slides were kept at room temperature for 30 minutes to allow solidification. The samples were kept at 37^{o}C during tracking. Images of swimming cells were recorded using a sCMOS camera (Andor Zyla 4.2, Oxford Instruments) at 20 frames per second using a 40X objective (Plan Fluor 40x, Nikon Instruments, Inc.) mounted on an inverted microscope (Eclipse Ti-E, Nikon Instruments, Inc.). Cell were illuminated using phase contrast in liquid or epifluorescence in mucus and agarose. Images were analyzed to detect and localize cells using custom scripts (Dufour et al., 2016) and cell trajectories were reconstructed using the µ-track package (Jaqaman et al., 2008). The analysis and plots of the cell trajectory statistics were done in MATLAB (The Mathworks, Inc.) as previously described (Dufour et al., 2016).

RESULTS

Higher flagellar number increases the speed and directional persistence of *S. enterica* in liquid.

Before tracking, *S. enterica* cultured in VB2Y to OD 1.0 was washed and transferred to VBG. Flagella-inducible *S. enterica* were tracked in VBG buffer at the near surface of a glass slide. At the concentration for one flagellum, most cells were immotile. At the inducer concentrations to produce two to five flagella, 89-95% of the population became motile. At these concentrations, the speed and directional persistence of *S. enterica* also increased which resulted in an increased diffusion coefficient. The tracking results from the condition for three or four flagella are similar with the results from the WT strain (Chapter 2). Coincidentally, the WT has an average number of 3.2±1.5 flagella (Partridge and Harshey, 2013). Of the inducer concentrations triggering motile behavior, the biggest increment in speed was between populations containing two and three flagella. Above that, the difference in speed increments between successive flagella number was smaller. It is observed that in the population with five flagella, there is more variation in speed with some cells having poor motility whereas other cells have high speed (Fig. 5.1B). Regarding tumbles, populations with more flagella have higher directional persistence time indicating that cells with more flagella spending more time swimming straight rather than tumbling (Fig. 5.1B).

Overall, it was observed that increasing the number of flagella increased the speed and run phase in liquid. This is the first time that flagella number has been reported to affect the swimming speed in a peritrichous bacterium.

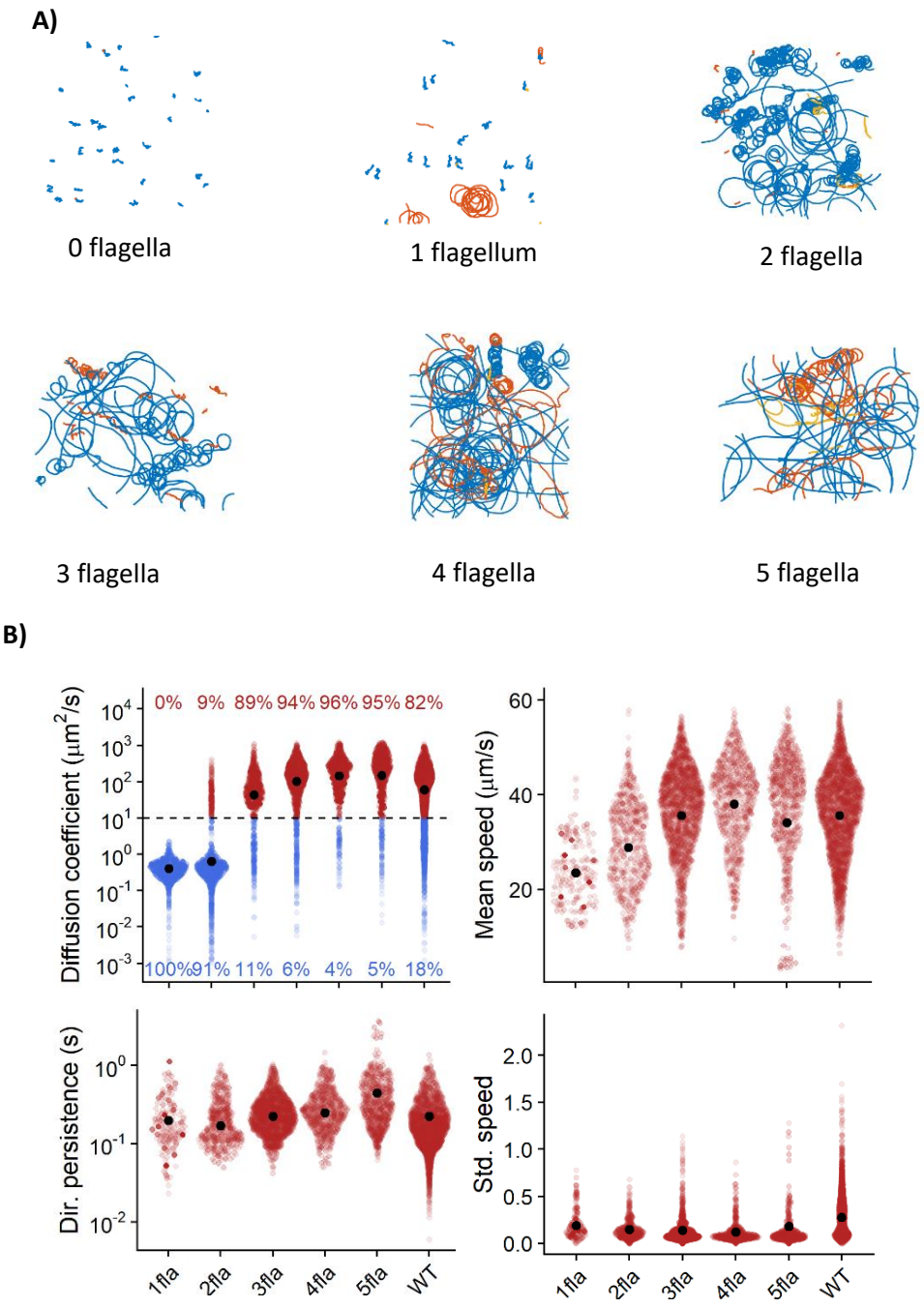

Figure 5.1: *S. enterica* swimming behavior A) The swimming trajectories of S. enterica at increasing induction and B) the distribution of diffusion coefficients, swimming speed, directional persistence time, and speed variance. Trajectory with diffusion coefficients below 10 $\mu m^2/s$ were categorized as non-

Figure 5.1 (cont'd)

motile (blue) and excluded from the remaining analyses. The dot represents the mean. The results are calculated from 188 to more than 3,000 trajectories.

***S. enterica* with higher flagellar number has better diffusion in hydrogels.**

S. enterica has adapted to the gastrointestinal tract of multiple animal species. To test the role of flagellar number in *S. enterica* motility in gels, I tracked *S. enterica* with different AnTc induction in LMA and raw mucus (Fig. 5.2). Among conditions with a high motile population (from two to five flagella), it was found that increased flagellar number also increased the swimming speed and diffusion of *S. enterica* in gels. Interestingly, significant differences in directional persistence time, and speed variance between inducing conditions was not observed.

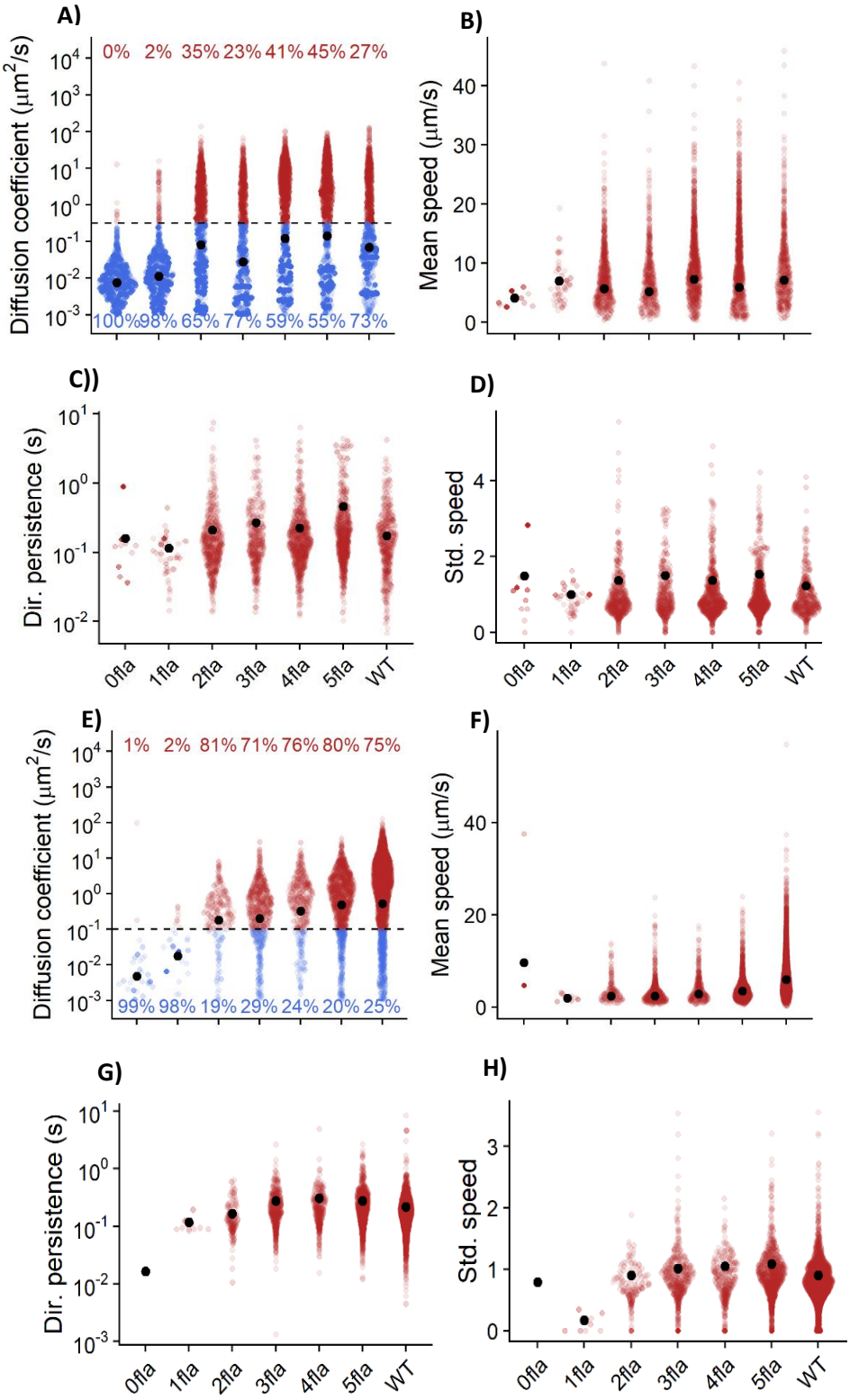

Figure 5.2: *S. enterica* with increasing AnTc induction in low-melting agarose and raw mucus. The plot shows the distribution of A) diffusion coefficients, B) swimming speed, C) directional persistence time,

Figure 5.2 (cont'd)

and D) speed variance from trajectories in LMA and E) diffusion coefficients, F) swimming speed, G) directional persistence time, and H) speed variance from trajectories in raw mucus. Trajectory with diffusion coefficients below $10^{-0.5}$ and 10^{-1} $\mu m^2/s$ were categorized as being trapped (blue) and excluded from the remaining analyses. The dot represents the mean. The results are calculated from ~200 to more than 3,000 trajectories.

DISCUSSION AND FUTURE DIRECTIONS

Even though mucus is effective at inhibiting *S. enterica* motility, there is still a proportion of cells that can navigate through this hydrogel. In this chapter, tracking was used to observe how the peritrichous nature of *Salmonella* helps with its motility. It was found that the swimming speed of *S. enterica* increases with flagellar number. Consequently, more flagella help *S. enterica* penetrate through hydrogels better.

It was shown that torque from a bundle of flagella is higher than torque from a single flagellum (Darnton et al., 2007). In addition, simulation studies show that more flagella may increase the propulsive force (Kanehl and Ishikawa, 2014). Our data agree with these models through the observation that higher number of flagella improve the swimming speed of *S. enterica* in liquid. Interestingly, the biggest increment in speed is between populations with two and three flagella. The swimming performance appeared to be negatively affected in five-flagellar population in which a proportion of cells swims poorly. It was reported that in *B. subtilis*, the swimming speed of mutants decreases when having less or more flagella comparing to WT (Najafi et al., 2018). In addition, flagellar production is costly in *Salmonella*. Our results might explain why *S. enterica* WT has an average number of three flagella given the cost and benefit of having multiple flagella.

S. enterica's natural habitat is an animal's gut. Therefore, it is presumed that its motility is best adapted to this environment. It was found that *S. enterica* motility in hydrogels increased with increasing flagellar number. Our results suggest that *S. enterica* achieves mucus penetration by improving its propulsion through the generation of torque from multiple flagella. It was previously shown that *H. pylori* with more flagella has higher swimming speed in porcine mucin (Martínez et al., 2016). This is the first time that the role of flagella number was shown to help a peritrichous bacterium penetrate mucus. However, having more flagella in mucus could be a bad strategy since it might be a target for the immune system. Therefore, bacteria in the gut must balance the need to be motile and to avoid triggering the host's immune response.

S. enterica swims with run and tumble model. In fact, it was shown that tumbling helps *E. coli* to escape from the porous environment (Licata et al., 2016). It was observed that it tumbles when one of the flagella change its rotational direction. However, other studies suggest that tumbling is a coordinated event where chemotaxis proteins change the rotation direction of all flagella. The second scenario is supported given that a higher number of flagella does not increase tumble bias (Mears et al., 2014). In this chapter, directional persistence time was used to evaluate the tumble bias. Directional persistence time has an opposite relationship with tumble bias. In contrary to my expectation, it was observed that the directional persistence time in liquid increases with flagellar number. However, the small increment makes its contribution to motility questionable. Nevertheless, this is a new finding that requires more studies to explain the phenomenon.

This is the first study reporting the additive propulsion of having multiple flagella. This propulsion promotes both the motility in liquid and mucus. This finding can be broadened to studies on other peritrichous bacteria found in the gut.

APPENDIX

APPENDIX

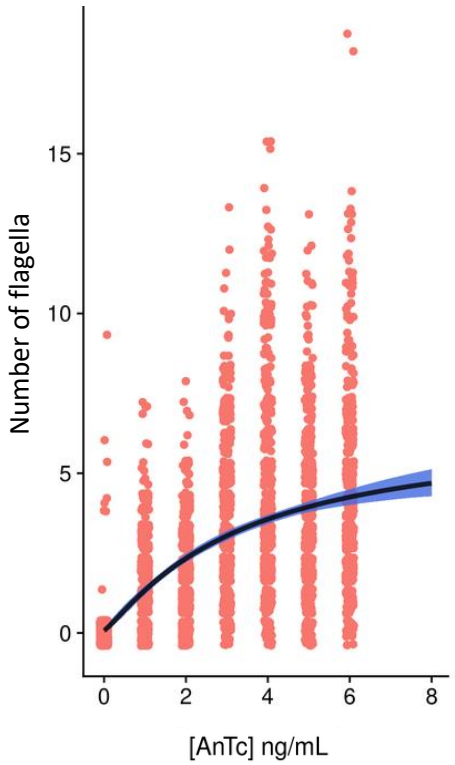

Figure 5.S1: Number of flagella as a function anhydrotetracycline (AnTc) inducer.

REFERENCES

REFERENCES

Beeby, M., Ribardo, D.A., Brennan, C.A., Ruby, E.G., Jensen, G.J., Hendrixson, D.R., and Hultgren, S.J. (2016). Diverse high-torque bacterial flagellar motors assemble wider stator rings using a conserved protein scaffold. Proc. Natl. Acad. Sci. U. S. A. *113*, 1–10.

Darnton, N.C., Turner, L., Rojevsky, S., and Berg, H.C. (2007). On torque and tumbling in swimming Escherichia coli. J. Bacteriol. *189*, 1756–1764.

Dufour, Y.S., Gillet, S., Frankel, N.W., Weibel, D.B., and Emonet, T. (2016). Direct Correlation between Motile Behavior and Protein Abundance in Single Cells. PLoS Comput. Biol. *12*, e1005149.

Erhardt, M., and Hughes, K.T. (2010). C-ring requirement in flagellar type III secretion is bypassed by FlhDC upregulation. Mol. Microbiol. *75*, 376–393.

Furter, M., Sellin, M.E., Hansson, G.C., and Hardt, W.D. (2019). Mucus Architecture and Near-Surface Swimming Affect Distinct Salmonella Typhimurium Infection Patterns along the Murine Intestinal Tract. Cell Rep. *27*, 2665-2678.e3.

Gustafsson, J.K., Ermund, A., Johansson, M.E.V. V., Schütte, A., Hansson, G.C., and Sjövall, H. (2012). An ex vivo method for studying mucus formation, properties, and thickness in human colonic biopsies and mouse small and large intestinal explants. Am. J. Physiol. Liver Physiol. *302*, G430–G438.

Iino, T. (1969). Polarity of flagellar growth in salmonella. J. Gen. Microbiol. *56*, 227–239.

Jaqaman, K., Loerke, D., Mettlen, M., Kuwata, H., Grinstein, S., Schmid, S.L., and Danuser, G. (2008). Robust single-particle tracking in live-cell time-lapse sequences. Nat. Methods. *5*, 695-702.

Kanehl, P., and Ishikawa, T. (2014). Fluid mechanics of swimming bacteria with multiple flagella. Phys. Rev. E - Stat. Nonlinear, Soft Matter Phys. *89*, 042704.

Koirala, S., Mears, P., Sim, M., Golding, I., Chemla, Y.R., Aldridge, P.D., and Rao, C. V. (2014). A nutrient-tunable bistable switch controls motility in Salmonella enterica serovar Typhimurium. MBio *5*, 01611–01614.

Licata, N.A.A., Mohari, B., Fuqua, C., and Setayeshgar, S. (2016). Diffusion of Bacterial Cells in Porous Media. Biophys. J. *110*, 247–257.

Liu, X., and Matsumura, P. (1994). The FlhD/FlhC complex, a transcriptional activator of the Escherichia coli flagellar class II operons. J. Bacteriol. *176*, 7345–7351.

Martínez, L.E., Hardcastle, J.M., Wang, J., Pincus, Z., Tsang, J., Hoover, T.R., Bansil, R., and Salama, N.R. (2016). Helicobacter pylori strains vary cell shape and flagellum number to maintain robust motility in viscous environments. Mol. Microbiol. *99*, 88–110.

Mears, P.J., Koirala, S., Rao, C. V., Golding, I., and Chemla, Y.R. (2014). Escherichia coli swimming is robust against variations in flagellar number. Elife *2014*, e01916.

Miao, E.A., and Rajan, J. V. (2011). Salmonella and Caspase-1: A complex interplay of detection and evasion. Front. Microbiol. *2*, 85.

Moens, S., and Vanderleyden, J. (1996). Functions of bacterial flagella. Crit. Rev. Microbiol. *22*, 67–100.

Najafi, J., Shaebani, M.R., John, T., Altegoer, F., Bange, G., and Wagner, C. (2018). Flagellar number governs bacterial spreading and transport efficiency. Sci. Adv. *4*, eaar6425.

Nakamura, S., and Minamino, T. (2019). Flagella-driven motility of bacteria. Biomolecules *9*, 279.

Parker, C.T., and Guard-Petter, J. (2001). Contribution of flagella and invasion proteins to pathogenesis of Salmonella enterica serovar enteritidis in chicks. FEMS Microbiol. Lett. *204*, 287–291.

Partridge, J.D., and Harshey, R.M. (2013). More than Motility: Salmonella Flagella Contribute to Overriding Friction and Facilitating Colony Hydration during Swarming. J. Bacteriol. *195*, 919–929.

Patel, S., and McCormick, B.A. (2014). Mucosal inflammatory response to Salmonella typhimurium infection. Front. Immunol. *5*, 5:311.

St. Paul, M., Brisbin, J.T., Abdul-Careem, M.F., and Sharif, S. (2013). Immunostimulatory properties of Toll-like receptor ligands in chickens. Vet. Immunol. Immunopathol. *152*, 191-199.

Salehi, S., Howe, K., Lawrence, M.L., Brooks, J.P., Hartford Bailey, R., and Karsi, A. (2017). Salmonella enterica serovar Kentucky flagella are required for broiler skin adhesion and Caco-2 cell invasion. Appl. Environ. Microbiol. *83*, e02115-16.

Stecher, B., Hapfelmeier, S., Müller, C., Kremer, M., Stallmach, T., and Hardt, W.D. (2004). Flagella and chemotaxis are required for efficient induction of Salmonella enterica serovar typhimurium colitis in streptomycin-pretreated mice. Infect. Immun. *72*, 4138-4150.

Stecher, B., Barthel, M., Schlumberger, M.C., Haberli, L., Rabsch, W., Kremer, M., and Hardt, W.D. (2008). Motility allows S. Typhimurium to benefit from the mucosal defence. Cell. Microbiol. *10*, 1166–1180.

Wang, F., Deng, L., Huang, F., Wang, Z., Lu, Q., and Xu, C. (2020). Flagellar Motility Is Critical for Salmonella enterica Serovar Typhimurium Biofilm Development. Front. Microbiol. *11*, 1695.

Yang, X., Thornburg, T., Suo, Z., Jun, S.M., Robison, A., Li, J., Lim, T., Cao, L., Hoyt, T., Avci, R., et al. (2012). Flagella Overexpression Attenuates Salmonella Pathogenesis. PLoS One. 7, e46828.

Chapter 6: CONCLUSION

My thesis presents a method for studying bacterial motility in raw mucus. By tracking single bacterial cells in mucus on a glass slide, a controlled environment can be established to selectively focus on the interaction between bacteria motility and mucus. The use of single cell tracking not only reveals more details about bacterial cell behavior, but this technique also avoids the effects of confounding factors, such as chemotaxis and growth. In addition, I can use this method to study the rheology by tracking microbeads. The movement of the beads reflects the physical properties of its environment at microscale. It was found that commercial mucins, including porcine gastric mucin (PGM) and bovine-submaxillary-gland mucin (BSM), and mucus behave differently. Whereas mucus behaves like a gel, PGM and BSM acts as a high viscous media (chapter 2 and 3). Raw mucus can trap 1 μm beads but allows 200 nm beads to freely disperse (chapter 3), suggesting that its pore size ranges from 200 nm to 1 μm.

Acting as the first line of defense, intestinal mucus is a harsh environmental constraint for enteric pathogens. It restricts the motility of most free-swimming *V. cholerae* and *S. enterica*, making it more effective than PGM (chapter 2) and BSM (chapter 3). Whereas mucus limits the diffusion of bacteria, commercial mucins still allows for long trajectories and large diffusion. Apart from the viscoelastic properties, mucus acidity can further affect *V. cholerae* motility (chapter 3), limiting them from penetrating most parts of the gut. In brief, *V. cholerae* is less motile in mucus at pH 6.0. The effect is observed on both *V. cholerae* strains, El Tor C6706 and Classical O395. In the small intestines, the pH is slightly alkaline at the ileum which is *V. cholerae* preferred site of infection. It was found that *V. cholerae* has higher diffusion at alkaline mucus. It is determined that the increment in diffusion is not a result of rheology change since mucus visco-elasticity is not different substantially between pH 8 and pH 6. The results might explain why the common site of infection is the ileum. On the other hand, while acting as a physical-biological barrier, the soluble components of mucus might promote the motility of *V. cholerae* and *S. enterica*, which are more motile in raw mucus than clarified mucus (chapter 2). The soluble components include lipid, soluble carbohydrate, and proteins.

V. cholerae seems to not rely on mucin digestion to increase the diffusion since I did not detect a micro-rheology change that is favorable to its movement after long incubation time in mucus (chapter 3). On the other hand, the role of curvature in *V. cholerae* motility in mucus still needs to be clarified (chapter 4). The same curvature that improves the speed in liquid, does not play the same role in mucus. The curvature appeared to help *V. cholerae* navigate through mucus to stay on track. However, the small increment in diffusion makes the efficiency of curvature on cell motility in mucus questionable. Moreover, migrating cells on the swim plate has less curvature and more inflections compared to the *V. cholerae* cells that I tracked in mucus. In fact, on the swim plate, the curved cells can swim 18.3% faster than rod-shaped mutant. It is noted that cells from swim plate have been dividing and growing in agar over the course of incubation. Thus, agar tracking results suggest that the curvature of *V. cholerae* might be different depending on the environments it lives in. For *V. cholerae* to move in mucus, its curvature might be tailored to cope with the thick inner layer, the fast mucin growing rate (240μm/hour) (Gustafsson et al., 2012) and the fluid circulation in the gut (Karthikeyan et al., 2021; Siryaporn et al., 2015).

Apart from the life in mucus, *V. cholerae* is more commonly found in aquatic environments which have low visco-elasticity. In this thesis, I tracked *V. cholerae* in phosphate buffer that has similar sodium content as sea water. Both *V. cholerae* strains, El Tor C6706 and Classical O395 swim fastest at pH 8.0, the pH of sea and brackish water. At pH 6.0, the Classical strain is still motile with decreased speed, but two-thirds of El Tor C6706 cells switch to a sessile lifestyle by extending its MshA pili to attach to the glass slide. Second messenger c-di-GMP regulates the motility or attachment in *V. cholerae*. Nevertheless, I did not detect the c-di-GMP level change when challenging El Tor C6706 at different pH. *V. cholerae* flagellar rotation is dependent on a sodium-driven motor. The difference in speed is likely due to the effect of pH on the Na^+-NQR pump of *V. cholerae*, which is more active at alkaline pH. In addition, El Tor had a higher growth rate than Classical at all pHs. This difference might

help El Tor to outcompete Classical in the natural habitats. When swimming in liquid, the curvature further improves the speed of *V. cholerae* WT, up to 11.0%. The increment is higher when swimming far away from the glass surface, suggesting that the curvature might be more important for navigating through the sea current. However, the curvature costs to *V. cholerae* is ~1.5% of its metabolism expenditure.

In contrast to *V. cholerae*, *S. enterica* is rod shaped and contains multiple flagella. It was found that *S. enterica* with a higher average number of flagella swam faster in liquid. The biggest increment in swimming speed is observed between population with the average number of two and three flagella. Above three flagella, the difference in speed in smaller. This result might explain why *S. enterica* is commonly found with an average of three flagella since it needs to balance between the benefits of motility and the cost of construction. I determined that *S. enterica* with more flagellar number can penetrate hydrogels better (chapter 5). *S. enterica* with higher number of flagella has higher swimming speed, resulting in higher diffusion in agarose and mucus. It is known that changing direction is necessary to escape the porous environment. I did not identify the correlation between increased flagellar number and frequency of changing direction among motile cells.

Overall, my thesis reported how mucus inhibits the motility of *V. cholerae* and *S. enterica*, and how these bacteria escape different environmental constraints. I found that mucus imposes constraints on bacteria such as the viscoelasticity and pH. On the other hand, bacteria develop different strategies for successful pathogenesis, such as navigating to and penetrating alkaline mucus or having multiple flagella**. My research has contributed to the understanding of bacterial motility in mucus, adding more knowledge about preferred site for *V. cholerae* infection, and the role of its curvature. I also presented the role of number of flagella in *S. enterica* motility. Based on these findings, my research opens some avenues for future research.**

Comparing to cells in liquid, *V. cholerae* in agar has higher number of inflections which makes the cell look spiral. I suspect that the spiral shape might facilitate the movement of *V. cholerae* in mucus and hydrogels by imitating the corkscrew motion of *H. pylori* and *C. jejuni*. To verify the role of spiral shape in *V. cholerae* movement, future studies can track cells at higher magnification to record the shape and the motility at the same time. Another method one can use is increasing the number of inflections of liquid-grown *V. cholerae* by cephalexin. In our lab, cells were obtained with two inflections by incubating exponential culture in 6µg/l Cephalexin for one hour. On the other hand, it is worth looking at *V. cholerae* with different curvature in mucus since it might promote its diffusion differently. The different curvature can be made by putting curvature-defined genes, Δ*crv*AB under an inducible promoter.

In many cases, chemotaxis guides the motility. This thesis focused mainly on motility behavior. Research looking at chemotaxis behavior in mucus will add additional knowledge about how pathogens move toward epithelial cells. It is interesting to integrate a chemical gradient into mucus and investigate if *V. cholerae* and *S. enterica* respond to a chemoattractant. On the other hand, the colony size of *V. cholerae* WT on swim plate is bigger than Δ*crv*A mutant. Chemotaxis plays a role in expanding colony. In addition, the high speed of *V. alginolyticus* was reported to increase the chemotaxis response by increasing the number of flicks. It was found that the curved shape increases the swimming speed. Therefore, it is interesting to investigate if the curved shape contributes to *V. cholerae* chemotaxis.

The mucus is not only a physical barrier but also a site of immune response. It was reported that antibodies can bind to *S. enterica* and *V. cholerae* surface proteins and inhibit bacterial motility in liquid. Using our method, one can look at the interaction between enteric pathogens and immune factors in mucus. In fact, I challenged *S. enterica*, *E. coli*, *V. cholerae* with secretory IgA from human colostrum at low concentration. I did not see an effect of sIgA on motility of these bacteria. Future studies can

continue to investigate more specific antibodies or challenge bacteria at higher concentrations of antibody.

Microbiota has been recognized recently as a part of our immune system. It is important to investigate the interaction between enteric pathogens and microbiota. By labelling two species with different fluorophores, one can track both at the same time and compare how their motility changes over time.

REFERENCES

REFERENCES

Gustafsson, J.K., Ermund, A., Johansson, M.E.V. V., Schütte, A., Hansson, G.C., and Sjövall, H. (2012). An ex vivo method for studying mucus formation, properties, and thickness in human colonic biopsies and mouse small and large intestinal explants. Am. J. Physiol. Liver Physiol. *302*, G430–G438.

Karthikeyan, J.S., Salvi, D., and Karwe, M. V. (2021). Modeling of fluid flow, carbohydrate digestion, and glucose absorption in human small intestine. J. Food Eng. *292*, 110339.

Siryaporn, A., Kim, M.K., Shen, Y., Stone, H.A., and Gitai, Z. (2015). Colonization, competition, and dispersal of pathogens in fluid flow networks. Curr. Biol. *25*, 1201–1207.